WIRELESS

communications

Principles & Practice

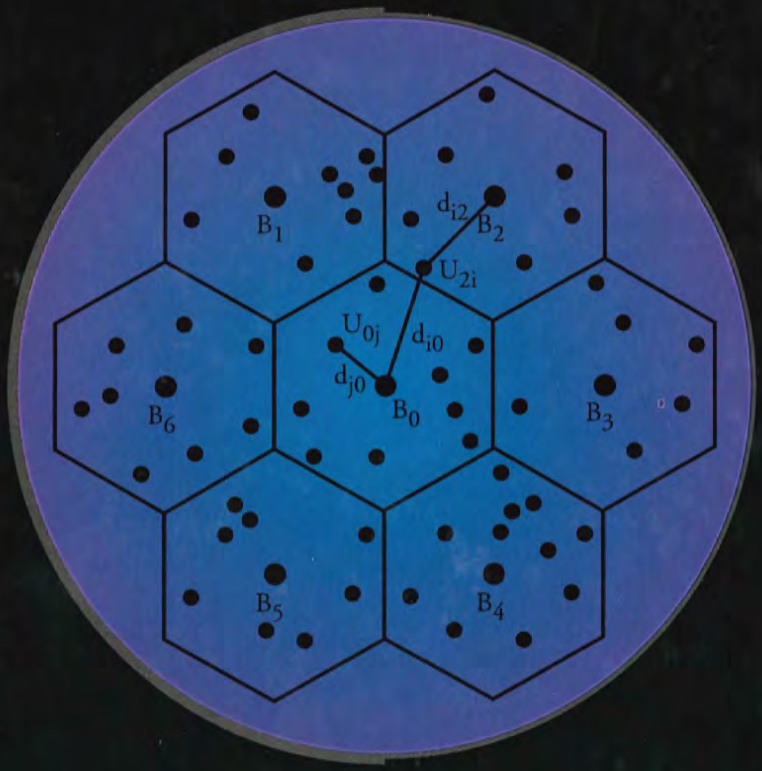

Theodore S. Rappaport

Wireless Communications

Principles and Practice

Theodore S. Rappaport

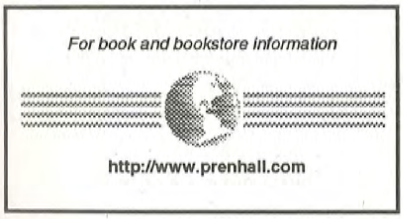

Prentice Hall PTR
Upper Saddle River, New Jersey 07458

Editorial/production manager: *Camille Trentacoste*
Cover design director: *Jerry Votta*
Cover designer: *Anthony Gemmellaro*
Manufacturing manager: *Alexis R. Heydt*
Acquisitions editor: *Karen Gettman*
Editorial assistant: *Barbara Alfieri*

Prentice-Hall, Inc.
A Simon & Schuster Company
Upper Saddle River, New Jersey 07458

The publisher offers discounts on this book when ordered in bulk quantities. For more information, contact Corporate Sales Department, Prentice Hall PTR, One Lake Street, Upper Saddle River, NJ 07458.
Phone: 800-382-3419; FAX: 201- 236-7141.
E-mail: corpsales@prenhall.com

Printed in the United States of America
10 9 8 7 6 5 4 3 2 1

ISBN 0-13-375536-3

Prentice-Hall International (UK) Limited, *London*
Prentice-Hall of Australia Pty. Limited, *Sydney*
Prentice-Hall Canada Inc., *Toronto*
Prentice-Hall Hispanoamericana, S.A., *Mexico*
Prentice-Hall of India Private Limited, *New Delhi*
Prentice-Hall of Japan, Inc., *Tokyo*
Simon & Schuster Asia Pte. Ltd., *Singapore*
Editora Prentice-Hall do Brasil, Ltda., *Rio de Janeiro*

Contents

Preface	**xi**
1 Introduction to Wireless Communication Systems	**1**
1.1 Evolution of Mobile Radio Communications	1
1.2 Mobile Radiotelephone in the U.S.	4
1.3 Mobile Radio Systems Around the World	6
1.4 Examples of Mobile Radio Systems	9
1.4.1 Paging Systems	11
1.4.2 Cordless Telephone Systems	13
1.4.3 Cellular Telephone Systems	14
1.4.4 Comparison of Common Mobile Radio Systems	17
1.5 Trends in Cellular Radio and Personal Communications	20
1.6 Problems	22
2 The Cellular Concept — System Design Fundamentals	**25**
2.1 Introduction	25
2.2 Frequency Reuse	26
2.3 Channel Assignment Strategies	30
2.4 Handoff Strategies	31
2.4.1 Prioritizing Handoffs	34
2.4.2 Practical Handoff Considerations	34
2.5 Interference and System Capacity	37
2.5.1 Co-channel Interference and System Capacity	37
2.5.2 Adjacent Channel Interference	41
2.5.3 Power Control for Reducing Interference	43
2.6 Trunking and Grade of Service	44

2.7 Improving Capacity in Cellular Systems 54
2.7.1 Cell Splitting 54
2.7.2 Sectoring 57
2.7.3 A Novel Microcell Zone Concept 61
2.8 Summary 63
2.9 Problems 63
3 Mobile Radio Propagation: Large-Scale Path Loss 69
3.1 Introduction to Radio Wave Propagation 69
3.2 Free Space Propagation Model 70
3.3 Relating Power to Electric Field 74
3.4 The Three Basic Propagation Mechanisms 78
3.5 Reflection 78
3.5.1 Reflection from Dielectrics 79
3.5.2 Brewster Angle 84
3.5.3 Reflection from Perfect Conductors 85
3.6 Ground Reflection (2-ray) Model 85
3.7 Diffraction 90
3.7.1 Fresnel Zone Geometry 91
3.7.2 Knife-edge Diffraction Model 94
3.7.3 Multiple Knife-edge Diffraction 99
3.8 Scattering 100
3.8.1 Radar Cross Section Model 101
3.9 Practical Link Budget Design using Path Loss Models 102
3.9.1 Log-distance Path Loss Model 102
3.9.2 Log-normal Shadowing 104
3.9.3 Determination of Percentage of Coverage Area 106
3.10 Outdoor Propagation Models 110
3.10.1 Longley-Rice Model 110
3.10.2 Durkin's Model — A Case Study 111
3.10.3 Okumura Model 116
3.10.4 Hata Model 119
3.10.5 PCS Extension to Hata Model 120
3.10.6 Walfisch and Bertoni Model 120
3.10.7 Wideband PCS Microcell Model 121
3.11 Indoor Propagation Models 123
3.11.1 Partition Losses (same floor) 123
3.11.2 Partition Losses between Floors 126
3.11.3 Log-distance Path Loss Model 126
3.11.4 Ericsson Multiple Breakpoint Model 128
3.11.5 Attenuation Factor Model 128
3.12 Signal Penetration into Buildings 131
3.13 Ray Tracing and Site Specific Modeling 132
3.14 Problems 133

54
54
57
61
63
63
69
69
70
74
78
78
79
84
85
85
90
91
94
99
100
101
102
102
104
106
110
110
111
116
119
120
120
121
123
123
126
126
128
128
131
132
133

4 Mobile Radio Propagation: Small-Scale Fading and Multipath 139
4.1 Small-Scale Multipath Propagation 139
4.1.1 Factors Influencing Small-Scale Fading 140
4.1.2 Doppler Shift 141
4.2 Impulse Response Model of a Multipath Channel 143
4.2.1 Relationship Between Bandwidth and Received Power 147
4.3 Small-Scale Multipath Measurements 153
4.3.1 Direct RF Pulse System 154
4.3.2 Spread Spectrum Sliding Correlator Channel Sounding 155
4.3.3 Frequency Domain Channel Sounding 158
4.4 Parameters of Mobile Multipath Channels 159
4.4.1 Time Dispersion Parameters 160
4.4.2 Coherence Bandwidth 163
4.4.3 Doppler Spread and Coherence Time 165
4.5 Types of Small-Scale Fading 167
4.5.1 Fading Effects Due to Multipath Time Delay Spread 168
4.5.2 Fading Effects Due to Doppler Spread 170
4.6 Rayleigh and Ricean Distributions 172
4.6.1 Rayleigh Fading Distribution 172
4.6.2 Ricean Fading Distribution 174
4.7 Statistical Models for Multipath Fading Channels 176
4.7.1 Clarke's Model for Flat Fading 177
4.7.2 Simulation of Clarke and Gans Fading Model 181
4.7.3 Level Crossing and Fading Statistics 185
4.7.4 Two-ray Rayleigh Fading Model 188
4.7.5 Saleh and Valenzuela Indoor Statistical Model 188
4.7.6 SIRCIM and SMRCIM Indoor and Outdoor Statistical Models 189
4.8 Problems 192
5 Modulation Techniques for Mobile Radio 197
5.1 Frequency Modulation vs. Amplitude Modulation 198
5.2 Amplitude Modulation 199
5.2.1 Single Sideband AM 202
5.2.2 Pilot Tone SSB 203
5.2.3 Demodulation of AM signals 206
5.3 Angle Modulation 206
5.3.1 Spectra and Bandwidth of FM Signals 208
5.3.2 FM Modulation Methods 209
5.3.3 FM Detection Techniques 211
5.3.4 Tradeoff Between SNR and Bandwidth in an FM Signal 219
5.4 Digital Modulation — an Overview 220
5.4.1 Factors That Influence the Choice of Digital Modulation 221
5.4.2 Bandwidth and Power Spectral Density of Digital Signals 224
5.4.3 Line Coding 225
5.5 Pulse Shaping Techniques 225
5.5.1 Nyquist Criterion for ISI Cancellation 227

5.5.2 Raised Cosine Rolloff Filter 229
5.5.3 Gaussian Pulse-shaping Filter 233
5.6 Geometric Representation of Modulation Signals 234
5.7 Linear Modulation Techniques 238
5.7.1 Binary Phase Shift Keying (BPSK) 238
5.7.2 Differential Phase Shift Keying (DPSK) 242
5.7.3 Quadrature Phase Shift Keying (QPSK) 243
5.7.4 QPSK Transmission and Detection Techniques 246
5.7.5 Offset QPSK 247
5.7.6 π/4 QPSK 249
5.7.7 π/4 QPSK Transmission Techniques 249
5.7.8 π/4 QPSK Detection Techniques 252
5.8 Constant Envelope Modulation 254
5.8.1 Binary Frequency Shift Keying 256
5.8.2 Minimum Shift Keying (MSK) 259
5.8.3 Gaussian Minimum Shift Keying (GMSK) 261
5.9 Combined Linear and Constant Envelope Modulation Techniques 267
5.9.1 M-ary Phase Shift Keying (MPSK) 267
5.9.2 M-ary Quadrature Amplitude Modulation (QAM) 270
5.9.3 M-ary Frequency Shift Keying (MFSK) 272
5.10 Spread Spectrum Modulation Techniques 274
5.10.1 Pseudo-noise (PN) Sequences 275
5.10.2 Direct Sequence Spread Spectrum (DS-SS) 276
5.10.3 Frequency Hopped Spread Spectrum (FH-SS) 278
5.10.4 Performance of Direct Sequence Spread Spectrum 280
5.10.5 Performance of Frequency Hopping Spread Spectrum 283
5.11 Modulation Performance in Fading and Multipath Channels 284
5.11.1 Performance of Digital Modulation in Slow, Flat Fading Channels 285
5.11.2 Digital Modulation in Frequency Selective Mobile Channels 289
5.11.3 Performance of π/4 DQPSK in Fading and Interference 290
5.12 Problems 294
6 Equalization, Diversity, and Channel Coding 299
6.1 Introduction 299
6.2 Fundamentals of Equalization 300
6.3 A Generic Adaptive Equalizer 303
6.4 Equalizers in a Communications Receiver 307
6.5 Survey of Equalization Techniques 308
6.6 Linear Equalizers 310
6.7 Nonlinear Equalization 312
6.7.1 Decision Feedback Equalization (DFE) 313
6.7.2 Maximum Likelihood Sequence Estimation (MLSE) Equalizer 315
6.8 Algorithms for Adaptive Equalization 316
6.8.1 Zero Forcing Algorithm 318
6.8.2 Least Mean Square Algorithm 319
6.8.3 Recursive Least Squares Algorithm 321
6.8.4 Summary of Algorithms 323

229
233
234
238
238
242
243
246
247
249
249
252
254
256
259
261
267
267
270
272
274
275
276
278
280
283
284
hannels 285
ls 289
290
294
299
299
300
303
307
308
310
312
313
zer 315
316
318
319
321
323

6.9 Fractionally Spaced Equalizers 323
6.10 Diversity Techniques 325
6.10.1 Derivation of Selection Diversity Improvement 326
6.10.2 Derivation of Maximal Ratio Combining Improvement 328
6.10.3 Practical Space Diversity Considerations 330
6.10.4 Polarization Diversity 332
6.10.5 Frequency Diversity 335
6.10.6 Time Diversity 335
6.11 RAKE Receiver 336
6.12 Interleaving 338
6.13 Fundamentals of Channel Coding 339
6.14 Block Codes 340
6.14.1 Examples of Block Codes 344
6.14.2 Case Study of Reed-Solomon Codes 346
6.15 Convolutional Codes 352
6.15.1 Decoding of Convolutional Codes 354
6.16 Coding Gain 356
6.17 Trellis Coded Modulation 356
6.18 Problems 357

7 Speech Coding 361

7.1 Introduction 361
7.2 Characteristics of Speech Signals 363
7.3 Quantization Techniques 365
7.3.1 Uniform Quantization 365
7.3.2 Nonuniform Quantization 365
7.3.3 Adaptive Quantization 368
7.3.4 Vector Quantization 368
7.4 Adaptive Differential Pulse Code Modulation 369
7.5 Frequency Domain Coding of Speech 371
7.5.1 Sub-band Coding 372
7.5.2 Adaptive Transform Coding 375
7.6 Vocoders 376
7.6.1 Channel Vocoders 376
7.6.2 Formant Vocoders 377
7.6.3 Cepstrum Vocoders 377
7.6.4 Voice-Excited Vocoder 378
7.7 Linear Predictive Coders 378
7.7.1 LPC Vocoders 378
7.7.2 Multi-pulse Excited LPC 381
7.7.3 Code-Excited LPC 382
7.7.4 Residual Excited LPC 383
7.8 Choosing Speech Codecs for Mobile Communications 384
7.9 The GSM Codec 387
7.10 The USDC Codec 389
7.11 Performance Evaluation of Speech Coders 389
7.12 Problems 392

8 Multiple Access Techniques for Wireless Communications 395
8.1 Introduction 395
8.1.1 Introduction to Multiple Access 396
8.2 Frequency Division Multiple Access (FDMA) 397
8.3 Time Division Multiple Access (TDMA) 400
8.4 Spread Spectrum Multiple Access 404
8.4.1 Frequency Hopped Multiple Access (FHMA) 404
8.4.2 Code Division Multiple Access (CDMA) 405
8.4.3 Hybrid Spread Spectrum Techniques 407
8.5 Space Division Multiple Access (SDMA) 409
8.6 Packet Radio 410
8.6.1 Packet Radio Protocols 411
8.6.2 Carrier Sense Multiple Access (CSMA) Protocols 415
8.6.3 Reservation Protocols 416
8.6.4 Capture Effect in Packet Radio 416
8.7 Capacity of Cellular Systems 417
8.7.1 Capacity of Cellular CDMA 422
8.7.2 Capacity of CDMA with Multiple Cells 425
8.7.3 Capacity of Space Division Multiple Access 431
8.8 Problems 437
9 Wireless Networking 439
9.1 Introduction to Wireless Networks 439
9.2 Differences Between Wireless and Fixed Telephone Networks 441
9.2.1 The Public Switched Telephone Network (PSTN) 441
9.2.2 Limitations in Wireless Networking 443
9.2.3 Merging Wireless Networks and the PSTN 444
9.3 Development of Wireless Networks 445
9.3.1 First Generation Wireless Networks 445
9.3.2 Second Generation Wireless Networks 448
9.3.3 Third Generation Wireless Networks 449
9.4 Fixed Network Transmission Hierarchy 449
9.5 Traffic Routing in Wireless Networks 450
9.5.1 Circuit Switching 452
9.5.2 Packet Switching 452
9.5.3 The X.25 Protocol 454
9.6 Wireless Data Services 455
9.6.1 Cellular Digital Packet Data (CDPD) 455
9.6.2 Advanced Radio Data Information Systems (ARDIS) 457
9.6.3 RAM Mobile Data (RMD) 457
9.7 Common Channel Signaling (CCS) 458
9.7.1 The Distributed Central Switching Office for CCS 459
9.8 Integrated Services Digital Network (ISDN) 461
9.8.1 Broadband ISDN and ATM 463
9.9 Signaling System No. 7 (SS7) 463
9.9.1 Network Services Part (NSP) of SS7 465

ons 395
395
396
397
400
404
404
405
407
409
410
411
415
416
416
417
422
425
431
437
439
439
441
441
443
444
445
445
448
449
449
450
452
452
454
455
455
457
457
458
459
461
463
463
465

9.9.2 The SS7 User Part 466
9.9.3 Signaling Traffic in SS7 467
9.9.4 SS7 Services 468
9.9.5 Performance of SS7 469
9.10 An example of SS7 — Global Cellular Network Interoperability 469
9.11 Personal Communication Services/Networks (PCS/PCN) 472
9.11.1 Packet vs. Circuit switching for PCN 472
9.11.2 Cellular Packet-Switched Architecture 473
9.12 Protocols for Network Access 477
9.12.1 Packet Reservation Multiple Access (PRMA) 478
9.13 Network Databases 479
9.13.1 Distributed Database for Mobility Management 479
9.14 Universal Mobile Telecommunication System (UMTS) 480
9.15 Summary 481

10 Wireless Systems and Standards 483

10.1 AMPS and ETACS 483
10.1.1 AMPS and ETACS System Overview 484
10.1.2 Call Handling in AMPS and ETACS 485
10.1.3 AMPS and ETACS Air Interface 487
10.1.4 N-AMPS 491
10.2 United States Digital Cellular (IS-54) 491
10.2.1 USDC Radio Interface 493
10.2.2 United States Digital Cellular Derivatives (IS-94 and IS-136) 500
10.3 Global System for Mobile (GSM) 500
10.3.1 GSM Services and Features 501
10.3.2 GSM System Architecture 502
10.3.3 GSM Radio Subsystem 505
10.3.4 GSM Channel Types 507
10.3.5 Example of a GSM Call 512
10.3.6 Frame Structure for GSM 513
10.3.7 Signal Processing in GSM 515
10.4 CDMA Digital Cellular Standard (IS-95) 519
10.4.1 Frequency and Channel Specifications 520
10.4.2 Forward CDMA Channel 521
10.4.3 Reverse CDMA Channel 527
10.4.4 IS-95 with 14.4 kbps Speech Coder [ANS95] 533
10.5 CT2 Standard For Cordless Telephones 533
10.5.1 CT2 Services and Features 533
10.5.2 The CT2 Standard 534
10.6 Digital European Cordless Telephone (DECT) 535
10.6.1 Features and Characteristics 535
10.6.2 DECT Architecture 536
10.6.3 DECT Functional Concept 537
10.6.4 DECT Radio Link 538

10.7 PACS — Personal Access Communication Systems 539
10.7.1 PACS System Architecture 540
10.7.2 PACS Radio Interface 541
10.8 Pacific Digital Cellular (PDC) 543
10.9 Personal Handyphone System (PHS) 544
10.10 U.S. PCS and ISM Bands 544
10.11 U.S. Wireless Cable Television 547
10.12 Summary of Standards Throughout the World 548
10.13 Problems 551

APPENDICES **555**
A Trunking Theory 556
A.1 Erlang B 556
A.1.1 Derivation of Erlang B 561
A.2 Erlang C 561
A.2.1 Derivation of Erlang C 565
B Noise Figure Calculations for Link Budgets 569
C Gaussian Approximations for Spread Spectrum CDMA 577
C.1 The Gaussian Approximation 582
C.2 The Improved Gaussian Approximation (IGA) 585
C.3 A Simplified Expression for the Improved Gaussian Approximation (SEIGA) 593
D Q, erf & erfc Functions 593
D.1 The Q-Function 595
D.2 The erf and erfc functions 599
E Mathematical Tables 607
F Abbreviations and Acronyms 617
G References 635
Index

Contents

539
540
541
543
544
544
547
548
551

555
556
556
561
561
565
A 569
577
582
on (SEIGA) 585
593
593
595
599
607
617
635

Preface

The purpose of this text is to initiate the newcomer to cellular radio and wireless personal communications, one of the fastest growing fields in the engineering world. Technical concepts which are at the core of design, implementation, research, and invention of wireless communication systems are presented in an order that is conducive to understanding general concepts, as well as those specific to particular cellular and personal communication systems and standards. This text is based upon my experiences as an educator, researcher, and consultant, and is modeled from an academic course developed for electrical engineering students as well as a self-study course for practicing engineers and technicians, developed at the request of the Institute of Electrical and Electronics Engineers (IEEE). References to journal articles are used liberally throughout this text to enable the interested reader to delve into additional reading that is always required to master any field. However, for handbook or classroom use, or for those who find it difficult to pursue outside reading, this text has been written as a complete, self-contained teaching and reference book. Numerous examples and problems have been provided to help the reader solidify the material.

This book has been designed for the student or practicing engineer who is already familiar with technical concepts such as probability, communication theory, and basic electromagnetics. However, like the wireless communications industry itself, this book combines material from many different technical disciplines, so it is unlikely that any one person will have had introductory courses for all of the topics covered. To accommodate a wide range of backgrounds, important concepts throughout the text are developed from first principles, so that readers learn the foundations of wireless communications. This approach

makes it possible to use this book as a handbook within industry, or as a teaching tool in a classroom setting.

The material and chapter sequence in this text have been adapted from an entry-level graduate course which I first taught in 1991 at the Virginia Polytechnic Institute and State University. Chapter 1 demonstrates the rapid growth of cellular radio throughout the world and provides a glimpse into the future. Chapter 2 covers cellular radio concepts such as frequency reuse and handoff, which are at the core of providing wireless communication service to subscribers on the move using limited radio spectrum. Chapter 2 also demonstrates how interference between mobiles and base stations affects the capacity of cellular systems. Chapter 3 presents radio propagation path loss and log-normal shadowing and describes different ways to model and predict the large-scale effects of radio propagation in many operating environments. Chapter 4 covers small-scale propagation effects such as fading, time delay spread, and Doppler spread, and describes how to measure and model the impact that signal bandwidth and motion have on the instantaneous received signal through the multipath channel. Radio wave propagation has historically been the most difficult problem to analyze and design for, since unlike a wired communication system which has a constant, stationary transmission channel (i.e., a wired path), radio channels are random and undergo shadowing and multipath fading, particularly when one of the terminals is in motion.

Chapter 5 provides extensive coverage of the most common analog and digital modulation techniques used in mobile communications and demonstrates trade-offs that must be made in selecting a modulation method. Issues such as receiver complexity, modulation and demodulation implementation, bit error rate analysis for fading channels, and spectral occupancy are presented. Channel coding, adaptive equalization, and antenna diversity concepts are presented in Chapter 6. In portable radio systems where people communicate while walking or driving, these methods may be used individually or in tandem to improve the quality (that is, reduce the bit error rate) of digital mobile radio communications in the presence of fading and noise.

Chapter 7 provides an introduction to speech coding. In the past decade there has been remarkable progress in decreasing the needed data rate of high quality digitized speech, which enables wireless system designers to match end-user services to network architectures. Principles which have driven the development of adaptive pulse code modulation and linear predictive coding techniques are presented, and how these techniques are used to evaluate speech quality in existing and proposed cellular, cordless, and personal communication systems are discussed. Chapter 8 introduces time, frequency, and code division multiple access, as well as more recent multiple access techniques such as packet reservation and space division multiple access. Chapter 8 also describes how each access method can accommodate a large number of mobile users and

demonstrates how multiple access impacts capacity and the network infrastructure of a cellular system. Chapter 9 describes networking considerations for wide area wireless communication systems, and presents practical networking approaches that are in use or have been proposed for future wireless systems. Chapter 10 unites all of the material from the first nine chapters by describing and comparing the major existing and proposed cellular, cordless, and personal communication systems throughout the world. The trade-offs made in the design and implementation of wireless personal communications systems are illuminated in this final chapter. The compilation of the major wireless standards makes Chapter 10 particularly useful as a single source of information for a wide range of systems.

Appendices which cover trunking theory, noise calculations, and the Gaussian approximation for spread spectrum code division systems provide details for those interested in solving practical wireless communications problems.

For industry use, Chapters 1—4 and 8 will benefit working engineers in the cellular system design and radio frequency (RF) testing/maintenance/measurement areas. Chapters 5—7 are tailored for modem designers and digital signal processing (DSP) engineers new to wireless. Chapters 9 and 10 should have broad appeal to network operators and managers, as well as working engineers.

To use this text at the undergraduate level, the instructor may wish to concentrate on Chapters 1—5, or Chapters 1—4, and 8, leaving the other chapters for treatment in a second semester undergraduate course or a graduate level course. Alternatively, traditional undergraduate courses on communications or network theory may find in Chapters 1, 2, 3, 5, 7, 8, and 9 useful material that can be inserted easily into the standard curriculum. In using this text at the graduate level, I have been successful in covering most of the material in Chapters 1—8 during a standard half-year semester. In Chapters 9 and 10, I have attempted to cover important but rarely compiled information on practical network implementations and worldwide standards.

Without the help and ingenuity of several former Virginia Tech graduate students, this text could not have been written. I am pleased to acknowledge the help and encouragement of Rias Muhamed, Varun Kapoor, Kevin Saldanha, and Anil Doradla – students I met in class while teaching the course *Cellular Radio and Personal Communications*. Kevin Saldanha also provided camera ready copy for this text (which turned out to be no small task!). The assistance of these students in compiling and editing materials for several chapters of this text was invaluable, and they were a source of constant encouragement throughout the project. Others who offered helpful suggestions, and whose research efforts are reflected in portions of this text, include Scott Seidel, Joe Liberti, Dwayne Hawbaker, Marty Feuerstein, Yingie Li, Ken Blackard, Victor Fung, Weifang Huang, Prabhakar Koushik, Orlando Landron, Francis Dominique, and Greg Bump. Zhi-

gang Rong, Jeff Laster, Michael Buehrer, Keith Brafford, and Sandip Sandhu also provided useful suggestions and helpful reviews of early drafts.

This text benefits greatly from practical input provided by several industry reviewers. Roman Zaputowycz of Bell Atlantic Mobile Systems, Mike Bamburak of McCaw Communications, David McKay of Allen Telecom Group, Jihad Hermes of Cellular One, Robert Rowe of AirTouch Communications, William Gardner of Qualcomm, and John Snapp of Blue Ridge Cellular provided extremely valuable input as to what materials were most important, and how they could best be presented for students and practicing engineers. Marty Feuerstein of U.S. West NewVector and Mike Lord of Cellular One provided comprehensive reviews which have greatly improved the manuscript. The technical staff at Grayson Electronics also provided feedback and practical suggestions during the development of this text.

From the academic perspective, a number of faculty in the wireless communications field provided useful suggestions which I readily incorporated. These reviewers include Prof. J. Keith Townsend of North Carolina State University and Prof. William H. Tranter of the University of Missouri-Rolla. Professors Jeffrey Reed and Brian Woerner of Virginia Tech also provided excellent recommendations from a teaching perspective. I am grateful for the invaluable contributions from all of these individuals.

I am pleased to acknowledge the support of the National Science Foundation, the Advanced Research Project Agency, and the many sponsors and friends of the Mobile & Portable Radio Research Group, who have supported our research and educational activities in wireless communications since 1990. It is from the excellent faculty at Purdue University, particularly my advisor, Clare D. McGillem, that I formally learned about communications and how to build a research program. I consider myself fortunate to have been one of the many graduate students who was stimulated to pursue a dual career in engineering and education upon graduation from Purdue.

Finally, it is a pleasure to acknowledge my family and students, who put up with my preoccupation on this project, Barbara Coburn and Jill Cals of the IEEE, who championed the IEEE self-study course on the same subject, and Karen Gettman and Camille Trentacoste of Prentice Hall, who commissioned this work and helped me bring this text to you.

Theodore S. Rappaport

CHAPTER 2

The Cellular Concept — System Design Fundamentals

The design objective of early mobile radio systems was to achieve a large coverage area by using a single, high powered transmitter with an antenna mounted on a tall tower. While this approach achieved very good coverage, it also meant that it was impossible to reuse those same frequencies throughout the system, since any attempts to achieve frequency reuse would result in interference. For example, the Bell mobile system in New York City in the 1970s could only support a maximum of twelve simultaneous calls over a thousand square miles [Cal88]. Faced with the fact that government regulatory agencies could not make spectrum allocations in proportion to the increasing demand for mobile services, it became imperative to restructure the radio telephone system to achieve high capacity with limited radio spectrum, while at the same time covering very large areas.

2.1 Introduction

The cellular concept was a major breakthrough in solving the problem of spectral congestion and user capacity. It offered very high capacity in a limited spectrum allocation without any major technological changes. The cellular concept is a system level idea which calls for replacing a single, high power transmitter (large cell) with many low power transmitters (small cells), each providing coverage to only a small portion of the service area. Each base station is allocated a portion of the total number of channels available to the entire system, and nearby base stations are assigned different groups of channels so that all the available channels are assigned to a relatively small number of neighboring base stations. Neighboring base stations are assigned different groups of channels so that the interference between base stations (and the mobile users

under their control) is minimized. By systematically spacing base stations and their channel groups throughout a market, the available channels are distributed throughout the geographic region and may be reused as many times as necessary, so long as the interference between co-channel stations is kept below acceptable levels.

As the demand for service increases (i.e., as more channels are needed within a particular market), the number of base stations may be increased (along with a corresponding decrease in transmitter power to avoid added interference), thereby providing additional radio capacity with no additional increase in radio spectrum. This fundamental principle is the foundation for all modern wireless communication systems, since it enables a fixed number of channels to serve an arbitrarily large number of subscribers by reusing the channels throughout the coverage region. Furthermore, the cellular concept allows every piece of subscriber equipment within a country or continent to be manufactured with the same set of channels, so that any mobile may be used anywhere within the region.

2.2 Frequency Reuse

Cellular radio systems rely on an intelligent allocation and reuse of channels throughout a coverage region [Oet83]. Each cellular base station is allocated a group of radio channels to be used within a small geographic area called a *cell*. Base stations in adjacent cells are assigned channel groups which contain completely different channels than neighboring cells. The base station antennas are designed to achieve the desired coverage within the particular cell. By limiting the coverage area to within the boundaries of a cell, the same group of channels may be used to cover different cells that are separated from one another by distances large enough to keep interference levels within tolerable limits. The design process of selecting and allocating channel groups for all of the cellular base stations within a system is called *frequency reuse* or *frequency planning* [Mac79].

Figure 2.1 illustrates the concept of cellular frequency reuse, where cells labeled with the same letter use the same group of channels. The frequency reuse plan is overlaid upon a map to indicate where different frequency channels are used. The hexagonal cell shape shown in Figure 2.1 is conceptual and is a simplistic model of the radio coverage for each base station, but it has been universally adopted since the hexagon permits easy and manageable analysis of a cellular system. The actual radio coverage of a cell is known as the *footprint* and is determined from field measurements or propagation prediction models. Although the real footprint is amorphous in nature, a regular cell shape is needed for systematic system design and adaptation for future growth. While it might seem natural to choose a circle to represent the coverage area of a base station, adjacent circles can not be overlaid upon a map without leaving gaps or

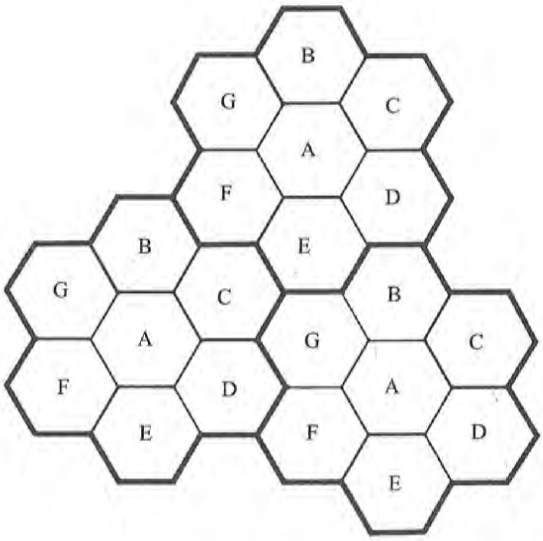

Figure 2.1
Illustration of the cellular frequency reuse concept. Cells with the same letter use the same set of frequencies. A cell cluster is outlined in bold and replicated over the coverage area. In this example, the cluster size, N, is equal to seven, and the frequency reuse factor is 1/7 since each cell contains one-seventh of the total number of available channels.

creating overlapping regions. Thus, when considering geometric shapes which cover an entire region without overlap and with equal area, there are three sensible choices: a square; an equilateral triangle; and a hexagon. A cell must be designed to serve the weakest mobiles within the footprint, and these are typically located at the edge of the cell. For a given distance between the center of a polygon and its farthest perimeter points, the hexagon has the largest area of the three. Thus, by using the hexagon geometry, the fewest number of cells can cover a geographic region, and the hexagon closely approximates a circular radiation pattern which would occur for an omni-directional base station antenna and free space propagation. Of course, the actual cellular footprint is determined by the contour in which a given transmitter serves the mobiles successfully.

When using hexagons to model coverage areas, base station transmitters are depicted as either being in the center of the cell (center-excited cells) or on three of the six cell vertices (edge-excited cells). Normally, omni-directional antennas are used in center-excited cells and sectored directional antennas are used in corner-excited cells. Practical considerations usually do not allow base stations to be placed exactly as they appear in the hexagonal layout. Most system designs permit a base station to be positioned up to one-fourth the cell radius away from the ideal location.

To understand the frequency reuse concept, consider a cellular system which has a total of S duplex channels available for use. If each cell is allocated a group of k channels ($k < S$), and if the S channels are divided among N cells into unique and disjoint channel groups which each have the same number of channels, the total number of available radio channels can be expressed as

$$S = kN \tag{2.1}$$

The N cells which collectively use the complete set of available frequencies is called a *cluster*. If a cluster is replicated M times within the system, the total number of duplex channels, C, can be used as a measure of capacity and is given

$$C = MkN = MS \tag{2.2}$$

As seen from equation (2.2), the capacity of a cellular system is directly proportional to the number of times a cluster is replicated in a fixed service area. The factor N is called the *cluster size* and is typically equal to 4, 7, or 12. If the cluster size N is reduced while the cell size is kept constant, more clusters are required to cover a given area and hence more capacity (a larger value of C) is achieved. A large cluster size indicates that the ratio between the cell radius and the distance between co-channel cells is large. Conversely, a small cluster size indicates that co-channel cells are located much closer together. The value for N is a function of how much interference a mobile or base station can tolerate while maintaining a sufficient quality of communications. From a design viewpoint, the smallest possible value of N is desirable in order to maximize capacity over a given coverage area (i.e., to maximize C in equation (2.2)). The *frequency reuse factor* of a cellular system is given by $1/N$, since each cell within a cluster is only assigned $1/N$ of the total available channels in the system.

Due to the fact that the hexagonal geometry of Figure 2.1 has exactly six equidistant neighbors and that the lines joining the centers of any cell and each of its neighbors are separated by multiples of 60 degrees, there are only certain cluster sizes and cell layouts which are possible [Mac79]. In order to tessellate — to connect without gaps between adjacent cells — the geometry of hexagons is such that the number of cells per cluster, N, can only have values which satisfy equation (2.3).

$$N = i^2 + ij + j^2 \tag{2.3}$$

where i and j are non-negative integers. To find the nearest co-channel neighbors of a particular cell, one must do the following: (1) move i cells along any chain of hexagons and then (2) turn 60 degrees counter-clockwise and move j cells. This is illustrated in Figure 2.2 for $i = 3$ and $j = 2$ (example, $N = 19$).

Example 2.1

If a total of 33 MHz of bandwidth is allocated to a particular FDD cellular telephone system which uses two 25 kHz simplex channels to provide full duplex

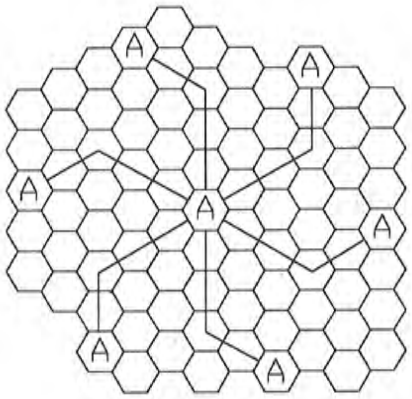

Figure 2.2
Method of locating co-channel cells in a cellular system. In this example, $N = 19$ (i.e., $i = 3, j = 2$). [Adapted from [Oet83] © IEEE].

voice and control channels, compute the number of channels available per cell if a system uses (a) 4-cell reuse, (b) 7-cell reuse (c) 12-cell reuse. If 1 MHz of the allocated spectrum is dedicated to control channels, determine an equitable distribution of control channels and voice channels in each cell for each of the three systems.

Solution to Example 2.1

Given:
Total bandwidth = 33 MHz
Channel bandwidth = 25 kHz × 2 simplex channels = 50 kHz/duplex channel
Total available channels = 33,000/50 = 660 channels
(a) For $N = 4$,
total number of channels available per cell = $660/4 \approx 165$ channels.
(b) For $N = 7$,
total number of channels available per cell = $660/7 \approx 95$ channels.
(c) For $N = 12$,
total number of channels available per cell = $660/12 \approx 55$ channels.

A 1 MHz spectrum for control channels implies that there are 1000/50 = 20 control channels out of the 660 channels available. To evenly distribute the control and voice channels, simply allocate the same number of channels in each cell wherever possible. Here, the 660 channels must be evenly distributed to each cell within the cluster. In practice, only the 640 voice channels would be allocated, since the control channels are allocated separately as 1 per cell.
(a) For $N = 4$, we can have 5 control channels and 160 voice channels per cell. In practice, however, each cell only needs a single control channel (the control

channels have a greater reuse distance than the voice channels). Thus, one control channel and 160 voice channels would be assigned to each cell.
(b) For $N = 7$, 4 cells with 3 control channels and 92 voice channels, 2 cells with 3 control channels and 90 voice channels, and 1 cell with 2 control channels and 92 voice channels could be allocated. In practice, however, each cell would have one control channel, four cells would have 91 voice channels, and three cells would have 92 voice channels.
(c) For $N = 12$, we can have 8 cells with 2 control channels and 53 voice channels, and 4 cells with 1 control channel and 54 voice channels each. In an actual system, each cell would have 1 control channel, 8 cells would have 53 voice channels, and 4 cells would have 54 voice channels.

2.3 Channel Assignment Strategies

For efficient utilization of the radio spectrum, a frequency reuse scheme that is consistent with the objectives of increasing capacity and minimizing interference is required. A variety of channel assignment strategies have been developed to achieve these objectives. Channel assignment strategies can be classified as either *fixed* or *dynamic*. The choice of channel assignment strategy impacts the performance of the system, particularly as to how calls are managed when a mobile user is handed off from one cell to another [Tek91], [LiC93], [Sun94], [Rap93b].

In a fixed channel assignment strategy, each cell is allocated a predetermined set of voice channels. Any call attempt within the cell can only be served by the unused channels in that particular cell. If all the channels in that cell are occupied, the call is *blocked* and the subscriber does not receive service. Several variations of the fixed assignment strategy exist. In one approach, called the *borrowing strategy*, a cell is allowed to borrow channels from a neighboring cell if all of its own channels are already occupied. The mobile switching center (MSC) supervises such borrowing procedures and ensures that the borrowing of a channel does not disrupt or interfere with any of the calls in progress in the donor cell.

In a dynamic channel assignment strategy, voice channels are not allocated to different cells permanently. Instead, each time a call request is made, the serving base station requests a channel from the MSC. The switch then allocates a channel to the requested cell following an algorithm that takes into account the likelihood of future blocking within the cell, the frequency of use of the candidate channel, the reuse distance of the channel, and other cost functions.

Accordingly, the MSC only allocates a given frequency if that frequency is not presently in use in the cell or any other cell which falls within the minimum restricted distance of frequency reuse to avoid co-channel interference. Dynamic channel assignment reduce the likelihood of blocking, which increases the trunking capacity of the system, since all the available channels in a market are accessible to all of the cells. Dynamic channel assignment strategies require the MSC

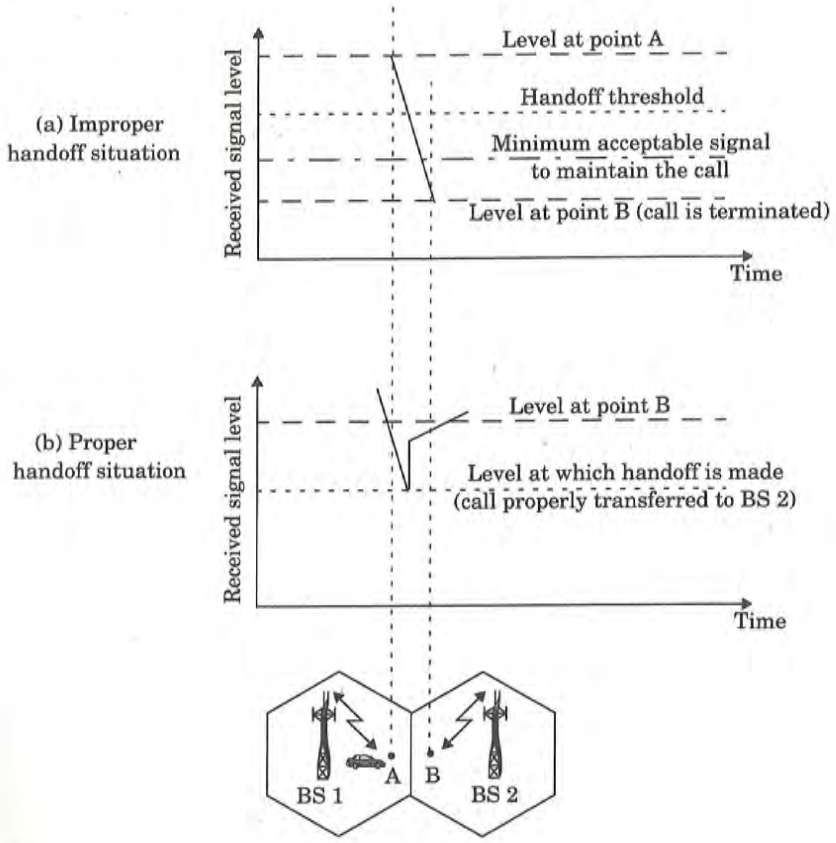

Figure 2.3
Illustration of a handoff scenario at cell boundary.

to collect real-time data on channel occupancy, traffic distribution, and *radio signal strength indications* (RSSI) of all channels on a continuous basis. This increases the storage and computational load on the system but provides the advantage of increased channel utilization and decreased probability of a blocked call.

2.4 Handoff Strategies

When a mobile moves into a different cell while a conversation is in progress, the MSC automatically transfers the call to a new channel belonging to the new base station. This handoff operation not only involves identifying a new base station, but also requires that the voice and control signals be allocated to channels associated with the new base station.

Processing handoffs is an important task in any cellular radio system. Many handoff strategies prioritize handoff requests over call initiation requests when allocating unused channels in a cell site. Handoffs must be performed successfully and as infrequently as possible, and be imperceptible to the users. In order to meet these requirements, system designers must specify an optimum signal level at which to initiate a handoff. Once a particular signal level is specified as the minimum usable signal for acceptable voice quality at the base station receiver (normally taken as between –90 dBm and –100 dBm), a slightly stronger signal level is used as a threshold at which a handoff is made. This margin, given by $\Delta = P_{r\ handoff} - P_{r\ minimum\ usable}$, cannot be too large or too small. If Δ is too large, unnecessary handoffs which burden the MSC may occur, and if Δ is too small, there may be insufficient time to complete a handoff before a call is lost due to weak signal conditions. Therefore, Δ is chosen carefully to meet these conflicting requirements. Figure 2.3 illustrates a handoff situation. Figure 2.3(a) demonstrates the case where a handoff is not made and the signal drops below the minimum acceptable level to keep the channel active. This dropped call event can happen when there is an excessive delay by the MSC in assigning a handoff, or when the threshold Δ is set too small for the handoff time in the system. Excessive delays may occur during high traffic conditions due to computational loading at the MSC or due to the fact that no channels are available on any of the nearby base stations (thus forcing the MSC to wait until a channel in a nearby cell becomes free).

In deciding when to handoff, it is important to ensure that the drop in the measured signal level is not due to momentary fading and that the mobile is actually moving away from the serving base station. In order to ensure this, the base station monitors the signal level for a certain period of time before a handoff is initiated. This running average measurement of signal strength should be optimized so that unnecessary handoffs are avoided, while ensuring that necessary handoffs are completed before a call is terminated due to poor signal level. The length of time needed to decide if a handoff is necessary depends on the speed at which the vehicle is moving. If the slope of the short-term average received signal level in a given time interval is steep, the handoff should be made quickly. Information about the vehicle speed, which can be useful in handoff decisions, can also be computed from the statistics of the received short-term fading signal at the base station.

The time over which a call may be maintained within a cell, without handoff, is called the *dwell time* [Rap93b]. The dwell time of a particular user is governed by a number of factors, which include propagation, interference, distance between the subscriber and the base station, and other time varying effects. Chapter 4 shows that even when a mobile user is stationary, ambient motion in the vicinity of the base station and the mobile can produce fading, thus even a stationary subscriber may have a random and finite dwell time. Analysis in

[Rap93b] indicates that the statistics of dwell time vary greatly, depending on the speed of the user and the type of radio coverage. For example, in mature cells which provide coverage for vehicular highway users, most users tend to have a relatively constant speed and travel along fixed and well-defined paths with good radio coverage. In such instances, the dwell time for an arbitrary user is a random variable with a distribution that is highly concentrated about the mean dwell time. On the other hand, for users in dense, cluttered microcell environments, there is typically a large variation of dwell time about the mean, and the dwell times are typically shorter than the cell geometry would otherwise suggest. It is apparent that the statistics of dwell time are important in the practical design of handoff algorithms [LiC93], [Sun94], [Rap93b].

In first generation analog cellular systems, signal strength measurements are made by the base stations and supervised by the MSC. Each base station constantly monitors the signal strengths of all of its reverse voice channels to determine the relative location of each mobile user with respect to the base station tower. In addition to measuring the RSSI of calls in progress within the cell, a spare receiver in each base station, called the locator receiver, is used to determine signal strengths of mobile users which are in neighboring cells. The *locator receiver* is controlled by the MSC and is used to monitor the signal strength of users in neighboring cells which appear to be in need of handoff and reports all RSSI values to the MSC. Based on the locator receiver signal strength information from each base station, the MSC decides if a handoff is necessary or not.

In second generation systems that use digital TDMA technology, handoff decisions are *mobile assisted*. In *mobile assisted handoff* (MAHO), every mobile station measures the received power from surrounding base stations and continually reports the results of these measurements to the serving base station. A handoff is initiated when the power received from the base station of a neighboring cell begins to exceed the power received from the current base station by a certain level or for a certain period of time. The MAHO method enables the call to be handed over between base stations at a much faster rate than in first generation analog systems since the handoff measurements are made by each mobile, and the MSC no longer constantly monitors signal strengths. MAHO is particularly suited for microcellular environments where handoffs are more frequent.

During the course of a call, if a mobile moves from one cellular system to a different cellular system controlled by a different MSC, an *intersystem handoff* becomes necessary. An MSC engages in an intersystem handoff when a mobile signal becomes weak in a given cell and the MSC cannot find another cell within its system to which it can transfer the call in progress. There are many issues that must be addressed when implementing an intersystem handoff. For instance, a local call may become a long-distance call as the mobile moves out of its home system and becomes a roamer in a neighboring system. Also, compati-

bility between the two MSCs must be determined before implementing an intersystem handoff. Chapter 9 demonstrates how intersystem handoffs are implemented in practice.

Different systems have different policies and methods for managing handoff requests. Some systems handle handoff requests in the same way they handle originating calls. In such systems, the probability that a handoff request will not be served by a new base station is equal to the blocking probability of incoming calls. However, from the user's point of view, having a call abruptly terminated while in the middle of a conversation is more annoying than being blocked occasionally on a new call attempt. To improve the quality of service as perceived by the users, various methods have been devised to prioritize handoff requests over call initiation requests when allocating voice channels.

2.4.1 Prioritizing Handoffs

One method for giving priority to handoffs is called the *guard channel concept*, whereby a fraction of the total available channels in a cell is reserved exclusively for handoff requests from ongoing calls which may be handed off into the cell. This method has the disadvantage of reducing the total carried traffic, as fewer channels are allocated to originating calls. Guard channels, however, offer efficient spectrum utilization when dynamic channel assignment strategies, which minimize the number of required guard channels by efficient demand-based allocation, are used.

Queuing of handoff requests is another method to decrease the probability of forced termination of a call due to lack of available channels. There is a trade-off between the decrease in probability of forced termination and total carried traffic. Queuing of handoffs is possible due to the fact that there is a finite time interval between the time the received signal level drops below the handoff threshold and the time the call is terminated due to insufficient signal level. The delay time and size of the queue is determined from the traffic pattern of the particular service area. It should be noted that queuing does not guarantee a zero probability of forced termination, since large delays will cause the received signal level to drop below the minimum required level to maintain communication and hence lead to forced termination.

2.4.2 Practical Handoff Considerations

In practical cellular systems, several problems arise when attempting to design for a wide range of mobile velocities. High speed vehicles pass through the coverage region of a cell within a matter of seconds, whereas pedestrian users may never need a handoff during a call. Particularly with the addition of microcells to provide capacity, the MSC can quickly become burdened if high speed users are constantly being passed between very small cells. Several schemes have been devised to handle the simultaneous traffic of high speed and

low speed users while minimizing the handoff intervention from the MSC. Another practical limitation is the ability to obtain new cell sites.

Although the cellular concept clearly provides additional capacity through the addition of cell sites, in practice it is difficult for cellular service providers to obtain new physical cell site locations in urban areas. Zoning laws, ordinances, and other nontechnical barriers often make it more attractive for a cellular provider to install additional channels and base stations at the same physical location of an existing cell, rather than find new site locations. By using different antenna heights (often on the same building or tower) and different power levels, it is possible to provide "large" and "small" cells which are co-located at a single location. This technique is called the *umbrella cell* approach and is used to provide large area coverage to high speed users while providing small area coverage to users traveling at low speeds. Figure 2.4 illustrates an umbrella cell which is co-located with some smaller microcells. The umbrella cell approach ensures that the number of handoffs is minimized for high speed users and provides additional microcell channels for pedestrian users. The speed of each user may be estimated by the base station or MSC by evaluating how rapidly the short-term average signal strength on the RVC changes over time, or more sophisticated algorithms may be used to evaluate and partition users [LiC93]. If a high speed user in the large umbrella cell is approaching the base station, and its velocity is rapidly decreasing, the base station may decide to hand the user into the co-located microcell, without MSC intervention.

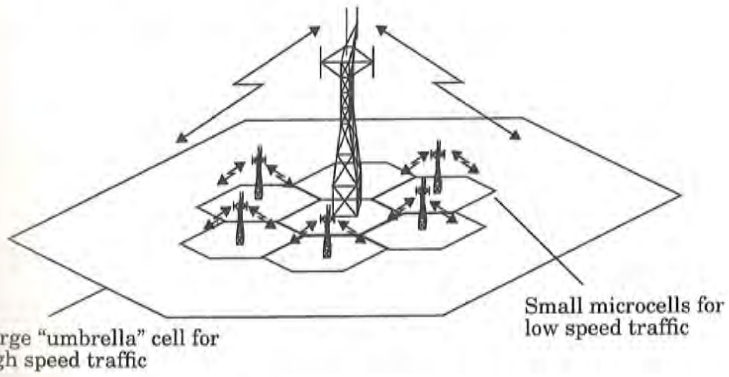

Figure 2.4
The umbrella cell approach.

Another practical handoff problem in microcell systems is known as *cell dragging*. Cell dragging results from pedestrian users that provide a very strong signal to the base station. Such a situation occurs in an urban environment when there is a line-of-sight (LOS) radio path between the subscriber and the base sta-

tion. As the user travels away from the base station at a very slow speed, the average signal strength does not decay rapidly. Even when the user has traveled well beyond the designed range of the cell, the received signal at the base station may be above the handoff threshold, thus a handoff may not be made. This creates a potential interference and traffic management problem, since the user has meanwhile traveled deep within a neighboring cell. To solve the cell dragging problem, handoff thresholds and radio coverage parameters must be adjusted carefully.

In first generation analog cellular systems, the typical time to make a handoff, once the signal level is deemed to be below the handoff threshold, is about 10 seconds. This requires that the value for Δ be on the order of 6 dB to 12 dB. In new digital cellular systems such as GSM, the mobile assists with the handoff procedure by determining the best handoff candidates, and the handoff, once the decision is made, typically requires only 1 or 2 seconds. Consequently, Δ is usually between 0 dB and 6 dB in modern cellular systems. The faster handoff process supports a much greater range of options for handling high speed and low speed users and provides the MSC with substantial time to "rescue" a call that is in need of handoff.

Another feature of newer cellular systems is the ability to make handoff decisions based on a wide range of metrics other than signal strength. The co-channel and adjacent channel interference levels may be measured at the base station or the mobile, and this information may be used with conventional signal strength data to provide a multi-dimensional algorithm for determining when a handoff is needed.

The IS-95 code division multiple access (CDMA) spread spectrum cellular system described in Chapter 10, provides a unique handoff capability that cannot be provided with other wireless systems. Unlike channelized wireless systems that assign different radio channels during a handoff (called a *hard handoff*), spread spectrum mobiles share the same channel in every cell. Thus, the term *handoff* does not mean a physical change in the assigned channel, but rather that a different base station handles the radio communication task. By simultaneously evaluating the received signals from a single subscriber at several neighboring base stations, the MSC may actually decide which version of the user's signal is best at any moment in time. This technique exploits macroscopic space diversity provided by the different physical locations of the base stations and allows the MSC to make a "soft" decision as to which version of the user's signal to pass along to the PSTN at any instance [Pad94]. The ability to select between the instantaneous received signals from a variety of base stations is called *soft handoff*.

2.5 Interference and System Capacity

Interference is the major limiting factor in the performance of cellular radio systems. Sources of interference include another mobile in the same cell, a call in progress in a neighboring cell, other base stations operating in the same frequency band, or any noncellular system which inadvertently leaks energy into the cellular frequency band. Interference on voice channels causes cross talk, where the subscriber hears interference in the background due to an undesired transmission. On control channels, interference leads to missed and blocked calls due to errors in the digital signaling. Interference is more severe in urban areas, due to the greater RF noise floor and the large number of base stations and mobiles. Interference has been recognized as a major bottleneck in increasing capacity and is often responsible for dropped calls. The two major types of system-generated cellular interference are *co-channel interference* and *adjacent channel interference*. Even though interfering signals are often generated within the cellular system, they are difficult to control in practice (due to random propagation effects). Even more difficult to control is interference due to out-of-band users, which arises without warning due to front end overload of subscriber equipment or intermittent intermodulation products. In practice, the transmitters from competing cellular carriers are often a significant source of out-of-band interference, since competitors often locate their base stations in close proximity to one another in order to provide comparable coverage to customers.

2.5.1 Co-channel Interference and System Capacity

Frequency reuse implies that in a given coverage area there are several cells that use the same set of frequencies. These cells are called *co-channel cells*, and the interference between signals from these cells is called *co-channel interference*. Unlike thermal noise which can be overcome by increasing the signal-to-noise ration (SNR), co-channel interference cannot be combated by simply increasing the carrier power of a transmitter. This is because an increase in carrier transmit power increases the interference to neighboring co-channel cells. To reduce co-channel interference, co-channel cells must be physically separated by a minimum distance to provide sufficient isolation due to propagation.

In a cellular system, when the size of each cell is approximately the same, co-channel interference is independent of the transmitted power and becomes a function of the radius of the cell (R), and the distance to the center of the nearest co-channel cell (D). By increasing the ratio of D/R, the spatial separation between co-channel cells relative to the coverage distance of a cell is increased. Thus interference is reduced from improved isolation of RF energy from the co-channel cell. The parameter Q, called the *co-channel reuse ratio*, is related to the cluster size. For a hexagonal geometry

$$Q = \frac{D}{R} = \sqrt{3N} \tag{2.4}$$

A small value of Q provides larger capacity since the cluster size N is small, whereas a large value of Q improves the transmission quality, due to a smaller level of co-channel interference. A trade-off must be made between these two objectives in actual cellular design.

Table 2.1 Co-channel Reuse Ratio for Some Values of N

	Cluster Size (N)	Co-channel Reuse Ratio(Q)
$i = 1, j = 1$	3	3
$i = 1, j = 2$	7	4.58
$i = 2, j = 2$	12	6
$i = 1, j = 3$	13	6.24

Let i_o be the number of co-channel interfering cells. Then, the signal-to-interference ratio (S/I or SIR) for a mobile receiver which monitors a forward channel can be expressed as

$$\frac{S}{I} = \frac{S}{\sum_{i=1}^{i_0} I_i} \tag{2.5}$$

where S is the desired signal power from the desired base station and I_i is the interference power caused by the i th interfering co-channel cell base station. If the signal levels of co-channel cells are known, then the S/I ratio for the forward link can be found using equation (2.5).

Propagation measurements in a mobile radio channel show that the average received signal strength at any point decays as a power law of the distance of separation between a transmitter and receiver. The average received power P_r at a distance d from the transmitting antenna is approximated by

$$P_r = P_0\left(\frac{d}{d_0}\right)^{-n} \tag{2.6}$$

or

$$P_r(\text{dBm}) = P_0(\text{dBm}) - 10n\log\left(\frac{d}{d_0}\right) \tag{2.7}$$

where P_0 is the power received at a close-in reference point in the far field region of the antenna at a small distance d_0 from the transmitting antenna, and n is the path loss exponent. Now consider the forward link where the desired signal is the serving base station and where the interference is due to co-channel base stations. If D_i is the distance of the i th interferer from the mobile, the received power at a given mobile due to the i th interfering cell will be proportional to

$(D_i)^{-n}$. The path loss exponent typically ranges between 2 and 4 in urban cellular systems [Rap92b].

When the transmit power of each base station is equal and the path loss exponent is the same throughout the coverage area, S/I for a mobile can be approximated as

$$\frac{S}{I} = \frac{R^{-n}}{\sum_{i=1}^{i_0} (D_i)^{-n}} \tag{2.8}$$

Considering only the first layer of interfering cells, if all the interfering base stations are equidistant from the desired base station and if this distance is equal to the distance D between cell centers, then equation (2.8) simplifies to

$$\frac{S}{I} = \frac{(D/R)^n}{i_0} = \frac{(\sqrt{3N})^n}{i_0} \tag{2.9}$$

Equation (2.9) relates S/I to the cluster size N, which in turn determines the overall capacity of the system from equation (2.2). For example, assume that the six closest cells are close enough to create significant interference and that they are all approximately equal distance from the desired base station. For the U.S. AMPS cellular system which uses FM and 30 kHz channels, subjective tests indicate that sufficient voice quality is provided when S/I is greater than or equal to 18 dB. Using equation (2.9) it can be shown in order to meet this requirement, the cluster size N should be at least 6.49, assuming a path loss exponent $n = 4$. Thus a minimum cluster size of 7 is required to meet an S/I requirement of 18 dB. It should be noted that equation (2.9) is based on the hexagonal cell geometry where all the interfering cells are equidistant from the base station receiver, and hence provides an optimistic result in many cases. For some frequency reuse plans (e.g. $N = 4$), the closest interfering cells vary widely in their distances from the desired cell.

From Figure 2.5, it can be seen for a 7-cell cluster, with the mobile unit is at the cell boundary, the mobile is a distance $D-R$ from the two nearest co-channel interfering cells and approximately $D + R/2$, D, $D - R/2$, and $D+R$ from the other interfering cells in the first tier [Lee86]. Using equation (2.9) and assuming n equals 4, the signal-to-interference ratio for the worst case can be closely approximated as (an exact expression is worked out by Jacobsmeyer [Jac94]).

$$\frac{S}{I} = \frac{R^{-4}}{2(D-R)^{-4} + (D-R/2)^{-4} + (D+R/2)^{-4} + (D+R)^{-4} + D^{-4}} \tag{2.10}$$

Equation (2.10) can be rewritten in terms of the co-channel reuse ratio Q, as

$$\frac{S}{I} = \frac{1}{\frac{2(Q+1)^4 + (Q-1)^4}{(Q^2-1)^4} + \frac{(Q+0.5)^4 + (Q-0.5)^4}{(Q^2-0.25)^4} + \frac{1}{Q^4}} \tag{2.11}$$

For $N = 7$, the co-channel reuse ratio Q is 4.6, and the worst case S/I is approximated as 49.56 (17 dB) using equation (2.11), whereas an exact solution using equation (2.8) yields 17.8 dB [Jac94]. Hence for a 7-cell cluster, the S/I ratio is slightly less than 18 dB for the worst case. To take the worst case into account, it would be necessary to increase N to the next possible value, which from equation (2.3) is found to be 12 (corresponding to $i = j = 2$). This obviously entails a significant decrease in capacity, since 12-cell reuse offers a spectrum utilization of 1/12 within each cell, whereas 7-cell reuse offers a spectrum utilization of 1/7. In practice, a capacity reduction of 7/12 would not be tolerable to accommodate for the worst case situation which rarely occurs. From the above discussion it is clear that co-channel interference determines link performance, which in turn dictates the frequency reuse plan and the overall capacity of cellular systems.

Example 2.2

If a signal to interference ratio of 15 dB is required for satisfactory forward channel performance of a cellular system, what is the frequency reuse factor and cluster size that should be used for maximum capacity if the path loss exponent is (a) $n = 4$, (b) $n = 3$? Assume that there are 6 co-channels cells in the first tier, and all of them are at the same distance from the mobile. Use suitable approximations.

Solution to Example 2.2

(a) $n = 4$

First, let us consider a 7-cell reuse pattern.

Using equation (2.4), the co-channel reuse ratio $D/R = 4.583$.

Using equation (2.9), the signal-to-noise interference ratio is given by

$S/I = (1/6) \times (4.583)^4 = 75.3 = 18.66$ dB.

Since this is greater than the minimum required S/I, $N = 7$ can be used.

b) $n = 3$

First, let us consider a 7-cell reuse pattern.

Using equation (2.9), the signal-to-interference ratio is given by

$S/I = (1/6) \times (4.583)^3 = 16.04 = 12.05$ dB.

Since this is less than the minimum required S/I, we need to use a larger N.

Using equation (2.3), the next possible value of N is 12, ($i = j = 2$).

The corresponding co-channel ratio is given by equation (2.4) as

$D/R = 6.0$.

Using equation (2.3) the signal-to-interference ratio is given by

$$S/I = (1/6) \times (6)^3 = 36 = 15.56 \text{ dB}.$$

Since this is greater than the minimum required S/I, $N = 12$ can be used.

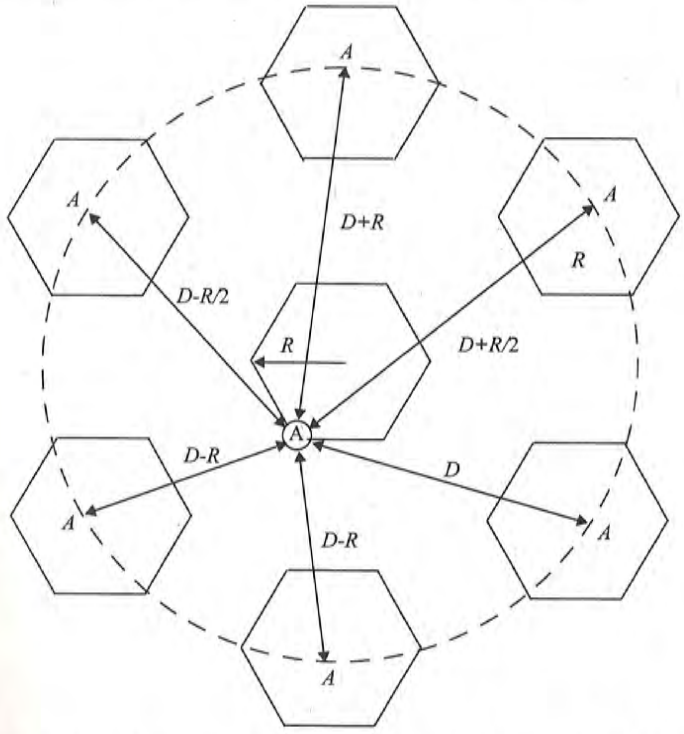

Figure 2.5
Illustration of the first tier of co-channel cells for a cluster size of N=7. When the mobile is at the cell boundary (point A), it experiences worst case co-channel interference on the forward channel. The marked distances between the mobile and different co-channel cells are based on approximations made for easy analysis.

2.5.2 Adjacent Channel Interference

Interference resulting from signals which are adjacent in frequency to the desired signal is called *adjacent channel interference*. Adjacent channel interference results from imperfect receiver filters which allow nearby frequencies to leak into the passband. The problem can be particularly serious if an adjacent channel user is transmitting in very close range to a subscriber's receiver, while the receiver attempts to receive a base station on the desired channel. This is referred to as the *near-far* effect, where a nearby transmitter (which may or may

not be of the same type as that used by the cellular system) captures the receiver of the subscriber. Alternatively, the near-far effect occurs when a mobile close to a base station transmits on a channel close to one being used by a weak mobile. The base station may have difficulty in discriminating the desired mobile user from the "bleedover" caused by the close adjacent channel mobile.

Adjacent channel interference can be minimized through careful filtering and channel assignments. Since each cell is given only a fraction of the available channels, a cell need not be assigned channels which are all adjacent in frequency. By keeping the frequency separation between each channel in a given cell as large as possible, the adjacent channel interference may be reduced considerably. Thus instead of assigning channels which form a contiguous band of frequencies within a particular cell, channels are allocated such that the frequency separation between channels in a given cell is maximized. By sequentially assigning successive channels in the frequency band to different cells, many channel allocation schemes are able to separate adjacent channels in a cell by as many as N channel bandwidths, where N is the cluster size. Some channel allocation schemes also prevent a secondary source of adjacent channel interference by avoiding the use of adjacent channels in neighboring cell sites.

If the frequency reuse factor is small, the separation between adjacent channels may not be sufficient to keep the adjacent channel interference level within tolerable limits. For example, if a mobile is 20 times as close to the base station as another mobile and has energy spill out of its passband, the signal-to-interference ratio for the weak mobile (before receiver filtering) is approximately

$$\frac{S}{I} = (20)^{-n} \tag{2.12}$$

For a path loss exponent $n = 4$, this is equal to -52 dB. If the intermediate frequency (IF) filter of the base station receiver has a slope of 20 dB/octave, then an adjacent channel interferer must be displaced by at least six times the passband bandwidth from the center of the receiver frequency passband to achieve 52 dB attenuation. Here, a separation of approximately six channel bandwidths is required for typical filters in order to provide 0 dB SIR from a close-in adjacent channel user. This implies that a channel separation greater than six is needed to bring the adjacent channel interference to an acceptable level, or tighter base station filters are needed when close-in and distant users share the same cell. In practice, each base station receiver is preceeded by a high Q cavity filter in order to reject adjacent channel interference.

Example 2.3

This example illustrates how channels are divided into subsets and allocated to different cells so that adjacent channel interference is minimized. The United States AMPS system initially operated with 666 duplex channels. In

1989, the FCC allocated an additional 10 MHz of spectrum for cellular services, and this allowed 166 new channels to be added to the AMPS system. There are now 832 channels used in AMPS. The forward channel (870.030 MHz) along with the corresponding reverse channel (825.030 MHz) is numbered as channel 1. Similarly the forward channel 889.98 MHz along with the reverse channel 844.98 MHz is numbered as channel 666 (see Figure 1.2). The extended band has channels numbered as 667 through 799, and 990 through 1023.

In order to encourage competition, the FCC licensed the channels to two competing operators in every service area, and each operator received half of the total channels. The channels used by the two operators are distinguished as *block A* and *block B* channels. Block B is operated by companies which have traditionally provided telephone services (called *wireline operators*), and Block A is operated by companies that have not traditionally provided telephone services (called *nonwireline operators*).

Out of the 416 channels used by each operator, 395 are voice channels and the remaining 21 are control channels. Channels 1 through 312 (voice channels) and channels 313 through 333 (control channels) are block A channels, and channels 355 through 666 (voice channels) and channels 334 through 354 (control channels) are block B channels. Channels 667 through 716 and 991 through 1023 are the extended Block A voice channels, and channels 717 through 799 are extended Block B voice channels.

Each of the 395 voice channels are divided into 21 subsets, each containing about 19 channels. In each subset, the closest adjacent channel is 21 channels away. In a 7-cell reuse system, each cell uses 3 subsets of channels. The 3 subsets are assigned such that every channel in the cell is assured of being separated from every other channel by at least 7 channel spacings. This channel assignment scheme is illustrated in Table 2.2. As seen in Table 2.2, each cell uses channels in the subsets, iA + iB + iC, where i is an integer from 1 to 7. The total number of voice channels in a cell is about 57. The channels listed in the upper half of the chart belong to block A and those in the lower half belong to block B. The shaded set of numbers correspond to the control channels which are standard to all cellular systems in North America.

2.5.3 Power Control for Reducing Interference

In practical cellular radio and personal communication systems the power levels transmitted by every subscriber unit are under constant control by the serving base stations. This is done to ensure that each mobile transmits the smallest power necessary to maintain a good quality link on the reverse channel. Power control not only helps prolong battery life for the subscriber unit, but also dramatically reduces the reverse channel S/I in the system. As shown in Chapters 8 and 10, power control is especially important for emerging CDMA spread spectrum systems that allow every user in every cell to share the same radio channel.

Table 2.2 AMPS channel allocation for A side and B side carriers

Channel allocation chart for the 832 channel AMPS system

1A	2A	3A	4A	5A	6A	7A	1B	2B	3B	4B	5B	6B	7B	1C	2C	3C	4C	5C	6C	7C	
1	2	3	4	5	6	7	8	9	10	11	12	13	14	15	16	17	18	19	20	21	
22	23	24	25	26	27	28	29	30	31	32	33	34	35	36	37	38	39	40	41	42	
43	44	45	46	47	48	49	50	51	52	53	54	55	56	57	58	59	60	61	62	63	
64	65	66	67	68	69	70	71	72	73	74	75	76	77	78	79	80	81	82	83	84	
85	86	87	88	89	90	91	92	93	94	95	96	97	98	99	100	101	102	103	104	105	
106	107	108	109	110	111	112	113	114	115	116	117	118	119	120	121	122	123	124	125	126	
127	128	129	130	131	132	133	134	135	136	137	138	139	140	141	142	143	144	145	146	147	
148	149	150	151	152	153	154	155	156	157	158	159	160	161	162	163	164	165	166	167	168	
169	170	171	172	173	174	175	176	177	178	179	180	181	182	183	184	185	186	187	188	189	A
190	191	192	193	194	195	196	197	198	199	200	201	202	203	204	205	206	207	208	209	210	SIDE
211	212	213	214	215	216	217	218	219	220	221	222	223	224	225	226	227	228	229	230	231	
232	233	234	235	236	237	238	239	240	241	242	243	244	245	246	247	248	249	250	251	252	
253	254	255	256	257	258	259	260	261	262	263	264	265	266	267	268	269	270	271	272	273	
274	275	276	277	278	279	280	281	282	283	284	285	286	287	288	289	290	291	292	293	294	
295	296	297	298	299	300	301	302	303	304	305	306	307	308	309	310	311	312	-	-	-	
313	314	315	316	317	318	319	320	321	322	323	324	325	326	327	328	329	330	331	332	333	
-	-	-	-	-	-	-	-	-	-	-	-	-	-	-	-	-	-	667	668	669	
670	671	672	673	674	675	676	677	678	679	680	681	682	683	684	685	686	687	688	689	690	
691	692	693	694	695	696	697	698	699	700	701	702	703	704	705	706	707	708	709	710	711	
712	713	714	715	716	-	-	-	-	997	992	993	994	995	996	997	998	999	1000	1001	1002	
1003	1004	1005	1006	1007	1008	1009	1010	1011	1012	1013	1014	1015	1016	1017	1018	1019	1020	1021	1022	1023	
334	335	336	337	338	339	340	341	342	343	344	345	346	347	348	349	350	351	352	353	354	
355	356	357	358	359	360	361	362	363	364	365	366	367	368	369	370	371	372	373	374	375	
376	377	378	379	380	381	382	383	384	385	386	387	388	389	390	391	392	393	394	395	396	
397	398	399	400	401	402	403	404	405	406	407	408	409	410	411	412	413	414	415	416	417	
418	419	420	421	422	423	424	425	426	427	428	429	430	431	432	433	434	435	436	437	438	
439	440	441	442	443	444	445	446	447	448	449	450	451	452	453	454	455	456	457	458	459	
460	461	462	463	464	465	466	467	468	469	470	471	472	473	474	475	476	477	478	479	480	
481	482	483	484	485	486	487	488	489	490	491	492	493	494	495	496	497	498	499	500	501	
502	503	504	505	506	507	508	509	510	511	512	513	514	515	516	517	518	519	520	521	522	B
523	524	525	526	527	528	529	530	531	532	533	534	535	536	537	538	539	540	541	542	543	SIDE
544	545	546	547	548	549	550	551	552	553	554	555	556	557	558	559	560	561	562	563	564	
565	566	567	568	569	570	571	572	573	574	575	576	577	578	579	580	581	582	583	584	585	
586	587	588	589	590	591	592	593	594	595	596	597	598	599	600	601	602	603	604	605	606	
607	608	609	610	611	612	613	614	615	616	617	618	619	620	621	622	623	624	625	626	627	
628	629	630	631	632	633	634	635	636	637	638	639	640	641	642	643	644	645	646	647	648	
649	650	651	652	653	654	655	656	657	658	659	660	661	662	663	664	655	656	657	658	659	
-	-	-	-	-	-	-	-	720	721	722	723	724	725	726	727	728	729	730	731	732	
733	734	735	736	737	738	739	740	741	742	743	744	745	746	747	748	749	750	751	752	753	
754	755	756	757	758	759	760	761	762	763	764	765	766	767	768	769	770	771	772	773	774	
775	776	777	778	779	780	781	782	783	784	785	786	787	788	789	790	791	792	793	794	795	
796	797	798	799																		

2.6 Trunking and Grade of Service

Cellular radio systems rely on *trunking* to accommodate a large number of users in a limited radio spectrum. The concept of trunking allows a large number of users to share the relatively small number of channels in a cell by providing access to each user, on demand, from a pool of available channels. In a trunked radio system, each user is allocated a channel on a per call basis, and upon termination of the call, the previously occupied channel is immediately returned to the pool of available channels.

Trunking exploits the statistical behavior of users so that a fixed number of channels or circuits may accommodate a large, random user community. The telephone company uses trunking theory to determine the number of telephone

circuits that need to be allocated for office buildings with hundreds of telephones, and this same principle is used in designing cellular radio systems. There is a trade-off between the number of available telephone circuits and the likelihood of a particular user finding that no circuits are available during the peak calling time. As the number of phone lines decreases, it becomes more likely that all circuits will be busy for a particular user. In a trunked mobile radio system, when a particular user requests service and all of the radio channels are already in use, the user is blocked, or denied access to the system. In some systems, a queue may be used to hold the requesting users until a channel becomes available.

To design trunked radio systems that can handle a specific capacity at a specific "grade of service", it is essential to understand trunking theory and queuing theory. The fundamentals of trunking theory were developed by Erlang, a Danish mathematician who, in the late 19th century, embarked on the study of how a large population could be accommodated by a limited number of servers [Bou88]. Today, the measure of traffic intensity bears his name. One Erlang represents the amount of traffic intensity carried by a channel that is completely occupied (i.e. 1 call-hour per hour or 1 call-minute per minute). For example, a radio channel that is occupied for thirty minutes during an hour carries 0.5 Erlangs of traffic.

The *grade of service (GOS)* is a measure of the ability of a user to access a trunked system during the busiest hour. The busy hour is based upon customer demand at the busiest hour during a week, month, or year. The busy hours for cellular radio systems typically occur during rush hours, between 4 p.m. and 6 p.m. on a Thursday or Friday evening. The grade of service is a benchmark used to define the desired performance of a particular trunked system by specifying a desired likelihood of a user obtaining channel access given a specific number of channels available in the system. It is the wireless designer's job to estimate the maximum required capacity and to allocate the proper number of channels in order to meet the *GOS*. *GOS* is typically given as the likelihood that a call is blocked, or the likelihood of a call experiencing a delay greater than a certain queuing time.

A number of definitions listed in Table 2.3 are used in trunking theory to make capacity estimates in trunked systems.

The traffic intensity offered by each user is equal to the call request rate multiplied by the holding time. That is, each user generates a traffic intensity of A_u Erlangs given by

$$A_u = \mu H \tag{2.13}$$

where H is the average duration of a call and μ is the average number of call requests per unit time. For a system containing U users and an unspecified number of channels, the total offered traffic intensity A, is given as

$$A = UA_u \tag{2.14}$$

Table 2.3 Definitions of Common Terms Used in Trunking Theory

Set-up Time: The time required to allocate a trunked radio channel to a requesting user.
Blocked Call: Call which cannot be completed at time of request, due to congestion. Also referred to as a *lost call*.
Holding Time: Average duration of a typical call. Denoted by H (in seconds).
Traffic Intensity: Measure of channel time utilization, which is the average channel occupancy measured in Erlangs. This is a dimensionless quantity and may be used to measure the time utilization of single or multiple channels. Denoted by A.
Load: Traffic intensity across the entire trunked radio system, measured in Erlangs.
Grade of Service (GOS): A measure of congestion which is specified as the probability of a call being blocked (for Erlang B), or the probability of a call being delayed beyond a certain amount of time (for Erlang C).
Request Rate: The average number of call requests per unit time. Denoted by μ seconds^{-1}.

Furthermore, in a C channel trunked system, if the traffic is equally distributed among the channels, then the traffic intensity per channel, A_c, is given as

$$A_c = UA_u/C \tag{2.15}$$

Note that the offered traffic is not necessarily the traffic which is *carried* by the trunked system, only that which is *offered* to the trunked system. When the offered traffic exceeds the maximum capacity of the system, the carried traffic becomes limited due to the limited capacity (i.e. limited number of channels). The maximum possible carried traffic is the total number of channels, C, in Erlangs. The AMPS cellular system is designed for a GOS of 2% blocking. This implies that the channel allocations for cell sites are designed so that 2 out of 100 calls will be blocked due to channel occupancy during the busiest hour.

There are two types of trunked systems which are commonly used. The first type offers no queuing for call requests. That is, for every user who requests service, it is assumed there is no setup time and the user is given immediate access to a channel if one is available. If no channels are available, the requesting user is blocked without access and is free to try again later. This type of trunking is called *blocked calls cleared* and assumes that calls arrive as determined by a Poisson distribution. Furthermore, it is assumed that there are an infinite number of users as well as the following: (a) there are memoryless arrivals of requests, implying that all users, including blocked users, may request a channel at any time; (b) the probability of a user occupying a channel is exponentially distributed, so that longer calls are less likely to occur as described by an exponential distribution; and (c) there are a finite number of channels available in the trunking pool. This is known as an M/M/m queue, and leads to the derivation of the Erlang B formula (also known as the *blocked calls cleared* formula). The Erlang B formula determines the probability that a call is blocked and is a measure of the GOS for a trunked system which provides no queuing for blocked calls. The Erlang B formula is derived in Appendix A and is given by

$$Pr[blocking] = \frac{\frac{A^C}{C!}}{\sum_{k=0}^{C}\frac{A^k}{k!}} = GOS \tag{2.16}$$

where C is the number of trunked channels offered by a trunked radio system and A is the total offered traffic. While it is possible to model trunked systems with finite users, the resulting expressions are much more complicated than the Erlang B result, and the added complexity is not warranted for typical trunked systems which have users that outnumber available channels by orders of magnitude. Furthermore, the Erlang B formula provides a conservative estimate of the GOS, as the finite user results always predict a smaller likelihood of blocking. The capacity of a trunked radio system where blocked calls are lost is tabulated for various values of GOS and numbers of channels in Table 2.4.

Table 2.4 Capacity of an Erlang B System

Number of Channels C	Capacity (Erlangs) for GOS = 0.01	= 0.005	= 0.002	= 0.001
2	0.153	0.105	0.065	0.046
4	0.869	0.701	0.535	0.439
5	1.36	1.13	0.900	0.762
10	4.46	3.96	3.43	3.09
20	12.0	11.1	10.1	9.41
24	15.3	14.2	13.0	12.2
40	29.0	27.3	25.7	24.5
70	56.1	53.7	51.0	49.2
100	84.1	80.9	77.4	75.2

The second kind of trunked system is one in which a queue is provided to hold calls which are blocked. If a channel is not available immediately, the call request may be delayed until a channel becomes available. This type of trunking is called *Blocked Calls Delayed*, and its measure of GOS is defined as the probability that a call is blocked after waiting a specific length of time in the queue. To find the GOS, it is first necessary to find the likelihood that a call is initially denied access to the system. The likelihood of a call not having immediate access to a channel is determined by the Erlang C formula derived in Appendix A

$$Pr[delay > 0] = \frac{A^C}{A^C + C!\left(1-\frac{A}{C}\right)\sum_{k=0}^{C-1}\frac{A^k}{k!}} \tag{2.17}$$

If no channels are immediately available the call is delayed, and the probability that the delayed call is forced to wait more than t seconds is given by the probability that a call is delayed, multiplied by the conditional probability that the delay is greater than t seconds. The GOS of a trunked system where blocked calls are delayed is hence given by

$$\begin{aligned} Pr[delay > t] &= Pr[delay > 0]\, Pr[delay > t | delay > 0] \\ &= Pr[delay > 0] \exp(-(C-A)t/H) \end{aligned} \tag{2.18}$$

The average delay D for all calls in a queued system is given by

$$D = Pr[delay > 0] \frac{H}{C-A} \tag{2.19}$$

where the average delay for those calls which are queued is given by $H/(C–A)$.

The Erlang B and Erlang C formulas are plotted in graphical form in Figure 2.6 and Figure 2.7. These graphs are useful for determining GOS in rapid fashion, although computer simulations are often used to determine transient behaviors experienced by particular users in a mobile system.

To use Figure 2.6 and Figure 2.7, locate the number of channels on the top portion of the graph. Locate the traffic intensity of the system on the bottom portion of the graph. The blocking probability $Pr[blocking]$ is shown on the abscissa of Figure 2.6, and $Pr[delay > 0]$ is shown on the abscissa of Figure 2.7. With two of the parameters specified it is easy to find the third parameter.

Example 2.4

How many users can be supported for 0.5% blocking probability for the following number of trunked channels in a blocked calls cleared system? (a) 1, (b) 5, (c) 10, (d) 20, (e) 100. Assume each user generates 0.1 Erlangs of traffic.

Solution to Example 2.4

From Table 2.4 we can find the total capacity in Erlangs for the 0.5% GOS for different numbers of channels. By using the relation $A = UA_u$, we can obtain the total number of users that can be supported in the system.

(a) Given $C = 1$, $A_u = 0.1$, $GOS = 0.005$
From Figure 2.6, we obtain $A = 0.005$.
Therefore, total number of users, $U = A/A_u = 0.005/0.1 = 0.05$ users.
But, actually one user could be supported on one channel. So, $U = 1$.

(b) Given $C = 5$, $A_u = 0.1$, $GOS = 0.005$
From Figure 2.6, we obtain $A = 1.13$.
Therefore, total number of users, $U = A/A_u = 1.13/0.1 \approx 11$ users.

(c) Given $C = 10$, $A_u = 0.1$, $GOS = 0.005$
From Figure 2.6, we obtain $A = 3.96$.
Therefore, total number of users, $U = A/A_u = 3.96/0.1 \approx 39$ users.

(d) Given $C = 20$, $A_u = 0.1$, $GOS = 0.005$
From Figure 2.6, we obtain $A = 11.10$.
Therefore, total number of users, $U = A/A_u = 11.1/0.1 = 110$ users.

(e) Given $C = 100$, $A_u = 0.1$, $GOS = 0.005$

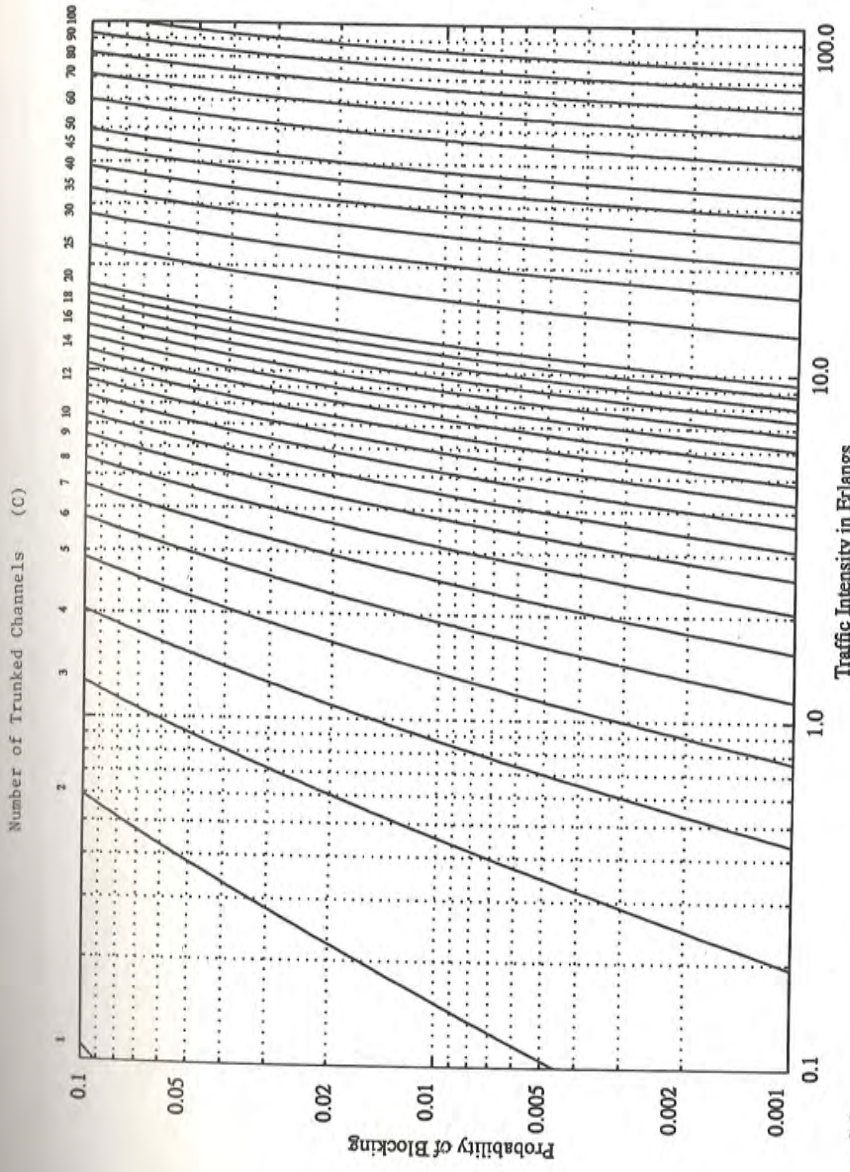

Figure 2.6
The Erlang B chart showing the probability of blocking as functions of the number of channels and traffic intensity in Erlangs.

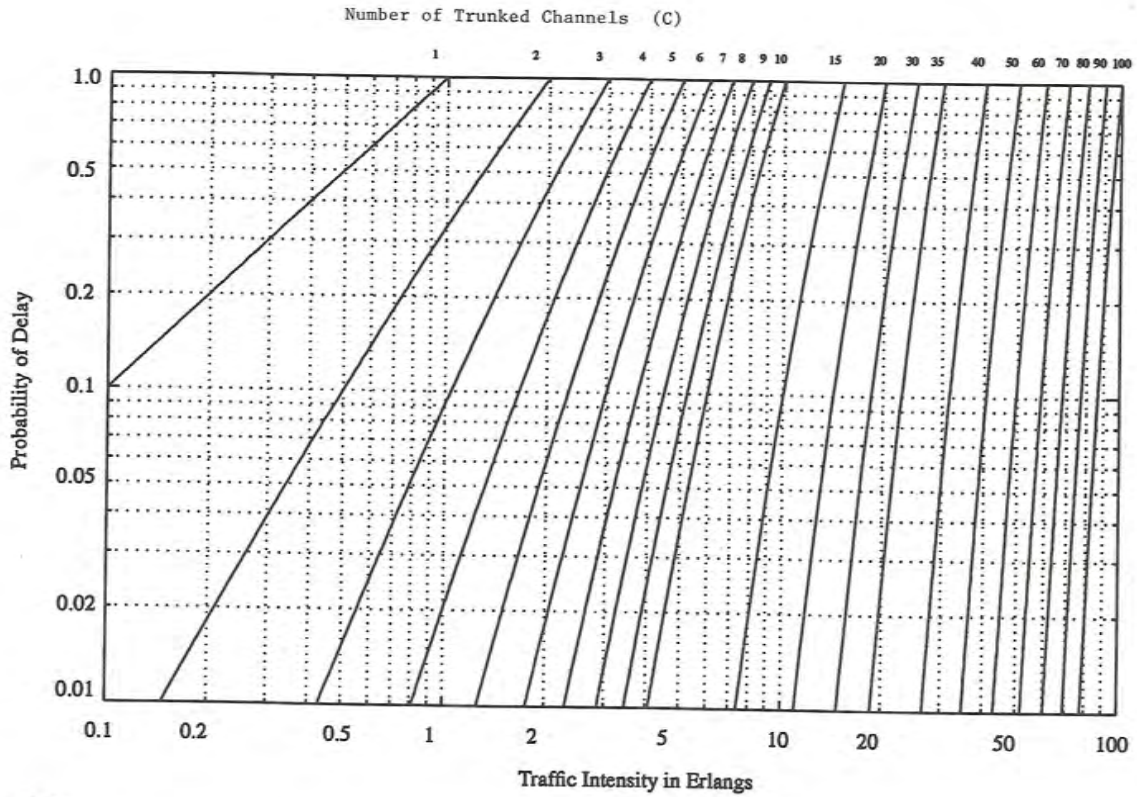

Figure 2.7
The Erlang C chart showing the probability of a call being delayed as a function of the number of channels and traffic intensity in Erlangs.

From Figure 2.6, we obtain $A = 80.9$.
Therefore, total number of users, $U = A/A_u = 80.9/0.1 = 809$ users.

Example 2.5

An urban area has a population of 2 million residents. Three competing trunked mobile networks (systems A, B, and C) provide cellular service in this area. System A has 394 cells with 19 channels each, system B has 98 cells with 57 channels each, and system C has 49 cells, each with 100 channels. Find the number of users that can be supported at 2% blocking if each user averages 2 calls per hour at an average call duration of 3 minutes. Assuming that all three trunked systems are operated at maximum capacity, compute the percentage market penetration of each cellular provider.

Solution to Example 2.5

System A
Given:
Probability of blocking = 2% = 0.02
Number of channels per cell used in the system, $C = 19$
Traffic intensity per user, $A_u = \mu H = 2 \times (3/60) = 0.1$ Erlangs

For $GOS = 0.02$ and $C = 19$, from the Erlang B chart, the total carried traffic, A, is obtained as 12 Erlangs.
Therefore, the number of users that can be supported per cell is
$U = A/A_u = 12/0.1 = 120$.
Since there are 394 cells, the total number of subscribers that can be supported by System A is equal to $120 \times 394 = 47280$.

System B
Given:
Probability of blocking = 2% = 0.02
Number of channels per cell used in the system, $C = 57$
Traffic intensity per user, $A_u = \mu H = 2 \times (3/60) = 0.1$ Erlangs

For $GOS = 0.02$ and $C = 57$, from the Erlang B chart, the total carried traffic, A, is obtained as 45 Erlangs.
Therefore, the number of users that can be supported per cell is
$U = A/A_u = 45/0.1 = 450$.
Since there are 98 cells, the total number of subscribers that can be supported by System B is equal to $450 \times 98 = 44100$.

System C
Given:
Probability of blocking = 2% = 0.02
Number of channels per cell used in the system, $C = 100$
Traffic intensity per user, $A_u = \mu H = 2 \times (3/60) = 0.1$ Erlangs

For $GOS = 0.02$ and $C = 100$, from the Erlang B chart, the total carried traffic, A, is obtained as 88 Erlangs.
Therefore, the number of users that can be supported per cell is

Figure 2.7
The Erlang C chart showing the probability of a call being delayed as a function of the number of channels and traffic intensity in Erlangs.

$U = A/A_u = 88/0.1 = 880$.

Since there are 49 cells, the total number of subscribers that can be supported by System C is equal to $880 \times 49 = 43120$

Therefore, total number of cellular subscribers that can be supported by these three systems are $47280 + 44100 + 43120 = 134500$ users.

Since there are 2 million residents in the given urban area and the total number of cellular subscribers in System A is equal to 47280 , the percentage market penetration is equal to

$47280/2000000 = 2.36\,\%$

Similarly, market penetration of System B is equal to

$44100/2000000 = 2.205\,\%$

and the market penetration of System C is equal to

$43120/2000000 = 2.156\,\%$

The market penetration of the three systems combined is equal to

$134500/2000000 = 6.725\,\%$

Example 2.6

A certain city has an area of 1,300 square miles and is covered by a cellular system using a 7-cell reuse pattern. Each cell has a radius of 4 miles and the city is allocated 40 MHz of spectrum with a full duplex channel bandwidth of 60 kHz. Assume a GOS of 2% for an Erlang B system is specified. If the offered traffic per user is 0.03 Erlangs, compute (a) the number of cells in the service area, (b) the number of channels per cell, (c) traffic intensity of each cell, (d) the maximum carried traffic, (e) the total number of users that can be served for 2% GOS, (f) the number of mobiles per channel, and (g) the theoretical maximum number of users that could be served at one time by the system.

Solution to Example 2.6

(a) Given:

Total coverage area = 1300 miles

Cell radius = 4 miles

The area of a cell (hexagon) can be shown to be $2.5981R^2$, thus each cell covers

$2.5981 \times (4)^2 = 41.57$ sq mi.

Hence, the total number of cells are $N_c = 1300/41.57 = 31$ cells.

(b) The total number of channels per cell (C)

= allocated spectrum / (channel width × frequency reuse factor)

$= 40,000,000/(60,000 \times 7) = 95$ channels/cell

(c) Given:

$C = 95$, and $GOS = 0.02$

From the Erlang B chart, we have

traffic intensity per cell $A = 84$ Erlangs/cell

(d) Maximum carried traffic = number of cells × traffic intensity per cell

$= 31 \times 84 = 2604$ Erlangs.

(e) Given traffic per user = 0.03 Erlangs

Total number of users = Total traffic / traffic per user

= 2604 / 0.03 = 86,800 users.

(f) Number of mobiles per channel = number of users/number of channels
= 86,800 / 666 = 130 mobiles/channel.

(g) The theoretical maximum number of served mobiles is the number of available channels in the system (all channels occupied)
$= C \times N_C = 95 \times 31 = 2945$ users, which is 3.4% of the customer base.

Example 2.7

A hexagonal cell within a 4-cell system has a radius of 1.387 km. A total of 60 channels are used within the entire system. If the load per user is 0.029 Erlangs, and $\mu = 1$ call/hour, compute the following for an Erlang C system with a GOS of 5%:

(a) How many users per square kilometer will this system support?

(a) What is the probability that a delayed call will have to wait for more than 10 s?

(c) What is the probability that a call will be delayed for more than 10 seconds?

Solution to Example 2.7

Given,

Cell radius, $R = 1.387$ km

Area covered per cell is $2.598 \times (1.387)^2 = 5$ sq km

Number of cells per cluster = 4

Total number of channels = 60

Therefore, number of channels per cell = 60 / 4 = 15 channels.

(a) From Erlang C chart, for 5% probability of delay with $C = 15$, traffic intensity = 8.8 Erlangs.

Therefore, number of users = total traffic intensity / traffic per user
= 8.8/0.029 = 303 users
= 303 users/5 sq km = 60 users/sq km

(b) Given $\mu = 1$, holding time
$H = A_u/\mu = 0.029$ hour = 104.4 seconds.

The probability that a delayed call will have to wait for more than 10 s is

$$Pr[delay > t|delay] = \exp(-(C-A)\,t/H)$$
$$= \exp(-(15-8.8)\,10/104.4) = 52.22\,\%$$

(c) Given GOS = 5% = 0.05

Probability that a call is delayed more than 10 seconds,

$$Pr[delay > 10] = Pr[delay > 0]\,Pr[delay > t|delay]$$
$$= 0.05 \times 0.5522 = 2.76\,\%$$

Trunking efficiency is a measure of the number of users which can be offered a particular GOS with a particular configuration of fixed channels. The way in which channels are grouped can substantially alter the number of users handled by a trunked system. For example, from Table 2.4, 10 trunked channels at a GOS of 0.01 can support 4.46 Erlangs of traffic, whereas 2 groups of 5 trunked channels can support 2×1.36 Erlangs, or 2.72 Erlangs of traffic.

Clearly, 10 channels trunked together support 60% more traffic at a specific GOS than do two 5 channel trunks! It should be clear that the allocation of channels in a trunked radio system has a major impact on overall system capacity.

2.7 Improving Capacity in Cellular Systems

As the demand for wireless service increases, the number of channels assigned to a cell eventually becomes insufficient to support the required number of users. At this point, cellular design techniques are needed to provide more channels per unit coverage area. Techniques such as *cell splitting*, *sectoring*, and *coverage zone approaches* are used in practice to expand the capacity of cellular systems. Cell splitting allows an orderly growth of the cellular system. Sectoring uses directional antennas to further control the interference and frequency reuse of channels. The *zone microcell* concept distributes the coverage of a cell and extends the cell boundary to hard-to-reach places. While cell splitting increases the number of base stations in order to increase capacity, sectoring and zone microcells rely on base station antenna placements to improve capacity by reducing co-channel interference. Cell splitting and zone microcell techniques do not suffer the trunking inefficiencies experienced by sectored cells, and enable the base station to oversee all handoff chores related to the microcells, thus reducing the computational load at the MSC. These three popular capacity improvement techniques will be explained in detail.

2.7.1 Cell Splitting

Cell splitting is the process of subdividing a congested cell into smaller cells, each with its own base station and a corresponding reduction in antenna height and transmitter power. Cell splitting increases the capacity of a cellular system since it increases the number of times that channels are reused. By defining new cells which have a smaller radius than the original cells and by installing these smaller cells (called *microcells*) between the existing cells, capacity increases due to the additional number of channels per unit area.

Imagine if every cell in Figure 2.1 were reduced in such a way that the radius of every cell was cut in half. In order to cover the entire service area with smaller cells, approximately four times as many cells would be required. This can be easily shown by considering a circle with radius R. The area covered by such a circle is four times as large as the area covered by a circle with radius $R/2$. The increased number of cells would increase the number of clusters over the coverage region, which in turn would increase the number of channels, and thus capacity, in the coverage area. Cell splitting allows a system to grow by replacing large cells with smaller cells, while not upsetting the channel allocation scheme required to maintain the minimum co-channel reuse ratio Q (see equation (2.4)) between co-channel cells.

An example of cell splitting is shown in Figure 2.8. In Figure 2.8, the base stations are placed at corners of the cells, and the area served by base station A is assumed to be saturated with traffic (i.e., the blocking of base station A exceeds acceptable rates). New base stations are therefore needed in the region to increase the number of channels in the area and to reduce the area served by the single base station. Note in the figure that the original base station A has been surrounded by three new microcell base stations. In the example shown in Figure 2.8, the three smaller cells were added in such a way as to preserve the frequency reuse plan of the system. For example, the microcell base station labeled G was placed half way between two larger stations utilizing the same channel set G. This is also the case for the other microcells in the figure. As can be seen from Figure 2.8, cell splitting merely scales the geometry of the cluster. In this case, the radius of each new microcell is half that of the original cell.

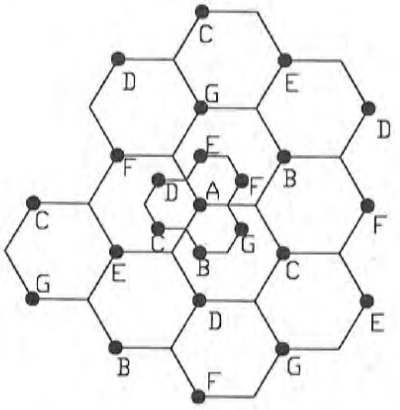

Figure 2.8
Illustration of cell splitting.

For the new cells to be smaller in size, the transmit power of these cells must be reduced. The transmit power of the new cells with radius half that of the original cells can be found by examining the received power P_r at the new and old cell boundaries and setting them equal to each other. This is necessary to ensure that the frequency reuse plan for the new microcells behaves exactly as for the original cells. For Figure 2.8

$$P_r\,[\text{at old cell boundary}] \propto P_{t1} R^{-n} \tag{2.20}$$

and

$$P_r\,[\text{at new cell boundary}] \propto P_{t2}\,(R/2)^{-n} \tag{2.21}$$

where P_{t1} an P_{t2} are the transmit powers of the larger and smaller cell base stations, respectively, and n is the path loss exponent. If we take $n = 4$ and set the received powers equal to each other, then

$$P_{t2} = \frac{P_{t1}}{16} \tag{2.22}$$

In other words, the transmit power must be reduced by 12 dB in order to fill in the original coverage area with microcells, while maintaining the S/I requirement.

In practice, not all cells are split at the same time. It is often difficult for service providers to find real estate that is perfectly situated for cell splitting. Therefore, different cell sizes will exist simultaneously. In such situations, special care needs to be taken to keep the distance between co-channel cells at the required minimum, and hence channel assignments become more complicated. Also, handoff issues must be addressed so that high speed and low speed traffic can be simultaneously accommodated (the umbrella cell approach of Section 2.4 is commonly used). When there are two cell sizes in the same region as shown in Figure 2.8, equation (2.22) shows that one can not simply use the original transmit power for all new cells or the new transmit power for all the original cells. If the larger transmit power is used for all cells, some channels used by the smaller cells would not be sufficiently separated from co-channel cells. On the other hand, if the smaller transmit power is used for all the cells, there would be parts of the larger cells left unserved. For this reason, channels in the old cell must be broken down into two channel groups, one that corresponds to the smaller cell reuse requirements and the other that corresponds to the larger cell reuse requirements. The larger cell is usually dedicated to high speed traffic so that handoffs occur less frequently.

The two channel group sizes depend on the stage of the splitting process. At the beginning of the cell splitting process there will be fewer channels in the small power groups. However, as demand grows, more channels will be required, and thus the smaller groups will require more channels. This splitting process continues until all the channels in an area are used in the lower power group, at which point cell splitting is complete within the region, and the entire system is rescaled to have a smaller radius per cell. *Antenna downtilting*, which deliberately focuses radiated energy from the base station towards the ground (rather than towards the horizon), is often used to limit the radio coverage of newly formed microcells.

Example 2.8

Consider Figure 2.9. Assume each base station uses 60 channels, regardless of cell size. If each original cell has a radius of 1 km and each microcell has a radius of 0.5 km. find the number of channels contained in a 3 km by 3 km

square centered around A, (a) without the use of microcells, (b) with the use of microcells as shown in Figure 2.9, and (c) if all the original base stations are replaced by microcells. Assume cells on the edge of the square to be contained within the square.

Solution to Example 2.8

(a) without the use of microcells:

A cell radius of 1 km implies that the sides of the larger hexagons are also 1 km in length. To cover the 3 km by 3 km square centered around base station A, we need to cover 1.5 km (1.5 times the hexagon radius) towards the right, left, top, and bottom of base station A. This is shown in Figure 2.9. From Figure 2.9 we see that this area contains 5 base stations. Since each base station has 60 channels, the total number of channels without cell splitting is equal to $5 \times 60 = 300$ channels.

(b) with the use of the microcells as shown in Figure 2.9:

In Figure 2.9, the base station A is surrounded by 6 microcells. Therefore, the total number of base stations in the square area under study is equal to $5 + 6 = 11$. Since each base station has 60 channels, the total number of channels will be equal to $11 \times 60 = 660$ channels. This is a 2.2 times increase in capacity when compared to case (a).

(c) if all the base stations are replaced by microcells:

From Figure 2.9, we see that there are a total of $5 + 12 = 17$ base stations in the square region under study. Since each base station has 60 channels, the total number of channels will be equal to $17 \times 60 = 1020$ channels. This is a 3.4 times increase in capacity when compared to case (a).

Theoretically, if all cells were microcells having half the radius of the original cell, the capacity increase would approach 4.

2.7.2 Sectoring

As shown in section 2.7.1, cell splitting achieves capacity improvement by essentially rescaling the system. By decreasing the cell radius R and keeping the co-channel reuse ratio D/R unchanged, cell splitting increases the number of channels per unit area. However, another way to increase capacity is to keep the cell radius unchanged and seek methods to decrease the D/R ratio. In this approach, capacity improvement is achieved by reducing the number of cells in a cluster and thus increasing the frequency reuse. However, in order to do this, it is necessary to reduce the relative interference without decreasing the transmit power.

The co-channel interference in a cellular system may be decreased by replacing a single omni-directional antenna at the base station by several directional antennas, each radiating within a specified sector. By using directional antennas, a given cell will receive interference and transmit with only a fraction

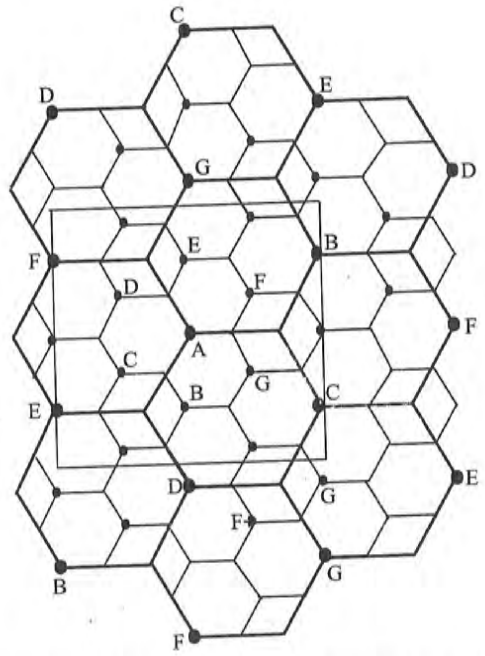

Figure 2.9
Illustration of cell splitting within a 3 km by 3 km square centered around base station A.

of the available co-channel cells. The technique for decreasing co-channel interference and thus increasing system capacity by using directional antennas is called *sectoring*. The factor by which the co-channel interference is reduced depends on the amount of sectoring used. A cell is normally partitioned into three 120° sectors or six 60° sectors as shown in Figure 2.10(a) and (b).

When sectoring is employed, the channels used in a particular cell are broken down into sectored groups and are used only within a particular sector, as illustrated in Figure 2.10(a) and (b). Assuming 7-cell reuse, for the case of 120° sectors, the number of interferers in the first tier is reduced from 6 to 2. This is because only 2 of the 6 co-channel cells receive interference with a particular sectored channel group. Referring to Figure 2.11, consider the interference experienced by a mobile located in the right-most sector in the center cell labeled "5". There are 3 co-channel cell sectors labeled "5" to the right of the center cell, and 3 to the left of the center cell. Out of these 6 co-channel cells, only 2 cells have sectors with antenna patterns which radiate into the center cell, and hence a mobile in the center cell will experience interference on the forward link from only these two sectors. The resulting S/I for this case can be found using equa-

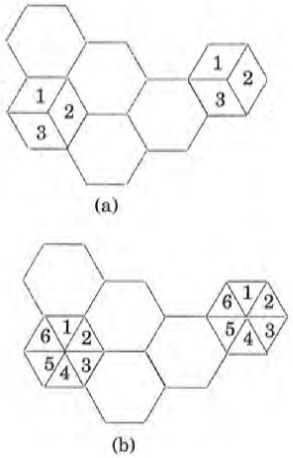

Figure 2.10
(a) 120° sectoring.
(b) 60° sectoring.

tion (2.8) to be 24.2 dB, which is a significant improvement over the omni-directional case in Section 2.5, where the worst case S/I was shown to be 17 dB. In practical systems, further improvement in S/I is achieved by downtilting the sector antennas such that the radiation pattern in the vertical (elevation) plane has a notch at the nearest co-channel cell distance.

The improvement in S/I implies that with 120° sectoring, the minimum required S/I of 18 dB can be easily achieved with 7-cell reuse, as compared to 12-cell reuse for the worst possible situation in the unsectored case (see Section 2.5.1). Thus, sectoring reduces interference, which amounts to an increase in capacity by a factor of 12/7, or 1.714. In practice, the reduction in interference offered by sectoring enable planners to reduce the cluster size N, and provides an additional degree of freedom in assigning channels. The penalty for improved S/I and the resulting capacity improvement is an increased number of antennas at each base station, and a decrease in trunking efficiency due to channel sectoring at the base station. Since sectoring reduces the coverage area of a particular group of channels, the number of handoffs increases, as well. Fortunately, many modern base stations support sectorization and allow mobiles to be handed off from sector to sector within the same cell without intervention from the MSC, so the handoff problem is often not a major concern.

It is the loss of traffic due to decreased trunking efficiency that causes some operators to shy away from the sectoring approach, particularly in dense urban areas where the directional antenna patterns are somewhat ineffective in controlling radio propagation. Because sectoring uses more than one antenna per base station, the available channels in the cell must be subdivided and dedicated

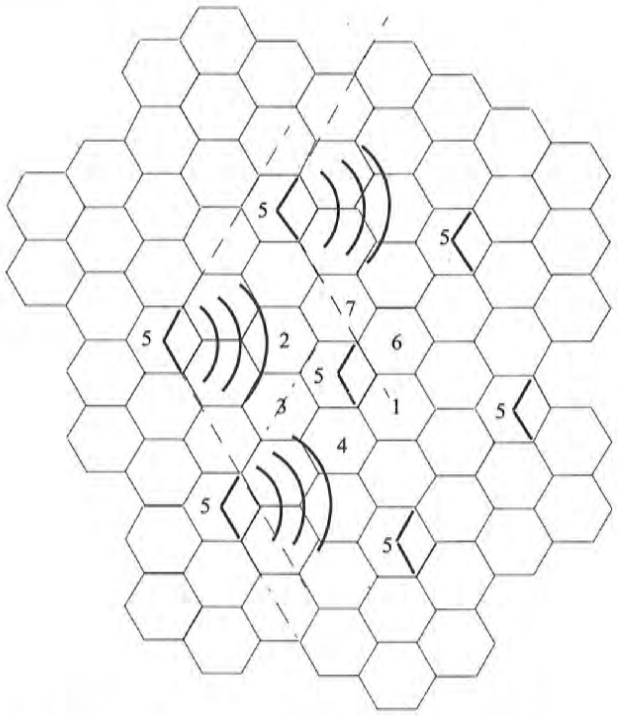

Figure 2.11
Illustration of how 120° sectoring reduces interference from co-channel cells. Out of the 6 co-channel cells in the first tier, only 2 of them interfere with the center cell. If omni-directional antennas were used at each base station, all 6 co-channel cells would interfere with the center cell.

to a specific antenna. This breaks up the available trunked channel pool into several smaller pools, and decreases trunking efficiency.

Example 2.9

Consider a cellular system in which an average call lasts 2 minutes, and the probability of blocking is to be no more than 1%. Assume that every subscriber makes 1 call per hour, on average. If there are a total of 395 traffic channels for a 7-cell reuse system, there will be about 57 traffic channels per cell. Assume that blocked calls are cleared so the blocking is described by the Erlang B distribution. From the Erlang B distribution, it can be found that the unsectored system may handle 44.2 Erlangs or 1326 calls per hour.

Now employing 120° sectoring, there are only 19 channels per antenna sector (57/3 antennas). For the same probability of blocking and average call length, it can be found from the Erlang B distribution that each sector can handle 11.2

Erlangs or 336 calls per hour. Since each cell consists of 3 sectors, this provides a cell capacity of $3 \times 336 = 1008$ calls per hour, which amounts to a 24% decrease when compared to the unsectored case. Thus, sectoring decreases the trunking efficiency while improving the S/I for each user in the system.

It can be found that using 60° sectors improves the S/I even more. In this case the number of first tier interferers is reduced from 6 to only 1. This results in $S/I = 29$ dB for a 7-cell system and enables 4-cell reuse. Of course, using 6 sectors per cell reduces the trunking efficiency and increases the number of necessary handoffs even more. If the unsectored system is compared to the 6 sector case, the degradation in trunking efficiency can be shown to be 44%. (The proof of this is left as an exercise).

2.7.3 A Novel Microcell Zone Concept

The increased number of handoffs required when sectoring is employed results in an increased load on the switching and control link elements of the mobile system. A solution to this problem was presented by Lee [Lee91b]. This proposal is based on a microcell concept for 7 cell reuse, as illustrated in Figure 2.12. In this scheme, each of the three (or possibly more) zone sites (represented as Tx/Rx in Figure 2.12) are connected to a single base station and share the same radio equipment. The zones are connected by coaxial cable, fiberoptic cable, or microwave link to base station multiple zones and single base station make up a cell. As a mobile travels within the cell, it is served by the zone with the strongest signal. This approach is superior to sectoring since antennas are placed at the outer edges of the cell, and any channel may be assigned to any zone by the base station.

As a mobile travels from one zone to another within the cell, it retains the same channel. Thus, unlike in sectoring, a handoff is not required at the MSC when the mobile travels between zones within the cell. The base station simply switches the channel to a different zone site. In this way, a given channel is active only in the particular zone in which the mobile is traveling, and hence the base station radiation is localized and interference is reduced. The channels are distributed in time and space by all three zones and are also reused in co-channel cells in the normal fashion. This technique is particularly useful along highways or along urban traffic corridors.

The advantage of the zone cell technique is that while the cell maintains a particular coverage radius, the co-channel interference in the cellular system is reduced since a large central base station is replaced by several lower powered transmitters (zone transmitters) on the edges of the cell. Decreased co-channel interference improves the signal quality and also leads to an increase in capacity, without the degradation in trunking efficiency caused by sectoring. As mentioned earlier, an S/I of 18 dB is typically required for satisfactory system performance in narrowband FM. For a system with $N = 7$, a D/R of 4.6 was

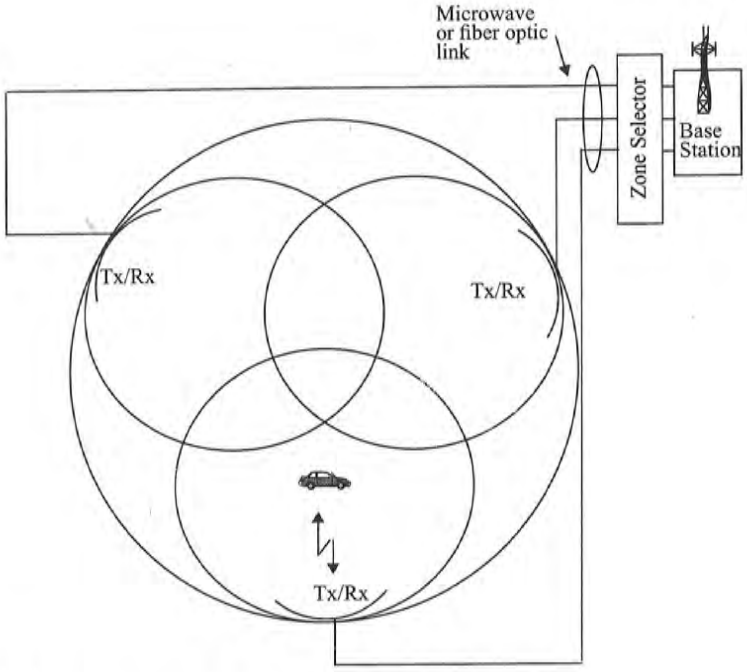

Figure 2.12
The microcell concept [adapted from [Lee91b] © IEEE].

shown to achieve this. With respect to the zone microcell system, since transmission at any instant is confined to a particular zone, this implies that a D_z/R_z of 4.6 (where D_z is the minimum distance between active co-channel zones and R_z is the zone radius) can achieve the required link performance. In Figure 2.13, let each individual hexagon represents a zone, while each group of three hexagons represents a cell. The zone radius R_z is approximately equal to one hexagon radius. Now, the capacity of the zone microcell system is directly related to the distance between co-channel cells, and not zones. This distance is represented as D in Figure 2.13. For a D_z/R_z value of 4.6, it can be seen from the geometry of Figure 2.13 that the value of co-channel reuse ratio, D/R, is equal to 3, where R is the radius of the cell and is equal to twice the length of the hexagon radius. Using equation (2.4), $D/R = 3$ corresponds to a cluster size of $N = 3$. This reduction in the cluster size from $N = 7$ to $N = 3$ amounts to a 2.33 times increase in capacity for a system completely based on the zone microcell concept. Hence for the same S/I requirement of 18 dB, this system provides a significant increase in capacity over conventional cellular planning.

By examining Figure 2.
case S/I of the zone microce
worst case, the system provi
interference ratio while incre
7-cell system using omni-dire
experienced. Zone cell archite
sonal communication systems

2.8 Summary

In this chapter, the fu
trunking efficiency, and frequ
required to pass mobile traffic
offs are implemented. The ca
variables. The S/I limits the
the number of channels within
the number of users that can a
by the number of available ch
cellular system. Trunking effic
ting, sectoring, and the zone m
ity by increasing S/I in some
methods is to increase the nun
gation characteristics influenc
actual system. Radio propagati

2.9 Problems

2.1 Prove that for a hexag
$Q = \sqrt{3N}$.

2.2 Show that the frequenc
where k is the average
of channels available to

2.3 A cellular service provi
tolerate a signal-to-inter
mal value of N for (a)
60° sectoring. Should se
be used? (Assume a pat
ciency).

2.4 If an intensive propagat
radio channel provided a
how would your design in

2.5 For a $N = 7$ system with
2 minutes, find the loss
tional antennas to 60°
cleared and the average

2.6 Assume that a cell name
Watt and a cell radius of

By examining Figure 2.13 and using equation (2.8) [Lee91b] the exact worst case S/I of the zone microcell system can be estimated to be 20 dB. Thus, in the worst case, the system provides a margin of 2 dB over the required signal-to-interference ratio while increasing the capacity by 2.33 times over a conventional 7-cell system using omni-directional antennas. No loss in trunking efficiency is experienced. Zone cell architectures are being adopted in many cellular and personal communication systems.

2.8 Summary

In this chapter, the fundamental concepts of handoff, frequency reuse, trunking efficiency, and frequency planning have been presented. Handoffs are required to pass mobile traffic from cell to cell, and there are various ways handoffs are implemented. The capacity of a cellular system is a function of many variables. The S/I limits the frequency reuse factor of a system, which limits the number of channels within the coverage area. The trunking efficiency limits the number of users that can access a trunked radio system. Trunking is affected by the number of available channels and how they are partitioned in a trunked cellular system. Trunking efficiency is quantified by the GOS. Finally, cell splitting, sectoring, and the zone microcell technique are all shown to improve capacity by increasing S/I in some fashion. The overriding objective in all of these methods is to increase the number of users within the system. The radio propagation characteristics influence the effectiveness of all of these methods in an actual system. Radio propagation is the subject of the following two chapters.

2.9 Problems

2.1 Prove that for a hexagonal geometry, the co-channel reuse ratio is given by $Q = \sqrt{3N}$.

2.2 Show that the frequency reuse factor for a cellular system is given by k/S, where k is the average number of channels per cell and S is the total number of channels available to the cellular service provider.

2.3 A cellular service provider decides to use a digital TDMA scheme which can tolerate a signal-to-interference ratio of 15 dB in the worst case. Find the optimal value of N for (a) omni-directional antennas, (b) 120° sectoring, and (c) 60° sectoring. Should sectoring be used? If so, which case (60° or 120°) should be used? (Assume a path loss exponent of $n = 4$ and consider trunking efficiency).

2.4 If an intensive propagation measurement campaign showed that the mobile radio channel provided a propagation path loss exponent of $n = 3$ instead of 4, how would your design in Problem 2.3 change?

2.5 For a $N = 7$ system with a $Pr[Blocking] = 1\%$ and an average call length of 2 minutes, find the loss in trunking efficiency when going from omni-directional antennas to 60° sectored antennas. (Assume that blocked calls are cleared and the average number of calls made by each user is 1 per hour).

2.6 Assume that a cell named "Radio Knob" has an effective radiated power of 32 Watt and a cell radius of 10 km. The grade of service is established to be a

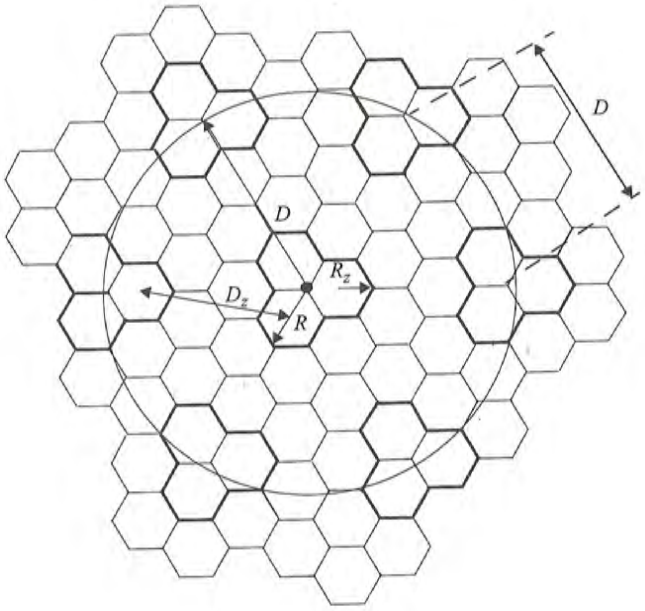

Figure 2.13
Defining D, D_z, R, R_z for a microcell architecture with N = 7. The smaller hexagons form zones and three hexagons (outlined in bold) together form a cell. Six nearest co-channel cells are shown.

probability of blocking of 5% (assuming blocked calls are cleared). Assume the average call length is 2 minutes, and each user averages 2 calls per hour. Further, assume the cell has just reached its maximum capacity and must be split into 4 cells using the techniques described in this chapter: (a) What is the current capacity of the "Radio Knob" cell? (b) What is the radius and transmit power of the new cells? (c) How many channels are needed in the new cells to maintain frequency reuse stability in the system? (d) If traffic is uniformly distributed, what is the new traffic carried by each new cell? Will the probability of blocking in these new cells be below 0.1% after the split?

2.7 Exercises in trunking (queueing) theory:

(a) What is the maximum system capacity (*total* and *per channel*) in Erlangs when providing a 2% blocking probability with 4 channels, with 20 channels, with 40 channels?

(b) How many users can be supported with 40 channels at 2% blocking? Assume H = 105 s, μ = 1 call/hour.

(c) Using the traffic intensity per channel calculated in part (a), find the grade of service in a lost call delayed system for the case of delays being greater than 20 seconds. Assume that H = 105 s, and determine the GOS for 4 channels, for 20 channels, for 40 channels.

(d) Comparing part (a) and part (c), does a lost call delayed system with a 20

second queue perform better than a system that drops blocked calls?

2.8 A receiver in an urban cellular radio system detects a 1 mW signal at $d = d_0 = 1$ meter from the transmitter. In order to mitigate co-channel interference effects, it is required that the signal received at any base station receiver from another base station transmitter which operates with the same channel must be below -100 dBm. A measurement team has determined that the average path loss exponent in the system is $n = 3$. Determine the major radius of each cell if a 7-cell reuse pattern is used. What is the major radius if a 4-cell reuse pattern is used?

2.9 A cellular system using a cluster size of 7 is described in Problem 2.8. It is operated with 660 channels, 30 of which are designated as setup (control) channels so that there are about 90 voice channels available per cell. If there is a potential user density of 9000 users/km^2 in the system, and each user makes an average of one call per hour and each call lasts 1 minute during peak hours, determine the probability that a user will experience a delay greater than 20 seconds if all calls are queued.

2.10 Show that if $n = 4$, a cell can be split into four smaller cells, each with half the radius and 1/16 of the transmitter power of the original cell. If extensive measurements show that the path loss exponent is 3, how should the transmitter power be changed in order to split a cell into four smaller cells? What impact will this have on the cellular geometry? Explain your answer and provide drawings that show how the new cells would fit within the original macrocells. For simplicity use omni-directional antennas.

2.11 Using the frequency assignment chart in Table 2.2, design a channelization scheme for a B-side carrier that uses 4-cell reuse and 3 sectors per cell. Include an allocation scheme for the 21 control channels.

2.12 Repeat Problem 2.11 for the case of 4-cell reuse and 6 sectors per cell.

2.13 In practical cellular radio systems, the MSC is programmed to allocate radio channels differently for the closest co-channel cells. This technique, called a *hunting sequence,* ensures that co-channel cells first use different channels from within the co-channel set, before the same channels are assigned to calls in nearby cells. This minimizes co-channel interference when the cellular system is not fully loaded. Consider 3 adjoining clusters, and design an algorithm that may be used by the MSC to hunt for appropriate channels when requested from co-channel cells. Assume a 7-cell reuse pattern with 3 sectors per cell, and use the U.S. cellular channel allocation scheme for the A-side carrier.

2.14 Determine the noise floor (in dBm) for mobile receivers which implement the following standards: (a) AMPS, (b) GSM, (c) USDC, (d) DECT, (e) IS-95, and (f) CT2. Assume all receivers have a noise figure of 10 dB.

2.15 If a base station provides a signal level of -90 dBm at the cell fringe, find the SNR for each of the mobile receivers described in Problem 2.14.

2.16 From first principles, derive the expression for Erlang B given in this chapter.

2.17 Carefully analyze the trade-off between sectoring and trunking efficiency for a 4-cell cluster size. While sectoring improves capacity by improving SNR, there is a loss due to decreased trunking efficiency, since each sector must be trunked separately. Consider a wide range of total available channels per cell and consider the impact of using 3 sectors and 6 sectors per cell. Your analysis may involve computer simulation, and should indicate the "break even" point when sectoring is not practical.

2.18 Assume each user of a single base station mobile radio system averages three

calls per hour, each call lasting an average of 5 minutes.

(a) What is the traffic intensity for each user?
(b) Find the number of users that could use the system with 1% blocking if only one channel is available.
(c) Find the number of users that could use the system with 1% blocking if five trunked channels are available.
(d) If the number of users you found in (c) is suddenly doubled, what is the new blocking probability of the five channel trunked mobile radio system? Would this be acceptable performance? Justify why or why not.

2.19 The U.S. AMPS system is allocated 50 MHz of spectrum in the 800 MHz range, and provides 832 channels. Forty-two of those channels are control channels. The forward channel frequency is exactly 45 MHz greater than the reverse channel frequency.

(a) Is the AMPS system simplex, half-duplex, or duplex? What is the bandwidth for each channel and how is it distributed between the base station and the subscriber?
(b) Assume a base station transmits control information on channel 352, operating at 880.560 MHz. What is the transmission frequency of a subscriber unit transmitting on channel 352?
(c) The A-side and B-side cellular carriers evenly split the AMPS channels. Find the number of voice channels and number of control channels for each carrier.
(d) Let's suppose you are chief engineer of a cellular carrier using 7-cell reuse. Propose a channel assignment strategy for a uniform distribution of users throughout your cellular system. Specifically, assume that each cell has 3 control channels (120° sectoring is employed) and specify the number of voice channels you would assign to each control channel in your system.
(e) For an ideal hexagonal cellular layout which has identical cell sites, what is the distance between the centers of two nearest co-channel cells for 7-cell reuse? for 4-cell reuse?

2.20 Pretend your company won a license to build a U.S. cellular system (the application cost for the license was only $500!). Your license is to cover 140 square km. Assume a base station costs $500,000 and a MTSO costs $1,500,000. An extra $500,000 is needed to advertise and start the business. You have convinced the bank to loan you $6 million, with the idea that in four years you will have earned $10 million in gross billing revenues, and will have paid off the loan.

(a) How many base stations (i.e. cell sites) will you be able to install for $6 million?
(b) Assuming the earth is flat and subscribers are uniformly distributed on the ground, what assumption can you make about the coverage area of each of your cell sites? What is the major radius of each of your cells, assuming a hexagonal mosaic?
(c) Assume that the average customer will pay $50 per month over a 4 year period. Assume that on the first day you turn your system on, you have a certain number of customers which remains fixed throughout the year. On the first day of each new year the number of customers using your system doubles and then remains fixed for the rest of that year. What is the minimum number of customers you must have on the first day of service in

order to have earned $10 million in gross billing revenues by the end of the 4th year of operation?

(d) For your answer in (c), how many users per square km are needed on the first day of service in order to reach the $10 million mark after the 4th year?

Problems

ver where,

ions).

CHAPTER 4

Mobile Radio Propagation: Small-Scale Fading and Multipath

Small-scale fading, or simply *fading*, is used to describe the rapid fluctuation of the amplitude of a radio signal over a short period of time or travel distance, so that large-scale path loss effects may be ignored. Fading is caused by interference between two or more versions of the transmitted signal which arrive at the receiver at slightly different times. These waves, called *multipath waves*, combine at the receiver antenna to give a resultant signal which can vary widely in amplitude and phase, depending on the distribution of the intensity and relative propagation time of the waves and the bandwidth of the transmitted signal.

4.1 Small-Scale Multipath Propagation

Multipath in the radio channel creates small-scale fading effects. The three most important effects are:

- Rapid changes in signal strength over a small travel distance or time interval
- Random frequency modulation due to varying Doppler shifts on different multipath signals
- Time dispersion (echoes) caused by multipath propagation delays.

In built-up urban areas, fading occurs because the height of the mobile antennas are well below the height of surrounding structures, so there is no single line-of-sight path to the base station. Even when a line-of-sight exists, multipath still occurs due to reflections from the ground and surrounding structures. The incoming radio waves arrive from different directions with different propagation delays. The signal received by the mobile at any point in space may consist of a large number of plane waves having randomly distributed amplitudes,

phases, and angles of arrival. These multipath components, combine vectorially at the receiver antenna, and can cause the signal received by the mobile to distort or fade. Even when a mobile receiver is stationary, the received signal may fade due to movement of surrounding objects in the radio channel.

If objects in the radio channel are static, and motion is considered to be only due to that of the mobile, then fading is purely a spatial phenomenon. The spatial variations of the resulting signal are seen as temporal variations by the receiver as it moves through the multipath field. Due to the constructive and destructive effects of multipath waves summing at various points in space, a receiver moving at high speed can pass through several fades in a small period of time. In a more serious case, a receiver may stop at a particular location at which the received signal is in a deep fade. Maintaining good communications can then become very difficult, although passing vehicles or people walking in the vicinity of the mobile can often disturb the field pattern, thereby diminishing the likelihood of the received signal remaining in a deep null for a long period of time. Antenna space diversity can prevent deep fading nulls, as shown in Chapter 6. Figure 3.1 shows typical rapid variations in the received signal level due to small-scale fading as a receiver is moved over a distance of a few meters.

Due to the relative motion between the mobile and the base station, each multipath wave experiences an apparent shift in frequency. The shift in received signal frequency due to motion is called the Doppler shift, and is directly proportional to the velocity and direction of motion of the mobile with respect to the direction of arrival of the received multipath wave.

4.1.1 Factors Influencing Small-Scale Fading

Many physical factors in the radio propagation channel influence small-scale fading. These include the following:

- **Multipath propagation** — The presence of reflecting objects and scatterers in the channel creates a constantly changing environment that dissipates the signal energy in amplitude, phase, and time. These effects result in multiple versions of the transmitted signal that arrive at the receiving antenna, displaced with respect to one another in time and spatial orientation. The random phase and amplitudes of the different multipath components cause fluctuations in signal strength, thereby inducing small-scale fading, signal distortion, or both. Multipath propagation often lengthens the time required for the baseband portion of the signal to reach the receiver which can cause signal smearing due to intersymbol interference.
- **Speed of the mobile** — The relative motion between the base station and the mobile results in random frequency modulation due to different Doppler shifts on each of the multipath components. Doppler shift will be positive or negative depending on whether the mobile receiver is moving toward or away from the base station.

- **Speed of surrounding objects** — If objects in the radio channel are in motion, they induce a time varying Doppler shift on multipath components. If the surrounding objects move at a greater rate than the mobile, then this effect dominates the small-scale fading. Otherwise, motion of surrounding objects may be ignored, and only the speed of the mobile need be considered.
- **The transmission bandwidth of the signal** — If the transmitted radio signal bandwidth is greater than the "bandwidth" of the multipath channel, the received signal will be distorted, but the received signal strength will not fade much over a local area (i.e., the small-scale signal fading will not be significant). As will be shown, the bandwidth of the channel can be quantified by the *coherence bandwidth* which is related to the specific multipath structure of the channel. The coherence bandwidth is a measure of the maximum frequency difference for which signals are still strongly correlated in amplitude. If the transmitted signal has a narrow bandwidth as compared to the channel, the amplitude of the signal will change rapidly, but the signal will not be distorted in time. Thus, the statistics of small-scale signal strength and the likelihood of signal smearing appearing over small-scale distances are very much related to the specific amplitudes and delays of the multipath channel, as well as the bandwidth of the transmitted signal.

4.1.2 Doppler Shift

Consider a mobile moving at a constant velocity v, along a path segment having length d between points X and Y, while it receives signals from a remote source S, as illustrated in Figure 4.1. The difference in path lengths traveled by the wave from source S to the mobile at points X and Y is $\Delta = d\cos\theta = v\Delta t\cos\theta$, where Δt is the time required for the mobile to travel from X to Y, and θ is assumed to be the same at points X and Y since the source is assumed to be very far away. The phase change in the received signal due to the difference in path lengths is therefore

$$\Delta\phi = \frac{2\pi\Delta l}{\lambda} = \frac{2\pi v\Delta t}{\lambda}\cos\theta \tag{4.1}$$

and hence the apparent change in frequency, or Doppler shift, is given by f_d, where

$$f_d = \frac{1}{2\pi}\cdot\frac{\Delta\phi}{\Delta t} = \frac{v}{\lambda}\cdot\cos\theta \tag{4.2}$$

Equation (4.2) relates the Doppler shift to the mobile velocity and the spatial angle between the direction of motion of the mobile and the direction of arrival of the wave. It can be seen from equation (4.2) that if the mobile is moving toward the direction of arrival of the wave, the Doppler shift is positive (i.e., the apparent received frequency is increased), and if the mobile is moving away from the direction of arrival of the wave, the Doppler shift is negative (i.e. the

apparent received frequency is decreased). As shown in section 4.7.1, multipath components from a CW signal, which arrive from different directions contribute to Doppler spreading of the received signal, thus increasing the signal bandwidth.

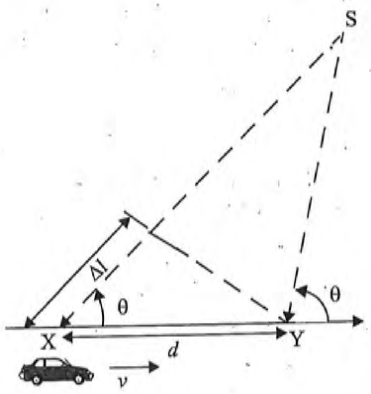

Figure 4.1
Illustration of Doppler effect.

Example 4.1

Consider a transmitter which radiates a sinusoidal carrier frequency of 1850 MHz. For a vehicle moving 60 mph, compute the received carrier frequency if the mobile is moving (a) directly towards the transmitter, (b) directly away from the transmitter, (c) in a direction which is perpendicular to the direction of arrival of the transmitted signal.

Solution to Example 4.1

Given:

Carrier frequency $f_c = 1850$ MHz

Therefore, wavelength $\lambda = c/f_c = \dfrac{3 \times 10^8}{1850 \times 10^6} = 0.162$ m

Vehicle speed $v = 60$ mph $= 26.82$ m/s

(a) The vehicle is moving directly towards the transmitter.
The Doppler shift in this case is positive and the received frequency is given by equation (4.2)

$$f = f_c + f_d = 1850 \times 10^6 + \frac{26.82}{0.162} = 1850.00016 \text{ MHz}$$

(b) The vehicle is moving directly away from the transmitter.
The Doppler shift in this case is negative and hence the received frequency is given by

$$f = f_c - f_d = 1850 \times 10^6 - \frac{26.82}{0.162} = 1849.999834 \text{ MHz}$$

(c) The vehicle is moving perpendicular to the angle of arrival of the transmitted signal.
In this case, $\theta = 90°$, $\cos\theta = 0$, and there is no Doppler shift.
The received signal frequency is the same as the transmitted frequency of 1850 MHz.

4.2 Impulse Response Model of a Multipath Channel

The small-scale variations of a mobile radio signal can be directly related to the impulse response of the mobile radio channel. The impulse response is a wideband channel characterization and contains all information necessary to simulate or analyze any type of radio transmission through the channel. This stems from the fact that a mobile radio channel may be modeled as a linear filter with a time varying impulse response, where the time variation is due to receiver motion in space. The filtering nature of the channel is caused by the summation of amplitudes and delays of the multiple arriving waves at any instant of time. The impulse response is a useful characterization of the channel, since it may be used to predict and compare the performance of many different mobile communication systems and transmission bandwidths for a particular mobile channel condition.

To show that a mobile radio channel may be modeled as a linear filter with a time varying impulse response, consider the case where time variation is due strictly to receiver motion in space. This is shown in Figure 4.2.

Figure 4.2
The mobile radio channel as a function of time and space.

In Figure 4.2, the receiver moves along the ground at some constant velocity v. For a fixed position d, the channel between the transmitter and the receiver can be modeled as a linear time invariant system. However, due to the different multipath waves which have propagation delays which vary over different spatial locations of the receiver, the impulse response of the linear time invariant channel should be a function of the position of the receiver. That is, the channel impulse response can be expressed as $h(d,t)$. Let $x(t)$ represent the transmitted signal, then the received signal $y(d,t)$ at position d can be expressed as a convolution of $x(t)$ with $h(d,t)$.

$$y(d,t) = x(t) \otimes h(d,t) = \int_{-\infty}^{\infty} x(\tau)\, h(d, t-\tau)\, d\tau \tag{4.3}$$

For a causal system, $h(d,t) = 0$ for $t<0$, thus equation (4.3) reduces to

$$y(d,t) = \int_{-\infty}^{t} x(\tau)\, h(d, t-\tau)\, d\tau \tag{4.4}$$

Since the receiver moves along the ground at a constant velocity v, the position of the receiver can by expressed as

$$d = vt \tag{4.5}$$

Substituting (4.5) in (4.4), we obtain

$$y(vt,t) = \int_{-\infty}^{t} x(\tau)\, h(vt, t-\tau)\, d\tau \tag{4.6}$$

Since v is a constant, $y(vt,t)$ is just a function of t. Therefore, equation (4.6) can be expressed as

$$y(t) = \int_{-\infty}^{t} x(\tau)\, h(vt, t-\tau)\, d\tau = x(t) \otimes h(vt,t) = x(t) \otimes h(d,t) \tag{4.7}$$

From equation (4.7) it is clear that the mobile radio channel can be modeled as a linear time varying channel, where the channel changes with time and distance.

Since v may be assumed constant over a short time (or distance) interval, we may let $x(t)$ represent the transmitted bandpass waveform, $y(t)$ the received waveform, and $h(t,\tau)$ the impulse response of the time varying multipath radio channel. The impulse response $h(t,\tau)$ completely characterizes the channel and is a function of both t and τ. The variable t represents the time variations due to motion, whereas τ represents the channel multipath delay for a fixed value of t. One may think of τ as being a vernier adjustment of time. The received signal $y(t)$ can be expressed as a convolution of the transmitted signal $x(t)$ with the channel impulse response (see Figure 4.3a).

$$y(t) = \int_{-\infty}^{\infty} x(\tau)\, h(t,\tau)\, d\tau = x(t) \otimes h(t,\tau) \tag{4.8}$$

If the multipath channel is assumed to be a bandlimited bandpass channel, which is reasonable, then $h(t,\tau)$ may be equivalently described by a complex baseband impulse response $h_b(t,\tau)$ with the input and output being the complex envelope representations of the transmitted and received signals, respectively (see Figure 4.3b). That is,

$$\frac{1}{2} r(t) = \frac{1}{2} c(t) \otimes \frac{1}{2} h_b(t,\tau) \tag{4.9}$$

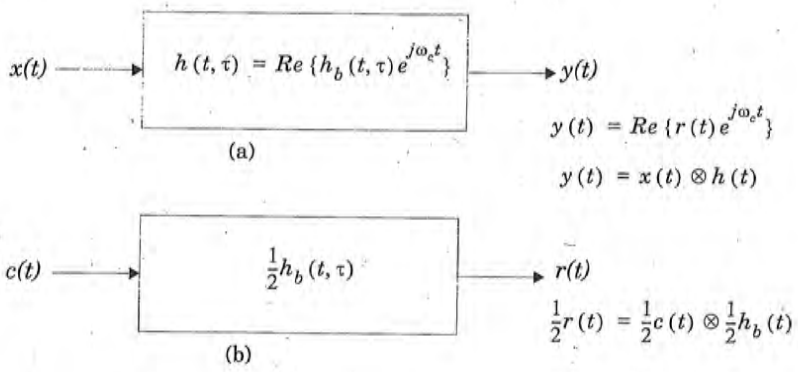

Figure 4.3
(a) Bandpass channel impulse response model.
(b) Baseband equivalent channel impulse response model.

where $c(t)$ and $r(t)$ are related to $x(t)$ and $y(t)$, respectively, through [Cou93]

$$x(t) = Re\{c(t) \exp(j2\pi f_c t)\} \tag{4.10}$$

$$y(t) = Re\{r(t) \exp(j2\pi f_c t)\} \tag{4.11}$$

The factors of $1/2$ in equation (4.9) are due to the properties of the complex envelope, in order to represent the passband radio system at baseband. The low-pass characterization removes the high frequency variations caused by the carrier, making the signal analytically easier to handle. It is shown by Couch [Cou93] that the average power of a bandpass signal $\overline{x^2(t)}$ is equal to $\frac{1}{2}\overline{|c(t)|^2}$, where the overbar denotes ensemble average for a stochastic signal, or time average for a deterministic or ergodic stochastic signal.

It is useful to discretize the multipath delay axis τ of the impulse response into equal time delay segments called *excess delay bins*, where each bin has time a delay width equal to $\tau_{i+1} - \tau_i$, where τ_0 is equal to 0, and represents the first arriving signal at the receiver. Letting i = 0, it is seen that $\tau_1 - \tau_0$ is equal to the time delay bin width given by $\Delta\tau$. For convention, $\tau_0 = 0$, $\tau_1 = \Delta\tau$, and $\tau_i = i\Delta\tau$, for $i = 0$ to $N-1$, where N represents the total number of possible equally-spaced multipath components, including the first arriving component. Any number of multipath signals received within the i th bin are represented by a single resolvable multipath component having delay τ_i. This technique of quantizing the delay bins determines the time delay resolution of the channel model, and the useful frequency span of the model can be shown to be $1/(2\Delta\tau)$. That is, the model may be used to analyze transmitted signals having bandwidths which are less than $1/(2\Delta\tau)$. Note that $\tau_0 = 0$ is the excess time delay

of the first arriving multipath component, and neglects the propagation delay between the transmitter and receiver. *Excess delay* is the relative delay of the i th multipath component as compared to the first arriving component and is given by τ_i. The *maximum excess delay* of the channel is given by $N\Delta\tau$.

Since the received signal in a multipath channel consists of a series of attenuated, time-delayed, phase shifted replicas of the transmitted signal, the baseband impulse response of a multipath channel can be expressed as

$$h_b(t,\tau) = \sum_{i=0}^{N-1} a_i(t,\tau) \exp\left[j2\pi f_c \tau_i(t) + \phi(t,\tau)\right] \delta(\tau - \tau_i(t)) \tag{4.12}$$

where $a_i(t,\tau)$ and $\tau_i(t)$ are the real amplitudes and excess delays, respectively, of i th multipath component at time t. The phase term $2\pi f_c \tau_i(t) + \phi_i(t,\tau)$ in (4.12) represents the phase shift due to free space propagation of the i th multipath component, plus any additional phase shifts which are encountered in the channel. In general, the phase term is simply represented by a single variable $\theta_i(t,\tau)$ which lumps together all the mechanisms for phase shifts of a single multipath component within the ith excess delay bin. Note that some excess delay bins may have no multipath at some time t and delay τ_i, since $a_i(t,\tau)$ may be zero. In equation (4.12), N is the total possible number of multipath components (bins), and $\delta(\cdot)$ is the unit impulse function which determines the specific multipath bins that have components at time t and excess delays τ_i. Figure 4.4 illustrates an example of different snapshots of $h_b(t,\tau)$, where t varies into the page, and the time delay bins are quantized to widths of $\Delta\tau$.

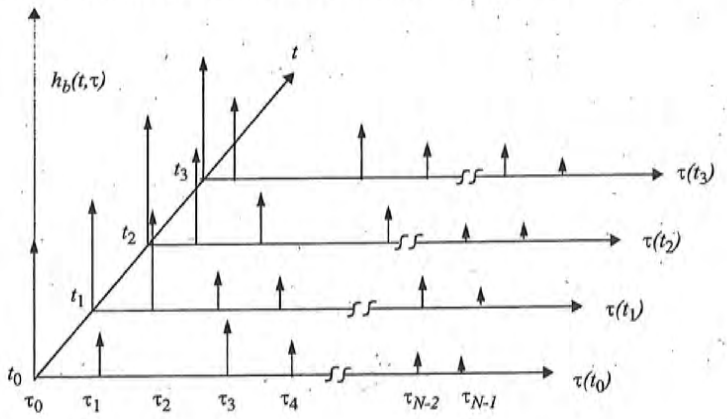

Figure 4.4
An example of the time varying discrete-time impulse response model for a multipath radio channel.

If the channel impulse response is assumed to be time invariant, or is at least wide sense stationary over a small-scale time or distance interval, then the channel impulse response may be simplified as

$$h_b(\tau) = \sum_{i=0}^{N-1} a_i \exp(-j\theta_i)\,\delta(\tau-\tau_i) \tag{4.13}$$

When measuring or predicting $h_b(\tau)$, a probing pulse $p(t)$ which approximates a delta function is used at the transmitter. That is,

$$p(t) \approx \delta(t-\tau) \tag{4.14}$$

is used to sound the channel to determine $h_b(\tau)$.

For small-scale channel modeling, the *power delay profile* of the channel is found by taking the spatial average of $|h_b(t;\tau)|^2$ over a local area. By making several local area measurements of $|h_b(t;\tau)|^2$ in different locations, it is possible to build an ensemble of power delay profiles, each one representing a possible small-scale multipath channel state [Rap91a].

Based on work by Cox [Cox72], [Cox75], if $p(t)$ has a time duration much smaller than the impulse response of the multipath channel, $p(t)$ does not need to be deconvolved from the received signal $r(t)$ in order to determine relative multipath signal strengths. The received power delay profile in a local area is given by

$$P(t;\tau) \approx k|h_b(t;\tau)|^2 \tag{4.15}$$

and many snapshots of $|h_b(t;\tau)|^2$ are typically averaged over a local (small-scale) area to provide a single time-invariant multipath power delay profile $P(\tau)$. The gain k in equation (4.15) relates the transmitted power in the probing pulse $p(t)$ to the total power received in a multipath delay profile.

4.2.1 Relationship Between Bandwidth and Received Power

In actual wireless communication systems, the impulse response of a multipath channel is measured in the field using channel sounding techniques. We now consider two extreme channel sounding cases as a means of demonstrating how the small-scale fading behaves quite differently for two signals with different bandwidths in the identical multipath channel.

Consider a pulsed, transmitted RF signal of the form

$$x(t) = \mathrm{Re}\{p(t)\exp(j2\pi f_c t)\}$$

where $p(t)$ is a repetitive baseband pulse train with very narrow pulse width T_{bb} and repetition period T_{REP} which is much greater than the maximum measured excess delay τ_{max} in the channel. Now let

$$p(t) = 2\sqrt{\tau_{max}/T_{bb}} \text{ for } 0 \le t \le T_{bb}$$

and let $p(t)$ be zero elsewhere for all excess delays of interest. The low pass channel output $r(t)$ closely approximates the impulse response $h_b(t)$ and is given by

$$\begin{aligned} r(t) &= \frac{1}{2}\sum_{i=0}^{N-1} a_i \left(\exp\left(-j\theta_i\right)\right) \cdot p\left(t-\tau_i\right) \\ &= \sum_{i=0}^{N-1} a_i \exp\left(-j\theta_i\right) \cdot \sqrt{\frac{\tau_{max}}{T_{bb}}}\ \text{rect}\left[t-\frac{T_{bb}}{2}-\tau_i\right] \end{aligned} \tag{4.16}$$

To determine the received power at some time t_0, the power $|r(t_0)|^2$ is measured. The quantity $|r(t_0)|^2$ is called the *instantaneous multipath power delay profile* of the channel, and is equal to the energy received over the time duration of the multipath delay divided by τ_{max}. That is, using equation (4.16)

$$\begin{aligned} |r(t_0)|^2 &= \frac{1}{\tau_{max}} \int_0^{\tau_{max}} r(t) \times r^*(t)\, dt \\ &= \frac{1}{\tau_{max}} \int_0^{\tau_{max}} \frac{1}{4}\text{Re}\left\{\sum_{j=0}^{N-1}\sum_{i=0}^{N-1} a_j(t_0)\, a_i(t_0)\, p\left(t-\tau_j\right) p\left(t-\tau_i\right) \exp\left(-j\left(\theta_j-\theta_i\right)\right)\right\} dt \end{aligned} \tag{4.17}$$

Note that if all the multipath components are resolved by the probe $p(t)$, then $|\tau_j-\tau_i| > T_{bb}$ for all $j \neq i$, and

$$\begin{aligned} |r(t_0)|^2 &= \frac{1}{\tau_{max}} \int_0^{\tau_{max}} \frac{1}{4}\left(\sum_{k=0}^{N-1} a_k^2(t_0)\, p^2\left(t-\tau_k\right)\right) dt \\ &= \frac{1}{\tau_{max}} \sum_{k=0}^{N-1} a_k^2(t_0) \int_0^{\tau_{max}} \left\{\sqrt{\frac{\tau_{max}}{T_{bb}}}\ \text{rect}\left[t-\frac{T_{bb}}{2}-\tau_k\right]\right\}^2 dt \\ &= \sum_{k=0}^{N-1} a_k^2(t_0) \end{aligned} \tag{4.18}$$

For a wideband probing signal $p(t)$, T_{bb} is smaller than the delays between multipath components in the channel, and equation (4.18) shows that the total received power is simply related to the sum of the powers in the individual multipath components, and is scaled by the ratio of the probing pulse's width and amplitude, and the maximum observed excess delay of the channel. Assuming that the received power from the multipath components forms a random process where each component has a random amplitude and phase at any time t, the average small-scale received power for the wideband probe is found from equation (4.17) as

$$E_{a,\theta}[P_{WB}] = E_{a,\theta}\left[\left|\sum_{i=0}^{N-1} a_i \exp(j\theta_i)\right|^2\right] \approx \sum_{i=0}^{N-1} \overline{a_i^2} \tag{4.19}$$

In equation (4.19), $E_{a,\theta}[\cdot]$ denotes the ensemble average over all possible values of a_i and θ_i in a local area, and the overbar denotes sample average over a local measurement area which is generally measured using multipath measurement equipment. The striking result of equations (4.18) and (4.19) is that if a transmitted signal is able to resolve the multipaths, then the *small-scale received power is simply the sum of the powers received in each multipath component*. In practice, the amplitudes of individual multipath components do not fluctuate widely in a local area. Thus, the received power of a wideband signal such as $p(t)$ does not fluctuate significantly when a receiver is moved about a local area [Rap89].

Now, instead of a pulse, consider a CW signal which is transmitted into the exact same channel, and let the complex envelope be given by $c(t) = 2$. Then, the instantaneous complex envelope of the received signal is given by the phasor sum

$$r(t) = \sum_{i=0}^{N-1} a_i \exp(j\theta_i(t,\tau)) \tag{4.20}$$

and the instantaneous power is given by

$$|r(t)|^2 = \left|\sum_{i=0}^{N-1} a_i \exp(j\theta_i(t,\tau))\right|^2 \tag{4.21}$$

As the receiver is moved over a local area, the channel changes, and the received signal strength will vary at a rate governed by the fluctuations of a_i and θ_i. As mentioned earlier, a_i varies little over local areas, but θ_i will vary greatly due to changes in propagation distance over space, resulting in large fluctuations of $r(t)$ as the receiver is moved over small distances (on the order of a wavelength). That is, since $r(t)$ is the phasor sum of the individual multipath components, the instantaneous phases of the multipath components cause the large fluctuations which typifies small-scale fading for CW signals. The average received power over a local area is then given by

$$E_{a,\theta}[P_{CW}] = E_{a,\theta}\left[\left[\left|\sum_{i=0}^{N-1} a_i \exp(j\theta_i)\right|^2\right]\right] \tag{4.22}$$

$$E_{a,\theta}[P_{CW}] \approx \overline{\left[\left(a_0 e^{j\theta_0} + a_1 e^{j\theta_1} + \ldots\ldots + a_{N-1} e^{j\theta_{N-1}}\right)\right.} \times \left.\left(a_0 e^{-j\theta_0} + a_1 e^{-j\theta_1} + \ldots\ldots + a_{N-1} e^{-j\theta_{N-1}}\right)\right] \tag{4.23}$$

$$E_{a,\theta}[P_{CW}] \approx \sum_{i=0}^{N-1} \overline{a_i^2} + 2\sum_{i=0}^{N-1} \sum_{i,j\neq i}^{N} r_{ij}\, \overline{\cos(\theta_i - \theta_j)} \tag{4.24}$$

where r_{ij} is the path amplitude correlation coefficient defined to be

$$r_{ij} = E_a[a_i a_j] \tag{4.25}$$

and the overbar denotes time average for CW measurements made by a mobile receiver over the local measurement area [Rap89]. Note that when $\overline{\cos(\theta_i - \theta_j)} = 0$ and/or $r_{ij} = 0$, then the average power for a CW signal is equivalent to the average received power for a wideband signal in a small-scale region. This is seen by comparing equation (4.19) and equation (4.24). This can occur when either the multipath phases are identically and independently distributed (i.i.d uniform) over $[0, 2\pi]$ or when the path amplitudes are uncorrelated. The i.i.d uniform distribution of θ is a valid assumption since multipath components traverse differential path lengths that measure hundreds of wavelengths and are likely to arrive with random phases. If for some reason it is believed that the phases are not independent, the average wideband power and average CW power will still be equal if the paths have uncorrelated amplitudes. However, if the phases of the paths are dependent upon each other, then the amplitudes are likely to be correlated, since the same mechanism which affects the path phases is likely to also affect the amplitudes. This situation is highly unlikely at transmission frequencies used in wireless mobile systems.

Thus it is seen that the *received local ensemble average power of wideband and narrowband signals are equivalent*. When the transmitted signal has a bandwidth much greater than the bandwidth of the channel, then the multipath structure is completely resolved by the received signal at any time, and the received power varies very little since the individual multipath amplitudes do not change rapidly over a local area. However, if the transmitted signal has a very narrow bandwidth (e.g., the baseband signal has a duration greater than the excess delay of the channel), then multipath is not resolved by the received signal, and large signal fluctuations (fading) occur at the receiver due to the phase shifts of the many unresolved multipath components.

Figure 4.5 illustrates actual indoor radio channel measurements made simultaneously with a wideband probing pulse having $T_{bb} = 10$ ns, and a CW transmitter. The carrier frequency was 4 GHz. It can be seen that the CW signal undergoes rapid fades, whereas the wideband measurements change little over the 5λ measurement track. However, the local average received powers of both signals were measured to be virtually identical [Haw91].

Example 4.2

Assume a discrete channel impulse response is used to model urban radio channels with excess delays as large as 100 μs and microcellular channels with excess delays no larger than 4 μs. If the number of multipath bins is fixed

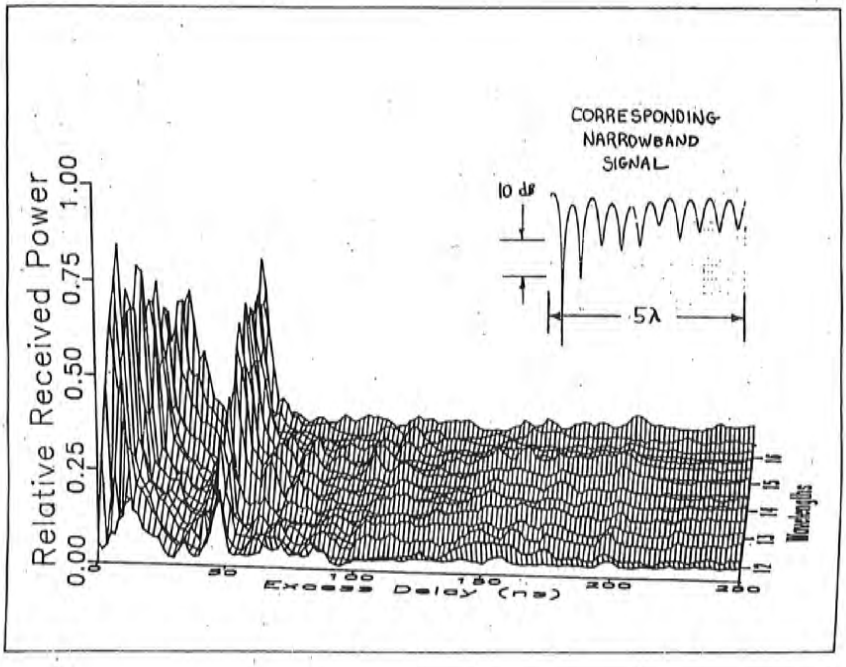

Figure 4.5
Measured wideband and narrowband received signals over a 5λ (0.375 m) measurement track inside a building. Carrier frequency is 4 GHz. Wideband power is computed using equation (4.19), which can be thought of as the area under the power delay profile.

at 64, find (a) $\Delta\tau$, and (b) the maximum bandwidth which the two models can accurately represent. Repeat the exercise for an indoor channel model with excess delays as large as 500 ns. As described in section 4.7.6, SIRCIM and SMRCIM are statistical channel models based on equation (4.12) that use parameters in this example.

Solution to Example 4.2

The maximum excess delay of the channel model is given by $\tau_N = N\Delta\tau$. Therefore, for $\tau_N = 100\mu s$, and $N = 64$ we obtain $\Delta\tau = \tau_N/N = 1.5625\,\mu s$. The maximum bandwidth that the SMRCIM model can accurately represent is equal to

$$1/(2\Delta\tau) = 1/(2(1.5625\mu s)) = 0.32 \text{ MHz}.$$

For the SMRCIM urban microcell model, $\tau_N = 4\mu s$, $\Delta\tau = \tau_N/N = 62.5$ ns. The maximum bandwidth that can be represented is

$$1/(2\Delta\tau) = 1/(2(62.5 \text{ ns})) = 8 \text{ MHz}.$$

Similarly, for indoor channels, $\Delta\tau = \tau_N/N = \frac{500 \times 10^{-9}}{64} = 7.8125$ ns.

The maximum bandwidth for the indoor channel model is

$$1/(2\Delta\tau) = 1/(2(7.8125 \text{ ns})) = 64 \text{ MHz}.$$

Example 4.3

Assume a mobile traveling at a velocity of 10 m/s receives two multipath components at a carrier frequency of 1000 MHz. The first component is assumed to arrive at $\tau = 0$ with an initial phase of 0° and a power of -70 dBm, and the second component which is 3 dB weaker than the first component is assumed to arrive at $\tau = 1\mu s$, also with an initial phase of 0°. If the mobile moves directly towards the direction of arrival of the first component and directly away from the direction of arrival of the second component, compute the narrowband instantaneous power at time intervals of 0.1 s from 0 s to 0.5 s. Compute the average narrowband power received over this observation interval. Compare average narrowband and wideband received powers over the interval.

Solution to Example 4.3

Given $v = 10$ m/s, time intervals of 0.1 s correspond to spatial intervals of 1 m. The carrier frequency is given to be 1000 MHz, hence the wavelength of the signal is

$$\lambda = \frac{c}{f} = \frac{3 \times 10^8}{1000 \times 10^6} = 0.3 \text{ m}$$

The narrowband instantaneous power can be computed using equation (4.21). Note -70 dBm = 100 pW. At time $t = 0$, the phases of both multipath components are 0°, hence the narrowband instantaneous power is equal to

$$|r(t)|^2 = \left| \sum_{i=0}^{N-1} a_i \exp(j\theta_i(t, \tau)) \right|^2$$

$$= \left| \sqrt{100 \text{ pW}} \times \exp(0) + \sqrt{50 \text{ pW}} \times \exp(0) \right|^2 = 291 \text{ pW}$$

Now, as the mobile moves, the phase of the two multipath components changes in opposite directions.

At $t = 0.1$ s, the phase of the first component is

$$\theta_i = \frac{2\pi d}{\lambda} = \frac{2\pi v t}{\lambda} = \frac{2\pi \times 10 \text{ (m/s)} \times 0.1 \text{ s}}{0.3 \text{ m}}$$

$$= 20.94 \text{ rad} = 2.09 \text{ rad} = 120°$$

Since the mobile moves towards the direction of arrival of the first component, and away from the direction of arrival of the second component, θ_1 is positive, and θ_2 is negative.

Therefore, at $t = 0.1$ s, $\theta_1 = 120°$, and $\theta_2 = -120°$, and the instantaneous power is equal to

$$|r(t)|^2 = \left|\sum_{i=0}^{N-1} a_i \exp(j\theta_i(t,\tau))\right|^2$$

$$= \left|\sqrt{100\ \text{pW}} \times \exp(j120°) + \sqrt{50\ \text{pW}} \times \exp(-j120°)\right|^2 = 78.2\ \text{pW}$$

Similarly, at $t = 0.2$ s, $\theta_2 = 240°$, and $\theta_2 = -240°$, and the instantaneous power is equal to

$$|r(t)|^2 = \left|\sum_{i=0}^{N-1} a_i \exp(j\theta_i(t,\tau))\right|^2$$

$$= \left|\sqrt{100\ \text{pW}} \times \exp(j240°) + \sqrt{50\ \text{pW}} \times \exp(-j240°)\right|^2 = 81.5\ \text{pW}$$

Similarly, at $t = 0.3$ s, $\theta_1 = 360° = 0°$, and $\theta_2 = -360° = 0°$, and the instantaneous power is equal to

$$|r(t)|^2 = \left|\sum_{i=0}^{N-1} a_i \exp(j\theta_i(t,\tau))\right|^2$$

$$= \left|\sqrt{100\ \text{pW}} \times \exp(j0°) + \sqrt{50\ \text{pW}} \times \exp(-j0°)\right|^2 = 291\ \text{pW}$$

It follows that at $t = 0.4$ s, $|r(t)|^2 = 78.2$ pW, and at $t = 0.5$ s, $|r(t)|^2 = 81.5$ pW.

The average narrowband received power is equal to

$$\frac{(2)(291) + (2)(78.2) + (2)(81.5)}{6}\ \text{pW} = 150.233\ \text{pW}$$

Using equation (4.19), the wideband power is given by

$$E_{a,\theta}[P_{W,B}] = E_{a,\theta}\left[\sum_{i=0}^{N-1} |a_i \exp(j\theta_i)|^2\right] \approx \sum_{i=0}^{N-1} \overline{a_i^2}$$

$$E_{a,\theta}[P_{W,B}] = 100\ \text{pW} + 50\ \text{pW} = 150\ \text{pW}$$

As can be seen, the narrowband and wideband received power are virtually identical when averaged over 0.5 s (or 5 m). While the CW signal fades over the observation interval, the wideband signal power remains constant.

4.3 Small-Scale Multipath Measurements

Because of the importance of the multipath structure in determining the small-scale fading effects, a number of wideband channel sounding techniques have been developed. These techniques may be classified as *direct pulse measurements*, *spread spectrum sliding correlator measurements*, and *swept frequency measurements*.

4.3.1 Direct RF Pulse System

A simple channel sounding approach is the direct RF pulse system (see Figure 4.6). This technique allows engineers to determine rapidly the power delay profile of any channel, as demonstrated by Rappaport and Seidel [Rap89], [Rap90]. Essentially a wide band pulsed bistatic radar, this system transmits a repetitive pulse of width τ_{bb} s, and uses a receiver with a wide bandpass filter ($BW = 2/\tau_{bb}$ Hz). The signal is then amplified, detected with an envelope detector, and displayed and stored on a high speed oscilloscope. This gives an immediate measurement of the square of the channel impulse response convolved with the probing pulse (see equation (4.17)). If the oscilloscope is set on averaging mode, then this system can provide a local average power delay profile. Another attractive aspect of this system is the lack of complexity, since off-the-shelf equipment may be used.

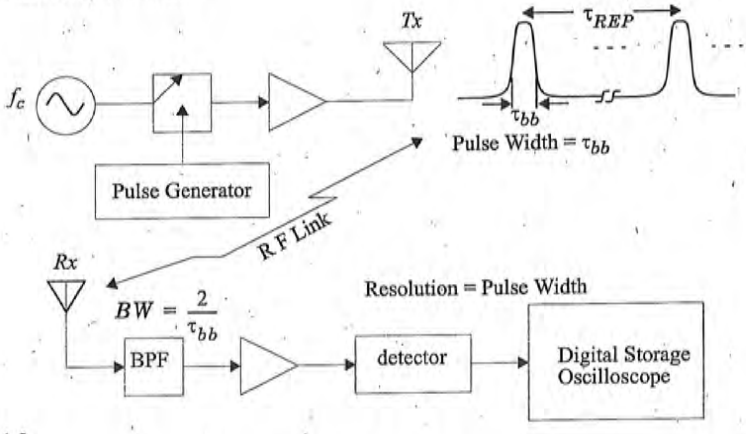

Figure 4.6
Direct RF channel impulse response measurement system.

The minimum resolvable delay between multipath components is equal to the probing pulse width τ_{bb}. The main problem with this system is that it is subject to interference and noise, due to the wide passband filter required for multipath time resolution. Also, the pulse system relies on the ability to trigger the oscilloscope on the first arriving signal. If the first arriving signal is blocked or fades, severe fading occurs, and it is possible the system may not trigger properly. Another disadvantage is that the phases of the individual multipath components are not received, due to the use of an envelope detector. However, use of a coherent detector permits measurement of the multipath phase using this technique.

4.3.2 Spread Spectrum Sliding Correlator Channel Sounding

The basic block diagram of a spread spectrum channel sounding system is shown in Figure 4.7. The advantage of a spread spectrum system is that, while the probing signal may be wideband, it is possible to detect the transmitted signal using a narrowband receiver preceded by a wideband mixer, thus improving the dynamic range of the system as compared to the direct RF pulse system.

In a spread spectrum channel sounder, a carrier signal is "spread" over a large bandwidth by mixing it with a binary pseudo-noise (PN) sequence having a chip duration T_c and a chip rate R_c equal to $1/T_c$ Hz. The power spectrum envelope of the transmitted spread spectrum signal is given by [Dix84] as

$$\left[\frac{\sin(f-f_c)T_c}{(f-f_c)T_c}\right]^2 \tag{4.26}$$

and the null-to-null bandwidth is

$$BW = 2R_c \tag{4.27}$$

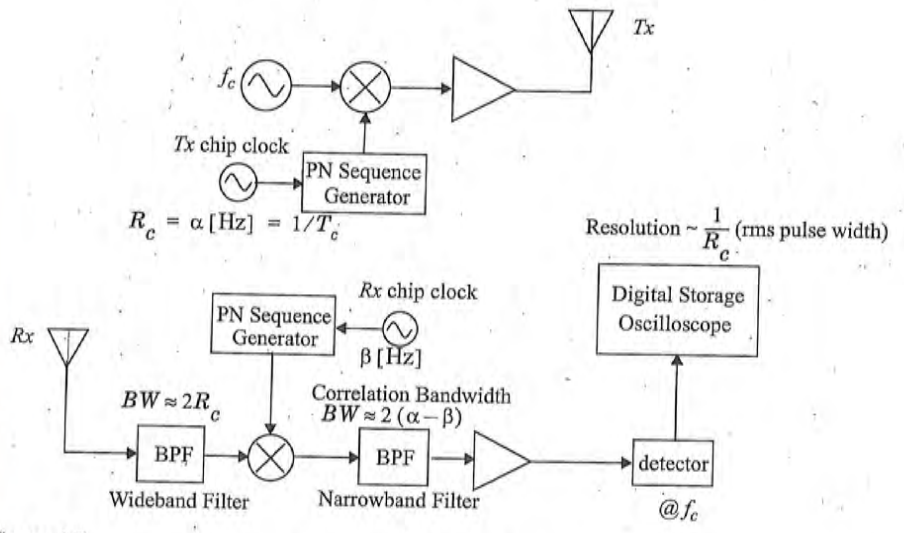

Figure 4.7
Spread spectrum channel impulse response measurement system.

The spread spectrum signal is then received, filtered, and *despread* using a PN sequence generator identical to that used at the transmitter. Although the two PN sequences are identical, the transmitter chip clock is run at a slightly faster rate than the receiver chip clock. Mixing the chip sequences in this fashion implements a *sliding correlator* [Dix84]. When the PN code of the faster chip

clock catches up with the PN code of the slower chip clock, the two chip sequences will be virtually identically aligned, giving maximal correlation. When the two sequences are not maximally correlated, mixing the incoming spread spectrum signal with the unsynchronized receiver chip sequence will spread this signal into a bandwidth at least as large as the receiver's reference PN sequence. In this way, the narrowband filter that follows the correlator can reject almost all of the incoming signal power. This is how *processing gain* is realized in a spread spectrum receiver and how it can reject passband interference, unlike the direct RF pulse sounding system.

Processing gain (PG) is given as

$$PG = \frac{2R_c}{R_{bb}} = \frac{2\tau_{bb}}{T_c} = \frac{(S/N)_{out}}{(S/N)_{in}} \tag{4.28}$$

where $\tau_{bb} = 1/R_{bb}$, is the period of the baseband information. For the case of a sliding correlator channel sounder, the baseband information rate is equal to the frequency offset of the PN sequence clocks at the transmitter and receiver.

When the incoming signal is correlated with the receiver sequence, the signal is collapsed back to the original bandwidth (i.e., "despread"), envelope detected, and displayed on an oscilloscope. Since different incoming multipaths will have different time delays, they will maximally correlate with the receiver PN sequence at different times. The energy of these individual paths will pass through the correlator depending on the time delay. Therefore, after envelope detection, the channel impulse response convolved with the pulse shape of a single chip is displayed on the oscilloscope. Cox [Cox72] first used this method to measure channel impulse responses in outdoor suburban environments at 910 MHz. Devasirvatham [Dev86], [Dev90a] successfully used a direct sequence spread spectrum channel sounder to measure time delay spread of multipath components and signal level measurements in office and residential buildings at 850 MHz. Bultitude [Bul89] used this technique for indoor and microcellular channel sounding work, as did Landron [Lan92].

The time resolution ($\Delta\tau$) of multipath components using a spread spectrum system with sliding correlation is

$$\Delta\tau = 2T_c = \frac{2}{R_c} \tag{4.29}$$

In other words, the system can resolve two multipath components as long as they are equal to or greater than $2T_c$ seconds apart. In actuality, multipath components with interarrival times smaller than $2T_c$ can be resolved since the rms pulse width is smaller than the absolute width of the triangular correlation pulse, and is on the order of T_c.

The sliding correlation process gives *equivalent time* measurements that are updated every time the two sequences are maximally correlated. The time between maximal correlations (T) can be calculated from equation (4.30)

$$\Delta T = T_c \gamma l = \frac{\gamma l}{R_c} \tag{4.30}$$

where T_c = chip period (s)
R_c = chip rate (Hz)
γ = slide factor (dimensionless)
l = sequence length (chips)

The slide factor is defined as the ratio between the transmitter chip clock rate and the difference between the transmitter and receiver chip clock rates [Dev86]. Mathematically, this is expressed as

$$\gamma = \frac{\alpha}{\alpha - \beta} \tag{4.31}$$

where α = transmitter chip clock rate (Hz)
β = receiver chip clock rate (Hz)

For a maximal length PN sequence, the sequence length is

$$l = 2^n - 1 \tag{4.32}$$

where n is the number of shift registers in the sequence generator [Dix84].

Since the incoming spread spectrum signal is mixed with a receiver PN sequence that is slower than the transmitter sequence, the signal is essentially down-converted ("collapsed") to a low-frequency narrowband signal. In other words, the relative rate of the two codes slipping past each other is the rate of information transferred to the oscilloscope. This narrowband signal allows narrowband processing, eliminating much of the passband noise and interference. The processing gain of equation (4.28) is then realized using a narrowband filter ($BW = 2(a - \beta)$).

The equivalent time measurements refer to the relative times of multipath components as they are displayed on the oscilloscope. The observed time scale on the oscilloscope using a sliding correlator is related to the actual propagation time scale by

$$\text{Actual Propagation Time} = \frac{\text{Observed Time}}{\gamma} \tag{4.33}$$

This effect is due to the relative rate of information transfer in the sliding correlator. For example, T_c of equation (4.30) is an observed time measured on an oscilloscope and not actual propagation time. This effect, known as *time dilation*, occurs in the sliding correlator system because the propagation delays are actually expanded in time by the sliding correlator.

Caution must be taken to ensure that the sequence length has a period which is greater than the longest multipath propagation delay. The PN sequence period is

$$\tau_{PNseq} = T_c l \tag{4.34}$$

The sequence period gives an estimate of the maximum unambiguous range of incoming multipath signal components. This range is found by multiplying the speed of light with τ_{PNseq} in equation (4.34).

There are several advantages to the spread spectrum channel sounding system. One of the key spread spectrum modulation characteristics is the ability to reject passband noise, thus improving the coverage range for a given transmitter power. Transmitter and receiver PN sequence synchronization is eliminated by the sliding correlator. Sensitivity is adjustable by changing the sliding factor and the post-correlator filter bandwidth. Also, required transmitter powers can be considerably lower than comparable direct pulse systems due to the inherent "processing gain" of spread spectrum systems.

A disadvantage of the spread spectrum system, as compared to the direct pulse system, is that measurements are not made in real time, but they are compiled as the PN codes slide past one another. Depending on system parameters and measurement objectives, the time required to make power delay profile measurements may be excessive. Another disadvantage of the system described here is that a noncoherent detector is used, so that phases of individual multipath components can not be measured. Even if coherent detection is used, the sweep time of a spread spectrum signal induces delay such that the phases of individual multipath components with different time delays would be measured at substantially different times, during which the channel might change.

4.3.3 Frequency Domain Channel Sounding

Because of the dual relationship between time domain and frequency domain techniques, it is possible to measure the channel impulse response in the frequency domain. Figure 4.8 shows a frequency domain channel sounder used for measuring channel impulse responses. A vector network analyzer controls a synthesized frequency sweeper, and an S-parameter test set is used to monitor the frequency response of the channel. The sweeper scans a particular frequency band (centered on the carrier) by stepping through discrete frequencies. The number and spacings of these frequency steps impact the time resolution of the impulse response measurement. For each frequency step, the S-parameter test set transmits a known signal level at port 1 and monitors the received signal level at port 2. These signal levels allow the analyzer to determine the complex response (i.e., transmissivity $S_{21}(\omega)$) of the channel over the measured frequency range. The transmissivity response is a frequency domain representation of the channel impulse response. This response is then converted to the time domain using inverse discrete Fourier transform (IDFT) processing, giving a band-limited version of the impulse response. In theory, this technique works well and indirectly provides amplitude and phase information in the time domain. However, the system requires careful calibration and hardwired synchronization between the transmitter and receiver, making it useful only for very close mea-

surements (e.g., indoor channel sounding). Another limitation with this system is the non-real-time nature of the measurement. For time varying channels, the channel frequency response can change rapidly, giving an erroneous impulse response measurement. To mitigate this effect, fast sweep times are necessary to keep the total swept frequency response measurement interval as short as possible. A faster sweep time can be accomplished by reducing the number of frequency steps, but this sacrifices time resolution and excess delay range in the time domain. The swept frequency system has been used successfully for indoor propagation studies by Pahlavan [Pah95] and Zaghloul, et.al. [Zag91a], [Zag91b].

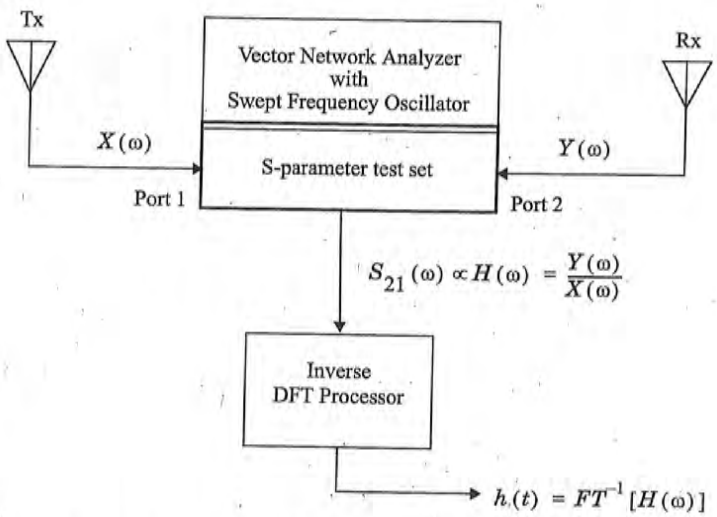

Figure 4.8
Frequency domain channel impulse response measurement system.

4.4 Parameters of Mobile Multipath Channels

Many multipath channel parameters are derived from the power delay profile, given by equation (4.18). Power delay profiles are measured using the techniques discussed in Section 4.4 and are generally represented as plots of relative received power as a function of excess delay with respect to a fixed time delay reference. Power delay profiles are found by averaging instantaneous power delay profile measurements over a local area in order to determine an average small-scale power delay profile. Depending on the time resolution of the probing pulse and the type of multipath channels studied, researchers often choose to sample at spatial separations of a quarter of a wavelength and over receiver movements no greater than 6 m in outdoor channels and no greater than 2 m in indoor channels in the 450 MHz - 6 GHz range. This small-scale sampling avoids

large-scale averaging bias in the resulting small-scale statistics. Figure 4.9 shows typical power delay profile plots from outdoor and indoor channels, determined from a large number of closely sampled instantaneous profiles.

4.4.1 Time Dispersion Parameters

In order to compare different multipath channels and to develop some general design guidelines for wireless systems, parameters which grossly quantify the multipath channel are used. The *mean excess delay, rms delay spread,* and *excess delay spread (X* dB*)* are multipath channel parameters that can be determined from a power delay profile. The time dispersive properties of wide band multipath channels are most commonly quantified by their mean excess delay ($\bar{\tau}$) and rms delay spread (σ_τ). The mean excess delay is the first moment of the power delay profile and is defined to be

$$\bar{\tau} = \frac{\sum_k a_k^2 \tau_k}{\sum_k a_k^2} = \frac{\sum_k P(\tau_k)\,\tau_k}{\sum_k P(\tau_k)} \tag{4.35}$$

The rms delay spread is the square root of the second central moment of the power delay profile and is defined to be

$$\sigma_\tau = \sqrt{\overline{\tau^2} - (\bar{\tau})^2} \tag{4.36}$$

where

$$\overline{\tau^2} = \frac{\sum_k a_k^2 \tau_k^2}{\sum_k a_k^2} = \frac{\sum_k P(\tau_k)\,\tau_k^2}{\sum_k P(\tau_k)} \tag{4.37}$$

These delays are measured relative to the first detectable signal arriving at the receiver at $\tau_0 = 0$. Equations (4.35) - (4.37) do not rely on the absolute power level of $P(\tau)$, but only the relative amplitudes of the multipath components within $P(\tau)$. Typical values of rms delay spread are on the order of microseconds in outdoor mobile radio channels and on the order of nanoseconds in indoor radio channels. Table 4.1 shows the typical measured values of rms delay spread.

It is important to note that the rms delay spread and mean excess delay are defined from a single power delay profile which is the temporal or spatial average of consecutive impulse response measurements collected and averaged over a local area. Typically, many measurements are made at many local areas in order to determine a statistical range of multipath channel parameters for a mobile communication system over a large-scale area [Rap90].

The *maximum excess delay (X* dB*)* of the power delay profile is defined to be the time delay during which multipath energy falls to X dB below the maxi-

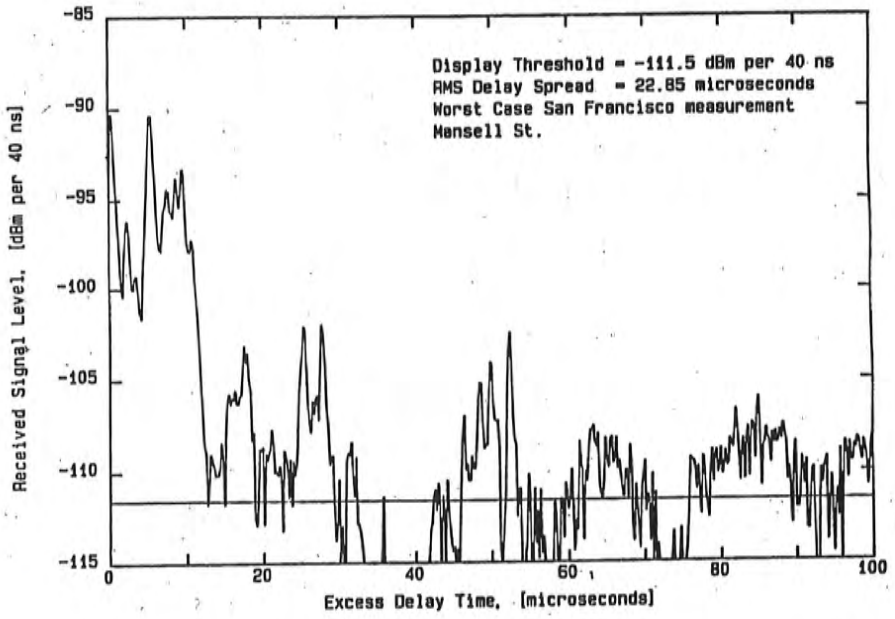

(a)

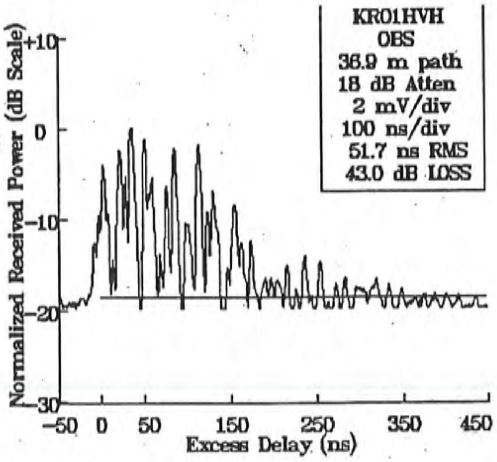

(b)

Figure 4.9
Measured multipath power delay profiles
a) From a 900 MHz cellular system in San Francisco [From [Rap90] © IEEE].
b) Inside a grocery store at 4 GHz [From [Haw91] © IEEE].

Table 4.1 Typical Measured Values of RMS Delay Spread

Environment	Frequency (MHz)	RMS Delay Spread (σ_τ)	Notes	Reference
Urban	910	1300 ns avg. 600 ns st. dev. 3500 ns max.	New York City	[Cox75]
Urban	892	10-25 μs	Worst case San Francisco	[Rap90]
Suburban	910	200-310 ns	Averaged typical case	[Cox72]
Suburban	910	1960-2110 ns	Averaged extreme case	[Cox72]
Indoor	1500	10-50 ns 25 ns median	Office building	[Sal87]
Indoor	850	270 ns max.	Office building	[Dev90a]
Indoor	1900	70-94 ns avg. 1470 ns max.	Three San Francisco buildings	[Sei92a]

mum. In other words, the maximum excess delay is defined as $\tau_X - \tau_0$, where τ_0 is the first arriving signal and τ_X is the maximum delay at which a multipath component is within X dB of the strongest arriving multipath signal (which does not necessarily arrive at τ_0). Figure 4.10 illustrates the computation of the maximum excess delay for multipath components within 10 dB of the maximum. The maximum excess delay (X dB) defines the temporal extent of the multipath that is above a particular threshold. The value of τ_X is sometimes called the *excess delay spread* of a power delay profile, but in all cases must be specified with a threshold that relates the multipath noise floor to the maximum received multipath component.

In practice, values for $\bar{\tau}$, $\overline{\tau^2}$, and σ_τ depend on the choice of noise threshold used to process $P(\tau)$. The noise threshold is used to differentiate between received multipath components and thermal noise. If the noise threshold is set too low, then noise will be processed as multipath, thus giving rise to values of $\bar{\tau}$, $\overline{\tau^2}$, and σ_τ that are artificially high.

It should be noted that the power delay profile and the magnitude frequency response (the spectral response) of a mobile radio channel are related through the Fourier transform. It is therefore possible to obtain an equivalent description of the channel in the frequency domain using its frequency response characteristics. Analogous to the delay spread parameters in the time domain, *coherence bandwidth* is used to characterize the channel in the frequency domain. The rms delay spread and coherence bandwidth are inversely proportional to one another, although their exact relationship is a function of the exact multipath structure.

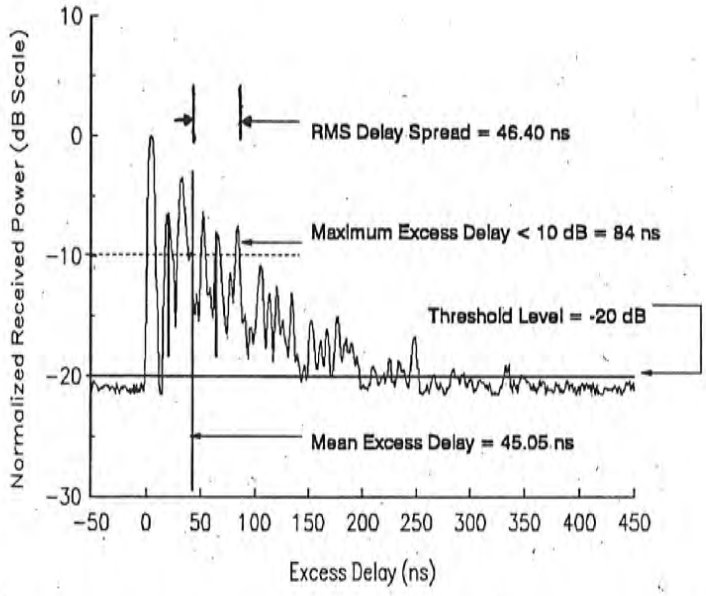

Figure 4.10
Example of an indoor power delay profile; rms delay spread, mean excess delay, maximum excess delay (10 dB), and threshold level are shown.

4.4.2 Coherence Bandwidth

While the delay spread is a natural phenomenon caused by reflected and scattered propagation paths in the radio channel, the coherence bandwidth, B_c, is a defined relation derived from the rms delay spread. Coherence bandwidth is a statistical measure of the range of frequencies over which the channel can be considered "flat" (i.e., a channel which passes all spectral components with approximately equal gain and linear phase). In other words, coherence bandwidth is the range of frequencies over which two frequency components have a strong potential for amplitude correlation. Two sinusoids with frequency separation greater than B_c are affected quite differently by the channel. If the coherence bandwidth is defined as the bandwidth over which the frequency correlation function is above 0.9, then the coherence bandwidth is approximately [Lee89b]

$$B_c \approx \frac{1}{50\sigma_\tau} \tag{4.38}$$

If the definition is relaxed so that the frequency correlation function is above 0.5, then the coherence bandwidth is approximately

$$B_c \approx \frac{1}{5\sigma_\tau} \tag{4.39}$$

It is important to note that an exact relationship between coherence bandwidth and rms delay spread does not exist, and equations (4.38) and (4.39) are "ball park estimates". In general, spectral analysis techniques and simulation are required to determine the exact impact that time varying multipath has on a particular transmitted signal [Chu87], [Fun93], [Ste94]. For this reason, accurate multipath channel models must be used in the design of specific modems for wireless applications [Rap91a], [Woe94].

Example 4.4

Calculate the mean excess delay, rms delay spread, and the maximum excess delay (10 dB) for the multipath profile given in the figure below. Estimate the 50% coherence bandwidth of the channel. Would this channel be suitable for AMPS or GSM service without the use of an equalizer?

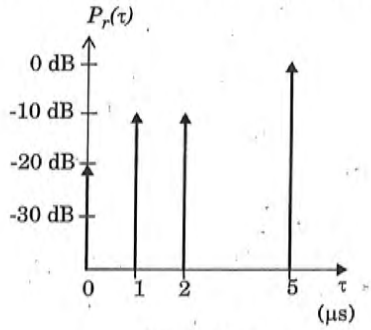

Figure E4.4

Solution to Example 4.4

The rms delay spread for the given multipath profile can be obtained using equations (4.35) — (4.37). The delays of each profile are measured relative to the first detectable signal. The mean excess delay for the given profile

$$\bar{\tau} = \frac{(1)(5) + (0.1)(1) + (0.1)(2) + (0.01)(0)}{[0.01 + 0.1 + 0.1 + 1]} = 4.38\mu s$$

The second moment for the given power delay profile can be calculated as

$$\overline{\tau^2} = \frac{(1)(5)^2 + (0.1)(1)^2 + (0.1)(2)^2 + (0.01)(0)}{1.21} = 21.07\mu s^2$$

Therefore the rms delay spread, $\sigma_\tau = \sqrt{21.07 - (4.38)^2} = 1.37\mu s$

The coherence bandwidth is found from equation (4.39) to be

$$B_c \approx \frac{1}{5\sigma_\tau} = \frac{1}{5(1.37\mu s)} = 146 \text{ kHz}$$

Since B_c is greater than 30 kHz, AMPS will work without an equalizer. However, GSM requires 200 kHz bandwidth which exceeds B_c, thus an equalizer would be needed for this channel.

4.4.3 Doppler Spread and Coherence Time

Delay spread and coherence bandwidth are parameters which describe the time dispersive nature of the channel in a local area. However, they do not offer information about the time varying nature of the channel caused by either relative motion between the mobile and base station, or by movement of objects in the channel. *Doppler spread* and *coherence time* are parameters which describe the time varying nature of the channel in a small-scale region.

Doppler spread B_D is a measure of the spectral broadening caused by the time rate of change of the mobile radio channel and is defined as the range of frequencies over which the received Doppler spectrum is essentially non-zero. When a pure sinusoidal tone of frequency f_c is transmitted, the received signal spectrum, called the Doppler spectrum, will have components in the range $f_c - f_d$ to $f_c + f_d$, where f_d is the Doppler shift. The amount of spectral broadening depends on f_d which is a function of the relative velocity of the mobile, and the angle θ between the direction of motion of the mobile and direction of arrival of the scattered waves. *If the baseband signal bandwidth is much greater than B_D, the effects of Doppler spread are negligible at the receiver.*

Coherence time T_c is the time domain dual of Doppler spread and is used to characterize the time varying nature of the frequency dispersiveness of the channel in the time domain. The Doppler spread and coherence time are inversely proportional to one another. That is,

$$T_C \approx \frac{1}{f_m} \tag{4.40.a}$$

Coherence time is actually a statistical measure of the time duration over which the channel impulse response is essentially invariant, and quantifies the similarity of the channel response at different times. In other words, coherence time is the time duration over which two received signals have a strong potential for amplitude correlation. If the reciprocal bandwidth of the baseband signal is greater than the coherence time of the channel, then the channel will change during the transmission of the baseband message, thus causing distortion at the receiver. If the coherence time is defined as the time over which the time correlation function is above 0.5, then the coherence time is approximately [Ste94]

$$T_C \approx \frac{9}{16\pi f_m} \tag{4.40.b}$$

where f_m is the maximum Doppler shift given by $f_m = v/\lambda$. In practice, (4.40.a) suggests a time duration during which a Rayleigh fading signal may fluctuate

wildly, and (4.40.b) is often too restrictive. A popular rule of thumb for modern digital communications is to define the coherence time as the geometric mean of equations (4.40.a) and (4.40.b). That is,

$$T_C = \sqrt{\frac{9}{16\pi f_m^2}} = \frac{0.423}{f_m} \qquad (4.40.c)$$

The definition of coherence time implies that two signals arriving with a time separation greater than T_C are affected differently by the channel. For example, for a vehicle traveling 60 mph using a 900 MHz carrier, a conservative value of T_C can be shown to be 2.22 ms from (4.40.b). If a digital transmission system is used, then as long as the symbol rate is greater than $1/T_C = 454$ bps, the channel will not cause distortion due to motion (however, distortion could result from multipath time delay spread, depending on the channel impulse response). Using the practical formula of (4.40.c), $T_C = 6.77$ ms and the symbol rate must exceed 150 bits/s in order to avoid distortion due to frequency dispersion.

Example 4.5

Determine the proper spatial sampling interval required to make small-scale propagation measurements which assume that consecutive samples are highly correlated in time. How many samples will be required over 10 m travel distance if $f_c = 1900$ MHz and $v = 50$ m/s. How long would it take to make these measurements, assuming they could be made in real time from a moving vehicle? What is the Doppler spread B_D for the channel?

Solution to Example 4.5

For correlation, ensure that the time between samples is equal to $T_C/2$, and use the smallest value of T_C for conservative design.
Using equation (4.40.b)

$$T_C \approx \frac{9}{16\pi f_m} = \frac{9\lambda}{16\pi v} = \frac{9c}{16\pi v f_c} = \frac{9 \times 3 \times 10^8}{16 \times 3.14 \times 50 \times 1900 \times 10^6}$$

$$T_C = 565\mu s$$

Taking time samples at less than half T_C, at $282.5\mu s$ corresponds to a spatial sampling interval of

$$\Delta x = \frac{vT_C}{2} = \frac{50 \times 565\mu s}{2} = 0.014125 \text{ m} = 1.41 \text{ cm}$$

Therefore, the number of samples required over a 10 m travel distance is

$$N_x = \frac{10}{\Delta x} = \frac{10}{0.014125} = 708 \text{ samples}$$

The time taken to make this measurement is equal to $\frac{10\text{m}}{50 \text{ m/s}} = 0.2$ s
The Doppler spread is

$$B_D = f_m = \frac{vf_c}{c} = \frac{50 \times 1900 \times 10^6}{3 \times 10^8} = 316.66 \text{ Hz}$$

4.5 Types of Small-Scale Fading

Section 4.3 demonstrated that the type of fading experienced by a signal propagating through a mobile radio channel depends on the nature of the transmitted signal with respect to the characteristics of the channel. Depending on the relation between the signal parameters (such as bandwidth, symbol period, etc.) and the channel parameters (such as rms delay spread and Doppler spread), different transmitted signals will undergo different types of fading. The time dispersion and frequency dispersion mechanisms in a mobile radio channel lead to four possible distinct effects, which are manifested depending on the nature of the transmitted signal, the channel, and the velocity. While multipath delay spread leads to *time dispersion* and *frequency selective fading*, Doppler spread leads to *frequency dispersion* and *time selective fading*. The two propagation mechanisms are independent of one another. Figure 4.11 shows a tree of the four different types of fading.

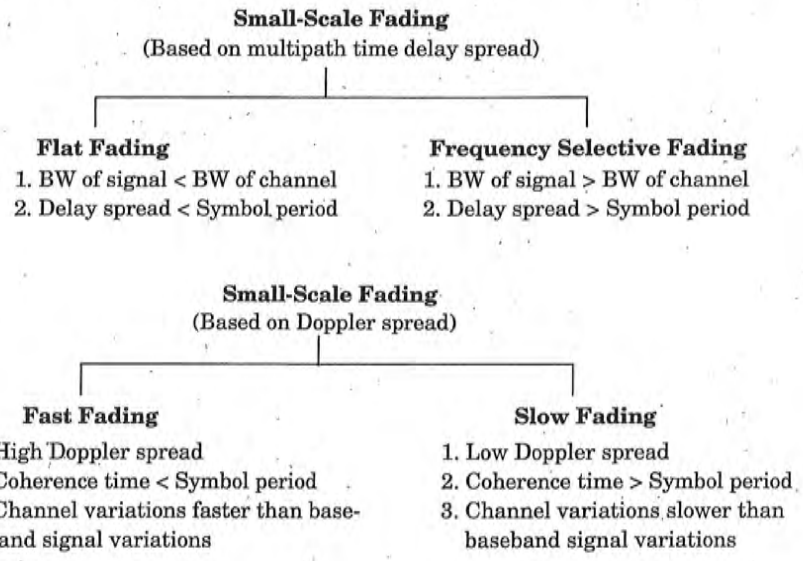

Figure 4.11
Types of small-scale fading.

4.5.1 Fading Effects Due to Multipath Time Delay Spread

Time dispersion due to multipath causes the transmitted signal to undergo either flat or frequency selective fading.

4.5.1.1 Flat fading

If the mobile radio channel has a constant gain and linear phase response over a bandwidth which is greater than the bandwidth of the transmitted signal, then the received signal will undergo *flat fading*. This type of fading is historically the most common type of fading described in the technical literature. In flat fading, the multipath structure of the channel is such that the spectral characteristics of the transmitted signal are preserved at the receiver. However the strength of the received signal changes with time, due to fluctuations in the gain of the channel caused by multipath. The characteristics of a flat fading channel are illustrated in Figure 4.12.

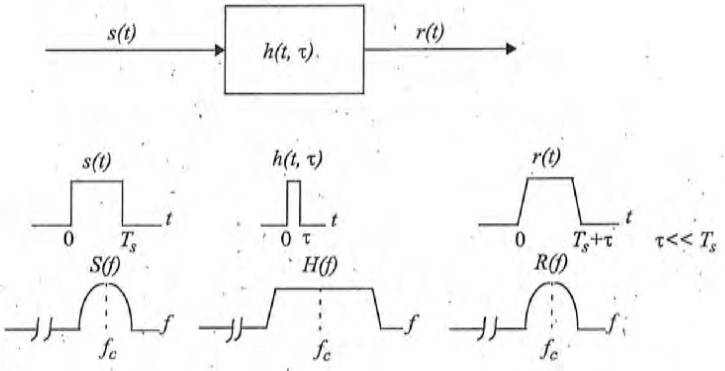

Figure 4.12
Flat fading channel characteristics.

It can be seen from Figure 4.12 that if the channel gain changes over time, a change of amplitude occurs in the received signal. Over time, the received signal $r(t)$ varies in gain, but the spectrum of the transmission is preserved. In a flat fading channel, the reciprocal bandwidth of the transmitted signal is much larger than the multipath time delay spread of the channel, and $h_b(t, \tau)$ can be approximated as having no excess delay (i.e., a single delta function with $\tau = 0$). Flat fading channels are also known as *amplitude varying channels* and are sometimes referred to as *narrowband channels*, since the bandwidth of the applied signal is *narrow* as compared to the channel flat fading bandwidth. Typical flat fading channels cause deep fades, and thus may require 20 or 30 dB more transmitter power to achieve low bit error rates during times of deep fades as

compared to systems operating over non-fading channels. The distribution of the instantaneous gain of flat fading channels is important for designing radio links, and the most common amplitude distribution is the Rayleigh distribution. The Rayleigh flat fading channel model assumes that the channel induces an amplitude which varies in time according to the Rayleigh distribution.

To summarize, a signal undergoes flat fading if

$$B_S \ll B_C \tag{4.41}$$

and

$$T_S \gg \sigma_\tau \tag{4.42}$$

where T_S is the reciprocal bandwidth (e.g., symbol period) and B_S is the bandwidth, respectively, of the transmitted modulation, and σ_τ and B_C are the rms delay spread and coherence bandwidth, respectively, of the channel.

4.5.1.2 Frequency Selective Fading

If the channel possesses a constant-gain and linear phase response over a bandwidth that is smaller than the bandwidth of transmitted signal, then the channel creates *frequency selective fading* on the received signal. Under such conditions the channel impulse response has a multipath delay spread which is greater than the reciprocal bandwidth of the transmitted message waveform. When this occurs, the received signal includes multiple versions of the transmitted waveform which are attenuated (faded) and delayed in time, and hence the received signal is distorted. Frequency selective fading is due to time dispersion of the transmitted symbols within the channel. Thus the channel induces *intersymbol interference* (ISI). Viewed in the frequency domain, certain frequency components in the received signal spectrum have greater gains than others.

Frequency selective fading channels are much more difficult to model than flat fading channels since each multipath signal must be modeled and the channel must be considered to be a linear filter. It is for this reason that wideband multipath measurements are made, and models are developed from these measurements. When analyzing mobile communication systems, statistical impulse response models such as the 2-ray Rayleigh fading model (which considers the impulse response to be made up of two delta functions which independently fade and have sufficient time delay between them to induce frequency selective fading upon the applied signal), or computer generated or measured impulse responses, are generally used for analyzing frequency selective small-scale fading. Figure 4.13 illustrates the characteristics of a frequency selective fading channel.

For frequency selective fading, the spectrum $S(f)$ of the transmitted signal has a bandwidth which is greater than the coherence bandwidth B_C of the channel. Viewed in the frequency domain, the channel becomes frequency selective, where the gain is different for different frequency components. Frequency selec-

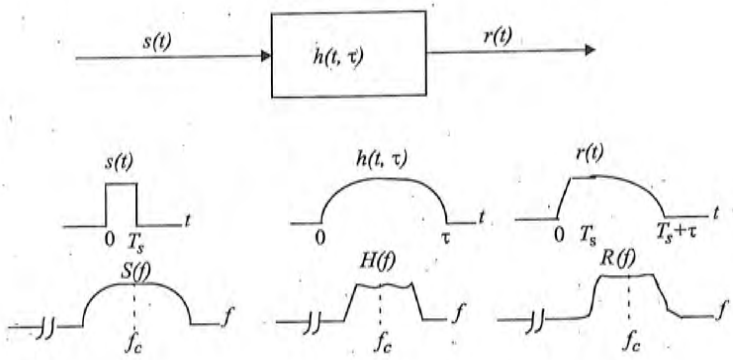

Figure 4.13
Frequency selective fading channel characteristics.

tive fading is caused by multipath delays which approach or exceed the symbol period of the transmitted symbol. Frequency selective fading channels are also known as *wideband channels* since the bandwidth of the signal $s(t)$ is wider than the bandwidth of the channel impulse response. As time varies, the channel varies in gain and phase across the spectrum of $s(t)$, resulting in time varying distortion in the received signal $r(t)$. To summarize, a signal undergoes frequency selective fading if

$$B_S > B_C \tag{4.43}$$

and

$$T_S < \sigma_\tau. \tag{4.44}$$

A common rule of thumb is that a channel is frequency selective if $\sigma_\tau > 0.1T_s$, although this is dependent on the specific type of modulation used. Chapter 5 presents simulation results which illustrate the impact of time delay spread on bit error rate (BER).

4.5.2 Fading Effects Due to Doppler Spread

4.5.2.1 Fast Fading

Depending on how rapidly the transmitted baseband signal changes as compared to the rate of change of the channel, a channel may be classified either as a *fast fading* or *slow fading* channel. In a *fast fading channel*, the channel impulse response changes rapidly within the symbol duration. That is, the coherence time of the channel is smaller than the symbol period of the transmitted signal. This causes frequency dispersion (also called time selective fading) due to Doppler spreading, which leads to signal distortion. Viewed in the frequency domain, signal distortion due to fast fading increases with increasing Doppler

spread relative to the bandwidth of the transmitted signal. Therefore, a signal undergoes fast fading if

$$T_S > T_C \tag{4.45}$$

and

$$B_S < B_D \tag{4.46}$$

It should be noted that when a channel is specified as a fast or slow fading channel, it does not specify whether the channel is flat fading or frequency selective in nature. Fast fading only deals with the rate of change of the channel due to motion. In the case of the flat fading channel, we can approximate the impulse response to be simply a delta function (no time delay). Hence, a *flat fading, fast fading* channel is a channel in which the amplitude of the delta function varies faster than the rate of change of the transmitted baseband signal. In the case of a *frequency selective, fast fading* channel, the amplitudes, phases, and time delays of any one of the multipath components vary faster than the rate of change of the transmitted signal. In practice, fast fading only occurs for very low data rates.

4.5.2.2 Slow Fading

In a *slow fading channel*, the channel impulse response changes at a rate much slower than the transmitted baseband signal *s(t)*. In this case, the channel may be assumed to be static over one or several reciprocal bandwidth intervals. In the frequency domain, this implies that the Doppler spread of the channel is much less than the bandwidth of the baseband signal. Therefore, a signal undergoes slow fading if

$$T_S \ll T_C \tag{4.47}$$

and

$$B_S \gg B_D \tag{4.48}$$

It should be clear that the velocity of the mobile (or velocity of objects in the channel) and the baseband signaling determines whether a signal undergoes fast fading or slow fading.

The relation between the various multipath parameters and the type of fading experienced by the signal are summarized in Figure 4.14. Over the years, some authors have confused the terms fast and slow fading with the terms large-scale and small-scale fading. It should be emphasized that fast and slow fading deal with the relationship between the time rate of change in the channel and the transmitted signal, and not with propagation path loss models.

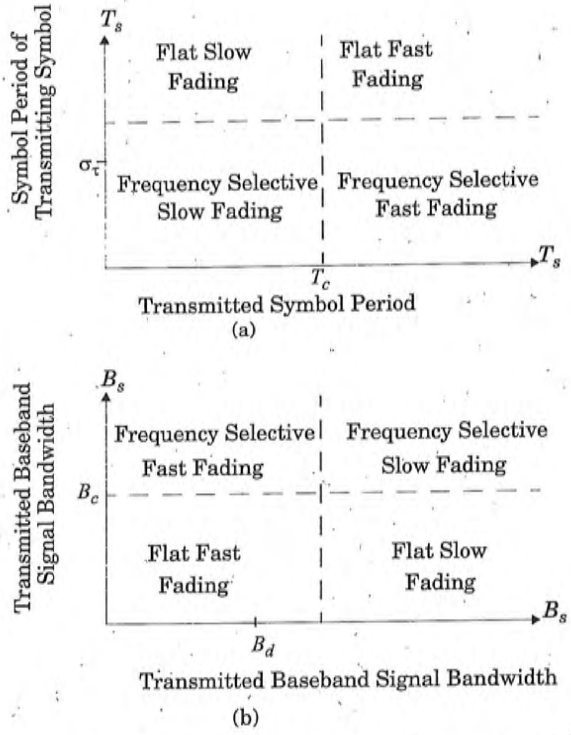

Figure 4.14
Matrix illustrating type of fading experienced by a signal as a function of
(a) symbol period
(b) baseband signal bandwidth.

4.6 Rayleigh and Ricean Distributions

4.6.1 Rayleigh Fading Distribution

In mobile radio channels, the Rayleigh distribution is commonly used to describe the statistical time varying nature of the received envelope of a flat fading signal, or the envelope of an individual multipath component. It is well known that the envelope of the sum of two quadrature Gaussian noise signals obeys a Rayleigh distribution. Figure 4.15 shows a Rayleigh distributed signal envelope as a function of time. The Rayleigh distribution has a probability density function (pdf) given by

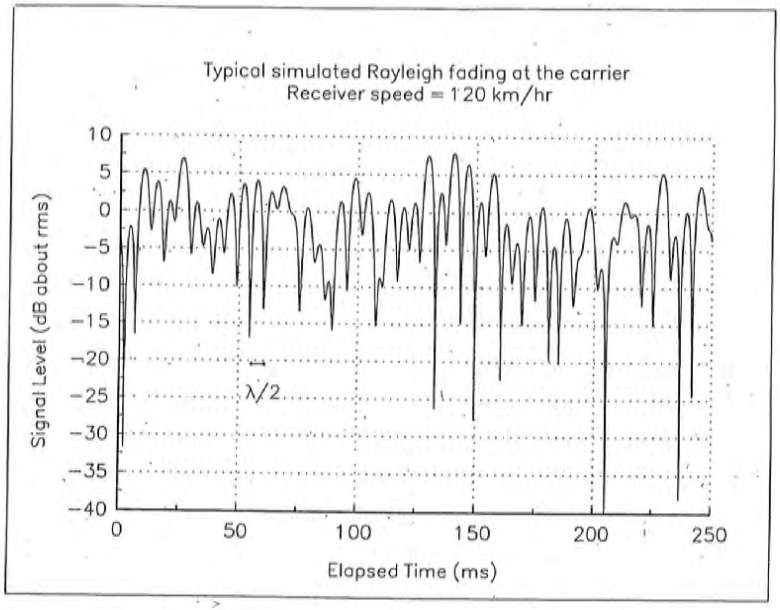

Figure 4.15
A typical Rayleigh fading envelope at 900 MHz [From [Fun93] © IEEE].

$$p(r) = \begin{cases} \dfrac{r}{\sigma^2}\exp\left(-\dfrac{r^2}{2\sigma^2}\right) & (0 \le r \le \infty) \\ 0 & (r < 0) \end{cases} \tag{4.49}$$

where σ is the rms value of the received voltage signal before *envelope detection*, and σ^2 is the time-average power of the received signal *before* envelope detection. The probability that the envelope of the received signal does not exceed a specified value R is given by the corresponding cumulative distribution function (CDF)

$$P(R) = Pr(r \le R) = \int_0^R p(r)\,dr = 1 - \exp\left(-\frac{R^2}{2\sigma^2}\right) \tag{4.50}$$

The mean value r_{mean} of the Rayleigh distribution is given by

$$r_{mean} = E[r] = \int_0^\infty r p(r)\,dr = \sigma\sqrt{\frac{\pi}{2}} = 1.2533\sigma \tag{4.51}$$

and the variance of the Rayleigh distribution is given by σ_r^2, which represents the ac power in the signal envelope

$$\sigma_r^2 = E[r^2] - E^2[r] = \int_0^\infty r^2 p(r)\,dr - \frac{\sigma^2\pi}{2} \tag{4.52}$$

$$= \sigma^2\left(2 - \frac{\pi}{2}\right) = 0.4292\sigma^2$$

The rms value of the envelope is the square root of the mean square, or $\sqrt{2}\sigma$.

The median value of r is found by solving

$$\frac{1}{2} = \int_0^{r_{median}} p(r)\,dr \tag{4.53}$$

and is

$$r_{median} = 1.177\sigma \tag{4.54}$$

Thus the mean and the median differ by only 0.55 dB in a Rayleigh fading signal. Note that the median is often used in practice, since fading data are usually measured in the field and a particular distribution cannot be assumed. By using median values instead of mean values it is easy to compare different fading distributions which may have widely varying means. Figure 4.16 illustrates the Rayleigh pdf. The corresponding Rayleigh cumulative distribution function (CDF) is shown in Figure 4.17.

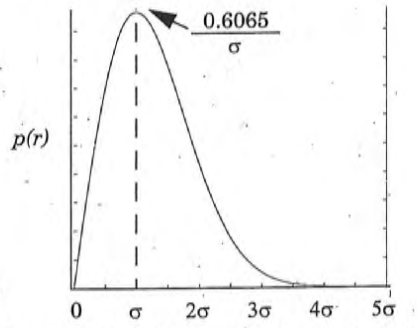

Figure 4.16
Rayleigh probability density function (pdf).

4.6.2 Ricean Fading Distribution

When there is a dominant stationary (nonfading) signal component present, such as a line-of-sight propagation path, the small-scale fading envelope

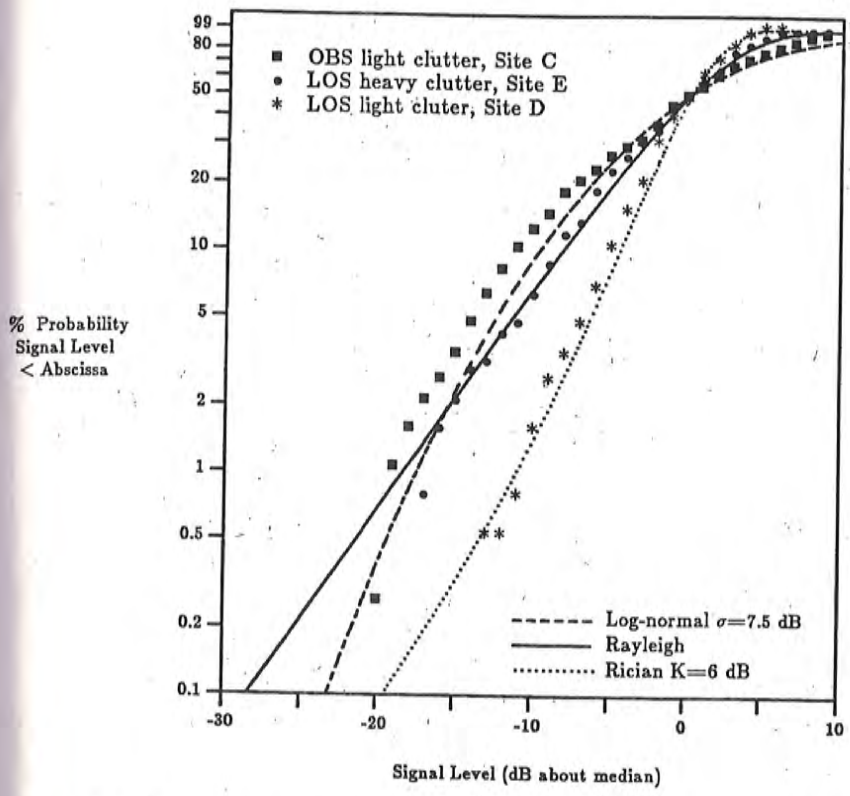

Figure 4.17
Cumulative distribution for three small-scale fading measurements and their fit to Rayleigh, Ricean, and log-normal distributions [From [Rap89] © IEEE].

distribution is Ricean. In such a situation, random multipath components arriving at different angles are superimposed on a stationary dominant signal. At the output of an envelope detector, this has the effect of adding a dc component to the random multipath.

Just as for the case of detection of a sine wave in thermal noise [Ric48], the effect of a dominant signal arriving with many weaker multipath signals gives rise to the Ricean distribution. As the dominant signal becomes weaker, the composite signal resembles a noise signal which has an envelope that is Rayleigh. Thus, the Ricean distribution degenerates to a Rayleigh distribution when the dominant component fades away.

The Ricean distribution is given by

$$p(r) = \begin{cases} \frac{r}{\sigma^2} e^{-\frac{(r^2+A^2)}{2\sigma^2}} I_0\left(\frac{Ar}{\sigma^2}\right) & \text{for } (A \geq 0, r \geq 0) \\ 0 & \text{for } (r < 0) \end{cases} \tag{4.55}$$

The parameter A denotes the peak amplitude of the dominant signal and $I_0(\cdot)$ is the modified Bessel function of the first kind and zero-order. The Ricean distribution is often described in terms of a parameter K which is defined as the ratio between the deterministic signal power and the variance of the multipath. It is given by $K = A^2/(2\sigma^2)$ or, in terms of dB

$$K(\text{dB}) = 10\log\frac{A^2}{2\sigma^2} \text{ dB} \tag{4.56}$$

The parameter K is known as the Ricean factor and completely specifies the Ricean distribution. As $A \to 0, K \to -\infty$ dB, and as the dominant path decreases in amplitude, the Ricean distribution degenerates to a Rayleigh distribution. Figure 4.18 shows the Ricean pdf. The Ricean CDF is compared with the Rayleigh CDF in Figure 4.17.

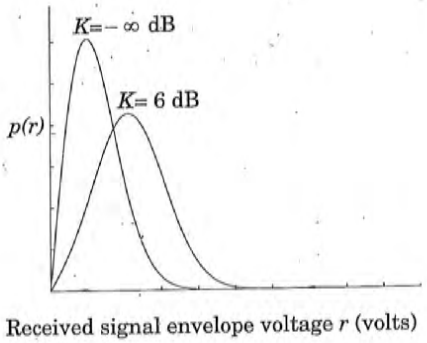

Figure 4.18
Probability density function of Ricean distributions: $K = -\infty$ dB (Rayleigh) and $K = 6$ dB. For K>>1, the Ricean pdf is approximately Gaussian about the mean.

4.7 Statistical Models for Multipath Fading Channels

Several multipath models have been suggested to explain the observed statistical nature of a mobile channel. The first model presented by Ossana [Oss64] was based on interference of waves incident and reflected from the flat sides of randomly located buildings. Although Ossana's model [Oss64] predicts flat fading power spectra that were in agreement with measurements in suburban

areas, it assumes the existence of a direct path between the transmitter and receiver, and is limited to a restricted range of reflection angles. Ossana's model is therefore rather inflexible and inappropriate for urban areas where the direct path is almost always blocked by buildings or other obstacles. Clarke's model [Cla68] is based on scattering and is widely used.

4.7.1 Clarke's Model for Flat Fading

Clarke [Cla68] developed a model where the statistical characteristics of the electromagnetic fields of the received signal at the mobile are deduced from scattering. The model assumes a fixed transmitter with a vertically polarized antenna. The field incident on the mobile antenna is assumed to comprise of N azimuthal plane waves with arbitrary carrier phases, arbitrary azimuthal angles of arrival, and each wave having equal average amplitude. It should be noted that the equal average amplitude assumption is based on the fact that in the absence of a direct line-of-sight path, the scattered components arriving at a receiver will experience similar attenuation over small-scale distances.

Figure 4.19 shows a diagram of plane waves incident on a mobile traveling at a velocity v, in the x-direction. The angle of arrival is measured in the x-y plane with respect to the direction of motion. Every wave that is incident on the mobile undergoes a Doppler shift due to the motion of the receiver and arrives at the receiver at the same time. That is, no excess delay due to multipath is assumed for any of the waves (flat fading assumption). For the n th wave arriving at an angle α_n to the x-axis, the Doppler shift in Hertz is given by

$$f_n = \frac{v}{\lambda}\cos\alpha_n \tag{4.57}$$

where λ is the wavelength of the incident wave.

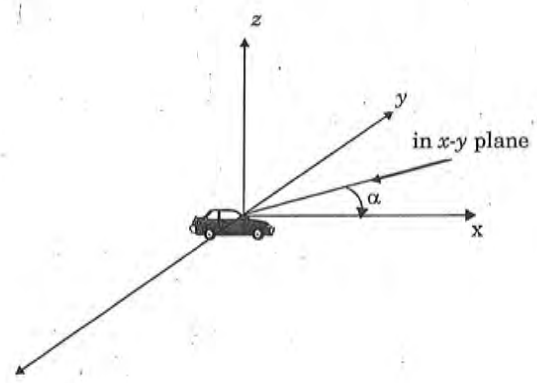

Figure 4.19
Illustrating plane waves arriving at random angles.

The vertically polarized plane waves arriving at the mobile have E and H field components given by

$$E_z = E_o \sum_{n=1}^{N} C_n \cos(2\pi f_c t + \theta_n) \tag{4.58}$$

$$H_x = -\frac{E_o}{\eta} \sum_{n=1}^{N} C_n \sin\alpha_n \cos(2\pi f_c t + \theta_n) \tag{4.59}$$

$$H_y = -\frac{E_o}{\eta} \sum_{n=1}^{N} C_n \cos\alpha_n \cos(2\pi f_c t + \theta_n) \tag{4.60}$$

where E_0 is the real amplitude of local average E-field (assumed constant), C_n is a real random variable representing the amplitude of individual waves, η is the intrinsic impedance of free space (377Ω), and f_c is the carrier frequency. The random phase of the n th arriving component θ_n is given by

$$\theta_n = 2\pi f_n t + \phi_n \tag{4.61}$$

The amplitudes of the E-and H-field are normalized such that the ensemble average of the C_n's is given by

$$\sum_{n=1}^{N} \overline{C_n^2} = 1 \tag{4.62}$$

Since the Doppler shift is very small when compared to the carrier frequency, the three field components may be modeled as narrow band random processes. The three components E_z, H_x, and H_y can be approximated as Gaussian random variables if N is sufficiently large. The phase angles are assumed to have a uniform probability density function (pdf) on the interval $(0,2\sigma]$. Based on the analysis by Rice [Ric48] the E-field can be expressed in an in-phase and quadrature form

$$E_z = T_c(t)\cos(2\pi f_c t) - T_s(t)\sin(2\pi f_c t) \tag{4.63}$$

where

$$T_c(t) = E_0 \sum_{n=1}^{N} C_n \cos(2\pi f_n t + \phi_n) \tag{4.64}$$

and

$$T_s(t) = E_0 \sum_{n=1}^{N} C_n \sin(2\pi f_n t + \phi_n) \tag{4.65}$$

Both $T_c(t)$ and $T_s(t)$ are Gaussian random processes which are denoted as T_c and T_s, respectively, at any time t. T_c and T_s are uncorrelated zero-mean Gaussian random variables with an equal variance given by

$$\overline{T_c^2} = \overline{T_s^2} = \overline{|E_z|^2} = E_0^2/2 \tag{4.66}$$

where the overbar denotes the ensemble average.

The envelope of the received E-field, $E_z(t)$, is given by

$$|E_z(t)| = \sqrt{T_c^2(t) + T_s^2(t)} = r(t) \tag{4.67}$$

Since T_c and T_s are Gaussian random variables, it can be shown through a Jacobean transformation [Pap91] that the random received signal envelope r has a Rayleigh distribution given by

$$p(r) = \begin{cases} \dfrac{r}{\sigma^2}\exp\left(-\dfrac{r^2}{2\sigma^2}\right) & 0 \le r \le \infty \\ 0 & r < 0 \end{cases} \tag{4.68}$$

where $\sigma^2 = E_0^2/2$

4.7.1.1 Spectral Shape Due to Doppler Spread in Clarke's Model

Gans [Gan72] developed a spectrum analysis for Clarke's model. Let $p(\alpha)\,d\alpha$ denote the fraction of the total incoming power within $d\alpha$ of the angle α, and let A denote the average received power with respect to an isotropic antenna. As $N \to \infty$, $p(\alpha)\,d\alpha$ approaches a continuous, rather than a discrete, distribution. If $G(\alpha)$ is the azimuthal gain pattern of the mobile antenna as a function of the angle of arrival, the total received power can be expressed as

$$P_r = \int_0^{2\pi} AG(\alpha)\,p(\alpha)\,d\alpha \tag{4.69}$$

where $AG(\alpha)\,p(\alpha)\,d\alpha$ is the differential variation of received power with angle. If the scattered signal is a CW signal of frequency f_c, then the instantaneous frequency of the received signal component arriving at an angle α is obtained using equation (4.57)

$$f(\alpha) = f = \frac{v}{\lambda}\cos(\alpha) + f_c = f_m \cos\alpha + f_c \tag{4.70}$$

where f_m is the maximum Doppler shift. It should be noted that $f(\alpha)$ is an even function of α, (i.e., $f(\alpha) = f(-\alpha)$).

If $S(f)$ is the power spectrum of the received signal, the differential variation of received power with frequency is given by

$$S(f)\,|df| \tag{4.71}$$

Equating the differential variation of received power with frequency to the differential variation in received power with angle, we have

$$S(f)\,|df| = A\,[p(\alpha)\,G(\alpha) + p(-\alpha)\,G(-\alpha)]\,|d\alpha| \tag{4.72}$$

Differentiating equation (4.70), and rearranging the terms, we have

$$|df| = |d\alpha|\,|-\sin\alpha| f_m \tag{4.73}$$

Using equation (4.70), α can be expressed as a function of f as

$$\alpha = \cos^{-1}\left[\frac{f-f_c}{f_m}\right] \tag{4.74}$$

This implies that

$$\sin\alpha = \sqrt{1-\left(\frac{f-f_c}{f_m}\right)^2} \tag{4.75}$$

Substituting equation (4.73) and (4.75) into both sides of (4.72), the power spectral density $S(f)$ can be expressed as

$$S(f) = \frac{A\,[p(\alpha)\,G(\alpha) + p(-\alpha)\,G(-\alpha)]}{f_m\sqrt{1-\left(\frac{f-f_c}{f_m}\right)^2}} \tag{4.76}$$

where

$$S(f) = 0, \qquad |f-f_c| > f_m \tag{4.77}$$

The spectrum is centered on the carrier frequency and is zero outside the limits of $f_c \pm f_m$. Each of the arriving waves has its own carrier frequency (due to its direction of arrival) which is slightly offset from the center frequency. For the case of a vertical $\lambda/4$ antenna ($G(\alpha) = 1.5$), and a uniform distribution $p(\alpha) = 1/2\pi$ over 0 to 2π, the output spectrum is given by (4.76) as

$$S_{E_z}(f) = \frac{1.5}{\pi f_m\sqrt{1-\left(\frac{f-f_c}{f_m}\right)^2}} \tag{4.78}$$

In equation (4.78) the power spectral density at $f = f_c \pm f_m$ is infinite, i.e., Doppler components arriving at exactly 0° and 180° have an infinite power spectral density. This is not a problem since α is continuously distributed and the probability of components arriving at exactly these angles is zero.

Figure 4.20 shows the power spectral density of the resulting RF signal due to Doppler fading. Smith [Smi75] demonstrated an easy way to simulate Clarke's model using a computer simulation as described Section 4.7.2.

After envelope detection of the Doppler-shifted signal, the resulting baseband spectrum has a maximum frequency of $2f_m$. It can be shown [Jak74] that the electric field produces a baseband power spectral density given by

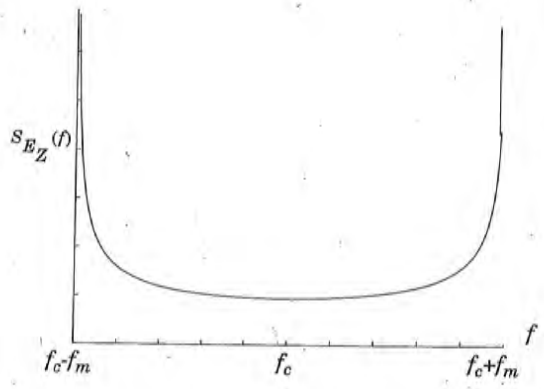

Figure 4.20
Doppler power spectrum for an unmodulated CW carrier [From [Gan72]] © IEEE].

$$S_{bbE_z}(f) = \frac{1}{8\pi f_m} K\left[\sqrt{1-\left(\frac{f}{2f_m}\right)^2}\right] \tag{4.79}$$

where $K[\cdot]$ is the complete elliptical integral of the first kind. Equation (4.79) is not intuitive and is a result of the temporal correlation of the received signal when passed through a nonlinear envelope detector. Figure 4.21 illustrates the baseband spectrum of the received signal after envelope detection.

The spectral shape of the Doppler spread determines the time domain fading waveform and dictates the temporal correlation and fade slope behaviors. Rayleigh fading simulators must use a fading spectrum such as equation (4.78) in order to produce realistic fading waveforms that have proper time correlation.

4.7.2 Simulation of Clarke and Gans Fading Model

It is often useful to simulate multipath fading channels in hardware or software. A popular simulation method uses the concept of in-phase and quadrature modulation paths to produce a simulated signal with spectral and temporal characteristics very close to measured data.

As shown in Figure 4.22, two independent Gaussian low pass noise sources are used to produce in-phase and quadrature fading branches. Each Gaussian source may be formed by summing two independent Gaussian random variables which are orthogonal (i.e., $g = a + jb$, where a and b are real Gaussian random variables and g is complex Gaussian). By using the spectral filter defined by equation (4.78) to shape the random signals in the frequency domain, accurate time domain waveforms of Doppler fading can be produced by using an inverse fast Fourier transform (IFFT) at the last stage of the simulator.

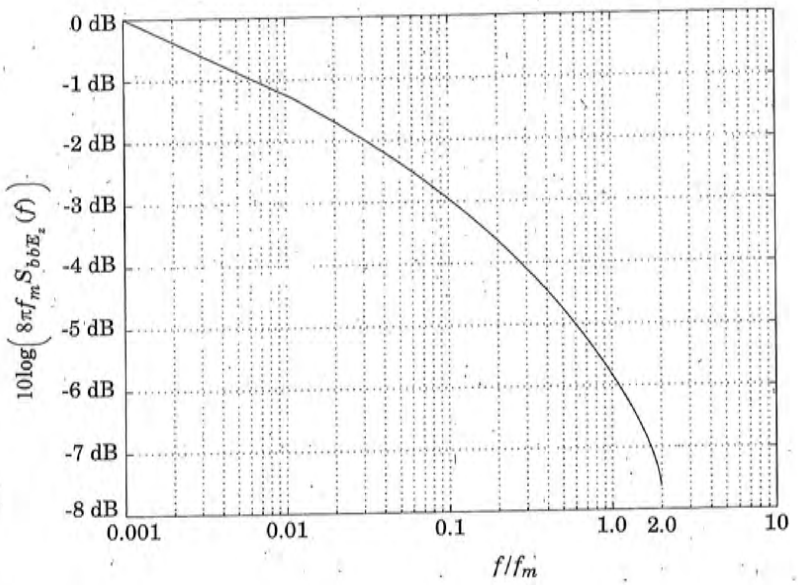

Figure 4.21
Baseband power spectral density of a CW Doppler signal after envelope detection.

Smith [Smi75] demonstrated a simple computer program that implements Figure 4.22(b). His method uses a complex Gaussian random number generator (noise source) to produce a baseband line spectrum with complex weights in the positive frequency band. The maximum frequency component of the line spectrum is f_m. Using the property of real signals, the negative frequency components are constructed by simply conjugating the complex Gaussian values obtained for the positive frequencies. Note that the IFFT of this signal is a purely real Gaussian random process in the time domain which is used in one of the quadrature arms shown in Figure 4.22. The random valued line spectrum is then multiplied with a discrete frequency representation of $\sqrt{S_{E_z}(f)}$ having the same number of points as the noise source. To handle the case where equation (4.78) approaches infinity at the passband edge, Smith truncated the value of $S_{E_z}(f_m)$ by computing the slope of the function at the sample frequency just prior to the passband edge and extended the slope to the passband edge. Simulations using the architecture in Figure 4.22 are usually implemented in the frequency domain using complex Gaussian line spectra to take advantage of easy implementation of equation (4.78). This, in turn, implies that the low pass Gaus-

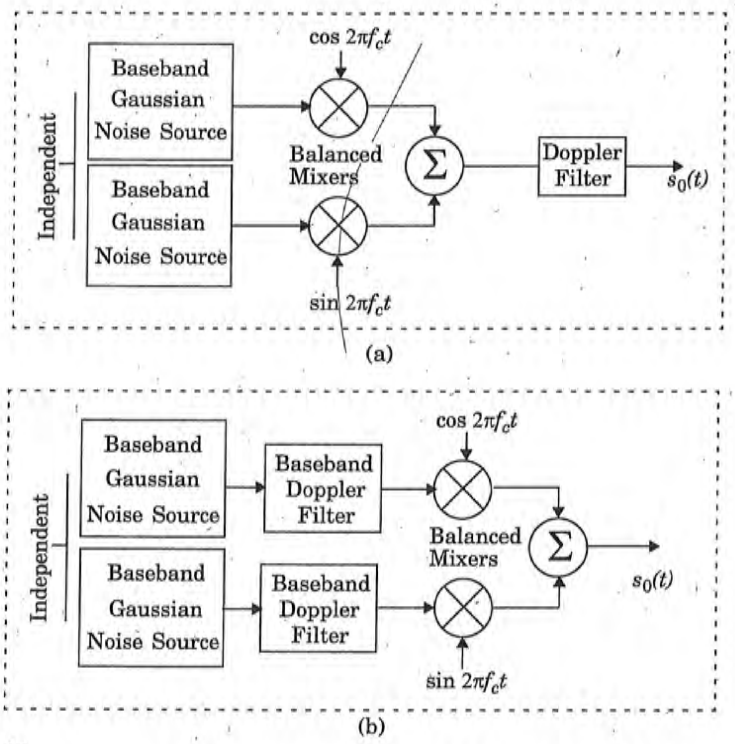

Figure 4.22
Simulator using quadrature amplitude modulation with (a) RF Doppler filter and (b) baseband Doppler filter.

sian noise components are actually a series of frequency components (line spectrum from $-f_m$ to f_m), which are equally spaced and each have a complex Gaussian weight. Smith's simulation methodology is shown in Figure 4.23.

To implement the simulator shown in Figure 4.23, the following steps are used:

(1) Specify the number of frequency domain points (N) used to represent $\sqrt{S_{E_z}(f)}$ and the maximum Doppler frequency shift (f_m). The value used for N is usually a power of 2.

(2) Compute the frequency spacing between adjacent spectral lines as $\Delta f = 2f_m/(N-1)$. This defines the time duration of a fading waveform, $T = 1/\Delta f$.

(3) Generate complex Gaussian random variables for each of the $N/2$ positive frequency components of the noise source.

(4) Construct the negative frequency components of the noise source by conju-

gating positive frequency values and assigning these at negative frequency values.

(5) Multiply the in-phase and quadrature noise sources by the fading spectrum $\sqrt{S_{E_z}(f)}$.

(6) Perform an IFFT on the resulting frequency domain signal from the in-phase and quadrature arms, and compute the sum of the squares of each signal.

(7) Take the square root of the sum obtained in step 6 to obtain an N point time series of a simulated Rayleigh fading signal with the proper Doppler spread and time correlation.

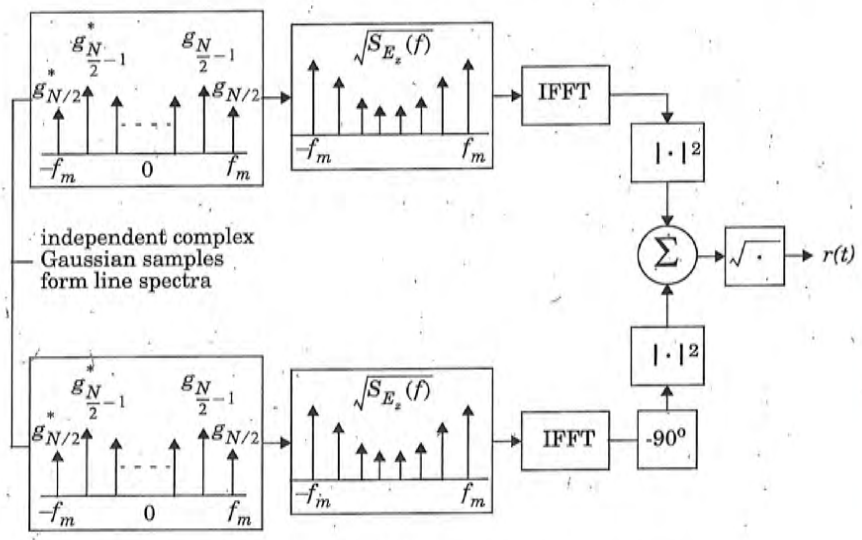

Figure 4.23
Frequency domain implementation of a Rayleigh fading simulator at baseband

Several Rayleigh fading simulators may be used in conjunction with variable gains and time delays to produce frequency selective fading effects. This is shown in Figure 4.24.

By making a single frequency component dominant in amplitude within $\sqrt{S_{E_z}(f)}$, the fading is changed from Rayleigh to Ricean. This can be used to alter the probability distributions of the individual multipath components in the simulator of Figure 4.24.

To determine the impact of flat fading on an applied signal $s(t)$, one merely needs to multiply the applied signal by $r(t)$, the output of the fading simulator. To determine the impact of more than one multipath component, a convolution must be performed as shown in Figure 4.24.

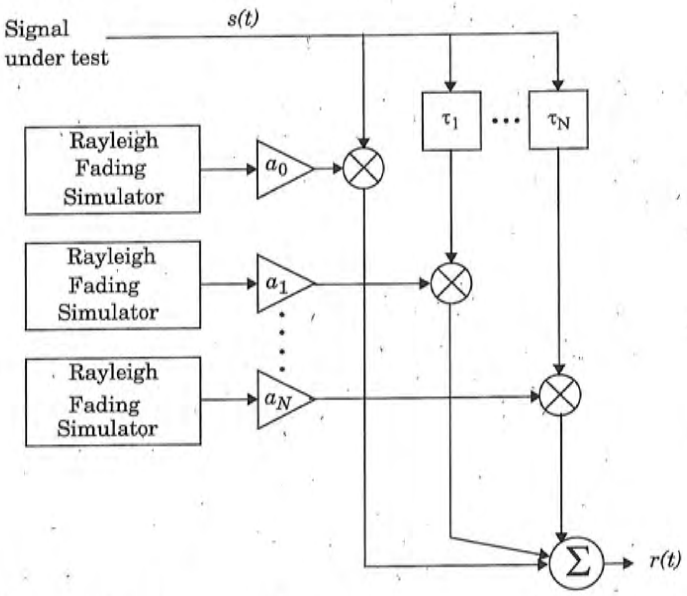

Figure 4.24
A signal may be applied to a Rayleigh fading simulator to determine performance in a wide range of channel conditions. Both flat and frequency selective fading conditions may be simulated, depending on gain and time delay settings.

4.7.3 Level Crossing and Fading Statistics

Rice computed joint statistics for a mathematical problem which is similar to Clarke's fading model [Cla68], and thereby provided simple expressions for computing the average number of level crossing and the duration of fades. The *level crossing rate* (LCR) and *average fade duration* of a Rayleigh fading signal are two important statistics which are useful for designing error control codes and diversity schemes to be used in mobile communication systems, since it becomes possible to relate the time rate of change of the received signal to the signal level and velocity of the mobile.

The *level crossing rate* (LCR) is defined as the expected rate at which the Rayleigh fading envelope, normalized to the local rms signal level, crosses a specified level in a positive-going direction. The number of level crossings per second is given by

$$N_R = \int_0^\infty \dot{r}\, p(R, \dot{r})\, d\dot{r} = \sqrt{2\pi} f_m \rho e^{-\rho^2} \tag{4.80}$$

where $\dot{r}$ is the time derivative of $r(t)$ (i.e., the slope), $p(R, \dot{r})$ is the joint density function of r and $\dot{r}$ at $r = R$, f_m is the maximum Doppler frequency and $\rho = R/R_{rms}$ is the value of the specified level R, normalized to the local rms amplitude of the fading envelope [Jak74]. Equation (4.80) gives the value of N_R, the average number of level crossings per second at specified R. The level crossing rate is a function of the mobile speed as is apparent from the presence of f_m in equation (4.80). There are few crossings at both high and low levels, with the maximum rate occurring at $\rho = 1/\sqrt{2}$, (i.e., at a level 3 dB below the rms level). The signal envelope experiences very deep fades only occasionally, but shallow fades are frequent.

Example 4.6

For a Rayleigh fading signal, compute the positive-going level crossing rate for $\rho = 1$, when the maximum Doppler frequency (f_m) is 20 Hz. What is the maximum velocity of the mobile for this Doppler frequency if the carrier frequency is 900 MHz?

Solution to Example 4.6

Using equation (4.80), the number of zero level crossings is

$$N_R = \sqrt{2\pi}\,(20)\,(1)\,e^{-1} = 18.44 \text{ crossings per second}$$

The maximum velocity of the mobile can be obtained using the Doppler relation, $f_{d,\,max} = v/\lambda$.

Therefore velocity of the mobile at $f_m = 20$ Hz is

$$v = f_d\lambda = 20 \text{ Hz}\,(1/3 \text{ m}) = 6.66 \text{ m/s} = 24 \text{ km/hr}$$

The *average fade duration* is defined as the average period of time for which the received signal is below a specified level R. For a Rayleigh fading signal, this is given by

$$\bar{\tau} = \frac{1}{N_R} Pr[r \le R] \tag{4.81}$$

where $Pr[r \le R]$ is the probability that the received signal r is less than R and is given by

$$Pr[r \le R] = \frac{1}{T}\sum_i \tau_i \tag{4.82}$$

where τ_i is the duration of the fade and T is the observation interval of the fading signal. The probability that the received signal r is less than the threshold R is found from the Rayleigh distribution as

$$P_r[r \le R] = \int_0^R p(r)\,dr = 1 - \exp(-\rho^2) \tag{4.83}$$

where $p(r)$ is the pdf of a Rayleigh distribution. Thus, using equations (4.80), (4.81), and (4.83), the average fade duration as a function of ρ and f_m can be expressed as

$$\bar{\tau} = \frac{e^{\rho^2} - 1}{\rho f_m \sqrt{2\pi}} \tag{4.84}$$

The average duration of a signal fade helps determine the most likely number of signaling bits that may be lost during a fade. Average fade duration primarily depends upon the speed of the mobile, and decreases as the maximum Doppler frequency f_m becomes large. If there is a particular fade margin built into the mobile communication system, it is appropriate to evaluate the receiver performance by determining the rate at which the input signal falls below a given level R, and how long it remains below the level, on average. This is useful for relating SNR during a fade to the instantaneous BER which results.

Example 4.7

Find the average fade duration for threshold levels $\rho = 0.01$, $\rho = 0.1$, and $\rho = 1$, when the Doppler frequency is 200 Hz.

Solution to Example 4.7

Average fade duration can be found by substituting the given values in equation (4.75)

For $\rho = 0.01$

$$\bar{\tau} = \frac{e^{0.01^2} - 1}{(0.01)\,200\sqrt{2\pi}} = 19.9\mu s$$

For $\rho = 0.1$

$$\bar{\tau} = \frac{e^{0.1^2} - 1}{(0.1)\,200\sqrt{2\pi}} = 200\mu s$$

For $\rho = 1$

$$\bar{\tau} = \frac{e^{1^2} - 1}{(1)\,200\sqrt{2\pi}} = 3.43 \text{ ms}$$

Example 4.8

Find the average fade duration for a threshold level of $\rho = 0.707$ when the Doppler frequency is 20 Hz. For a binary digital modulation with bit duration of 50 bps, is the Rayleigh fading slow or fast? What is the average number of bit errors per second for the given data rate. Assume that a bit error occurs whenever any portion of a bit encounters a fade for which $\rho < 0.1$.

Solution to Example 4.8

The average fade duration can be obtained using equation (4.84).

$$\bar{\tau} = \frac{e^{0.707^2} - 1}{(0.707)\, 20\sqrt{2\pi}} = 18.3 \text{ ms}$$

For a data rate of 50 bps, the bit period is 20 ms. Since the bit period is greater than the average fade duration, for the given data rate the signal undergoes fast Rayleigh fading. Using equation (4.84), the average fade duration for $\rho = 0.1$ is equal to 0.002 s. This is less than the duration of one bit. Therefore, only one bit on average will be lost during a fade. Using equation (4.80), the number of level crossings for $\rho = 0.1$ is $N_r = 4.96$ crossings per seconds. Since a bit error is assumed to occur whenever a portion of a bit encounters a fade, and since average fade duration spans only a fraction of a bit duration, the total number of bits in error is 5 per second, resulting in a BER = (5/50) = 0.1.

4.7.4 Two-ray Rayleigh Fading Model

Clarke's model and the statistics for Rayleigh fading are for flat fading conditions and do not consider multipath time delay. In modern mobile communication systems with high data rates, it has become necessary to model the effects of multipath delay spread as well as fading. A commonly used multipath model is an independent Rayleigh fading 2-ray model (which is a specific implementation of the generic fading simulator shown in Figure 4.24). Figure 4.25 shows a block diagram of the 2-ray independent Rayleigh fading channel model. The impulse response of the model is represented as

$$h_b(t) = \alpha_1 \exp(j\phi_1)\, \delta(t) + \alpha_2 \exp(j\phi_2)\, \delta(t-\tau) \tag{4.85}$$

where α_1 and α_2 are independent and Rayleigh distributed, ϕ_1 and ϕ_2 are independent and uniformly distributed over $[0, 2\pi]$, and τ is the time delay between the two rays. By setting α_2 equal to zero, the special case of a flat Rayleigh fading channel is obtained as

$$h_b(t) = \alpha_1 \exp(j\phi_1)\, \delta(t) \tag{4.86}$$

By varying τ, it is possible to create a wide range of frequency selective fading effects. The proper time correlation properties of the Rayleigh random variables α_1 and α_2 are guaranteed by generating two independent waveforms, each produced from the inverse Fourier transform of the spectrum described in Section 4.7.2.

4.7.5 Saleh and Valenzuela Indoor Statistical Model

Saleh and Valenzuela [Sal87] reported the results of indoor propagation measurements between two vertically polarized omni-directional antennas located on the same floor of a medium sized office building. Measurements were made using 10 ns, 1.5 GHz, radar-like pulses. The method involved averaging the square law detected pulse response while sweeping the frequency of the

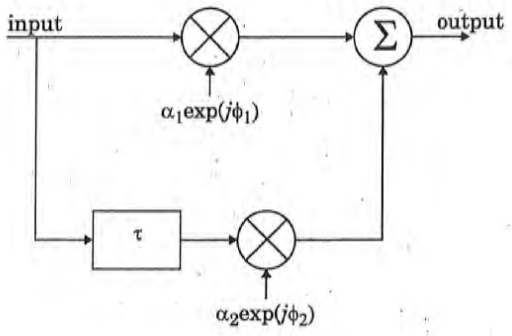

Figure 4.25
Two-ray Rayleigh fading model.

transmitted pulse. Using this method, multipath components within 5 ns were resolvable.

The results obtained by Saleh and Valenzula show that: (a) the indoor channel is quasi-static or very slowly time varying, and (b) the statistics of the channel impulse response are independent of transmitting and receiving antenna polarization, if there is no line-of-sight path between them. They reported a maximum multipath delay spread of 100 ns to 200 ns within the rooms of a building, and 300 ns in hallways. The measured rms delay spread within rooms had a median of 25 ns and a maximum of 50 ns. The large-scale path loss with no line-of-sight path was found to vary over a 60 dB range and obey a log-distance power law (see equation (3.68)) with an exponent between 3 and 4.

Saleh and Valenzuela developed a simple multipath model for indoor channels based on measurement results. The model assumes that the multipath components arrive in clusters. The amplitudes of the received components are independent Rayleigh random variables with variances that decay exponentially with cluster delay as well as excess delay within a cluster. The corresponding phase angles are independent uniform random variables over $[0,2\pi]$. The clusters and multipath components within a cluster form Poisson arrival processes with different rates. The clusters and multipath components within a cluster have exponentially distributed interarrival times. The formation of the clusters is related to the building structure, while the components within the cluster are formed by multiple reflections from objects in the vicinity of the transmitter and the receiver.

4.7.6 SIRCIM and SMRCIM Indoor and Outdoor Statistical Models

Rappaport and Seidel [Rap91a] reported measurements at 1300 MHz in five factory buildings and carried out subsequent measurements in other types of

buildings. The authors developed an elaborate, empirically derived statistical model based on the discrete impulse response channel model and wrote a computer program called SIRCIM (Simulation of Indoor Radio Channel Impulse-response Models). SIRCIM generates realistic samples of small-scale indoor channel impulse response measurements [Rap91a]. Subsequent work by Huang produced SMRCIM (Simulation of Mobile Radio Channel Impulse-response Models), a similar program that generates small-scale urban cellular and microcellular channel impulse responses [Rap93a]. These programs are currently in use at over 100 institutions throughout the world.

By recording power delay profile impulse responses at $\lambda/4$ intervals on a 1 m track at many indoor measurement locations, the authors were able to characterize local small-scale fading of individual multipath components, and the small-scale variation in the number and arrival times of multipath components within a local area. Thus, the resulting statistical models are functions of multipath time delay bin τ_i, the small-scale receiver spacing, X_l, within a 1 m local area, the topography S_m which is either line-of-sight (LOS) or obstructed, the large-scale T-R separation distance D_n, and the particular measurement location P_n. Therefore, each individual baseband power delay profile is expressed in a manner similar to equation (4.13), except the random amplitudes and time delays are random variables which depend on the surrounding environment. Phases are synthesized using a pseudo-deterministic model which provides realistic results, so that a complete time varying complex baseband channel impulse response $h_b(t;\tau_i)$ may be obtained over a local area through simulation.

$$h_b(t, X_l, S_m, D_n, P_n) = \sum_i A_i(\tau_i, X_l, S_m, D_n, P_n)\, e^{j\theta_i[\tau_i, X_l, S_m, D_n, P_n]} \delta(t - \tau_i(X_l, S_m, D_n, P_n)) \tag{4.87}$$

In equation (4.87), A_i^2 is the average multipath receiver power within a discrete excess delay interval of 7.8125 ns.

The measured multipath delays inside open-plan buildings ranged from 40 ns to 800 ns. Mean multipath delay and rms delay spread values ranged from 30 ns to 300 ns, with median values of 96 ns in LOS paths and 105 ns in obstructed paths. Delay spreads were found to be uncorrelated with T-R separation but were affected by factory inventory, building construction materials, building age, wall locations, and ceiling heights. Measurements in a food processing factory that manufactures dry-goods and has considerably less metal inventory than other factories had an rms delay spread that was half of those observed in factories producing metal products. Newer factories which incorporate steel beams and steel reinforced concrete in the building structure have stronger multipath signals and less attenuation than older factories which used wood and brick for perimeter walls. The data suggested that radio propagation in buildings may be described by a hybrid geometric/statistical model that accounts for both reflec-

tions from walls and ceilings and random scattering from inventory and equipment.

By analyzing the measurements from fifty local areas in many buildings, it was found that the number of multipath components, N_p, arriving at a certain location is a function of X, S_m, and P_n, and almost always has a Gaussian distribution. The average number of multipath components ranges between 9 and 36, and is generated based on an empirical fit to measurements. The probability that a multipath component will arrive at a receiver at a particular excess delay T_i in a particular environment S_m is denoted as $P_R(T_i, S_m)$. This was found from measurements by counting the total number of detected multipath components at a particular discrete excess delay time, and dividing by the total number of possible multipath components for each excess delay interval. The probabilities for multipath arriving at a particular excess delay values may be modeled as piecewise functions of excess delay, and are given by

$$P_R(T_i, S_1)_{\text{for LOS}} = \begin{cases} 1 - \dfrac{T_i}{367} & (T_i < 110 \text{ ns}) \\ 0.65 - \dfrac{(T_i - 110)}{360} & (110 \text{ ns} < T_i < 200 \text{ ns}) \\ 0.22 - \dfrac{(T_i - 200)}{1360} & (200 \text{ ns} < T_i < 500 \text{ ns}) \end{cases} \tag{4.88}$$

$$P_R(T_i, S_2)_{\text{for OBS}} = \begin{cases} 0.55 + \dfrac{T_i}{667} & (T_i < 100 \text{ ns}) \\ 0.08 + 0.62 \exp\left(-\dfrac{(T_i - 100)}{75}\right) & (100 \text{ ns} < T_i < 500 \text{ ns}) \end{cases} \tag{4.89}$$

where S_1 corresponds to the LOS topography, and S_2 corresponds to obstructed topography. SIRCIM uses the probability of arrival distributions described by equation (4.88) or (4.89) along with the probability distribution of the number of multipath components, $N_P(X, S_m, P_n)$, to simulate power delay profiles over small-scale distances. A recursive algorithm repeatedly compares equation (4.88) or (4.89) with a uniformly distributed random variable until the proper N_P is generated for each profile [Hua91], [Rap91a].

Figure 4.26 shows an example of measured power delay profiles at 19 discrete receiver locations along a 1 m track, and illustrates accompanying narrowband information which SIRCIM computes based on synthesized phases for each multipath component [Rap91a]. Measurements reported in the literature provide excellent agreement with impulse responses predicted by SIRCIM.

Using similar statistical modeling techniques, urban cellular and microcellular multipath measurement data from [Rap90], [Sei91], [Sei92a] were used to develop SMRCIM. Both large cell and microcell models were developed. Figure

4.27 shows an example of SMRCIM output for an outdoor microcell environment [Rap93a].

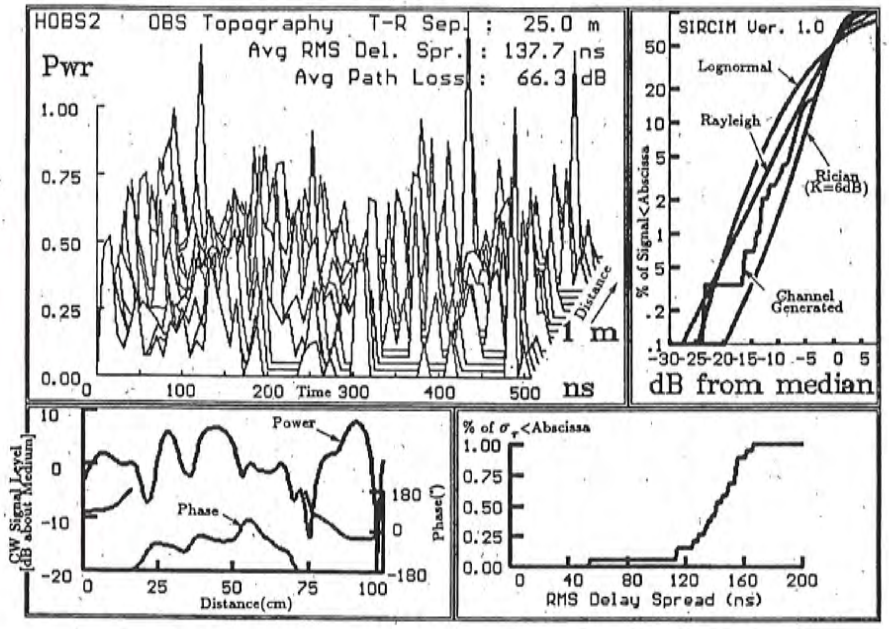

Figure 4.26
Indoor wide band impulse responses simulated by SIRCIM at 1.3 GHz. Also shown are the distributions of the rms delay spread and the narrowband signal power distribution. The channel is simulated as being obstructed in an open-plan building, T-R separation is 25 m. The rms delay spread is 137.7 ns. All multipath components and parameters are stored on disk [From [Rap93a] © IEEE].

4.8 Problems

4.1 Draw a block diagram of a binary spread spectrum sliding correlator multipath measurement system. Explain in words how it is used to measure power delay profiles.

(a) If the transmitter chip period is 10 ns, the PN sequence has length 1023, and a 6 GHz carrier is used at the transmitter, find the time between maximal correlation and the slide factor if the receiver uses a PN sequence clock that is 30 kHz slower than the transmitter.

(b) If an oscilloscope is used to display one complete cycle of the PN sequence (that is, if two successive maximal correlation peaks are to be displayed on the oscilloscope), and if 10 divisions are provided on the oscilloscope time axis, what is the most appropriate sweep setting (in seconds/divi-

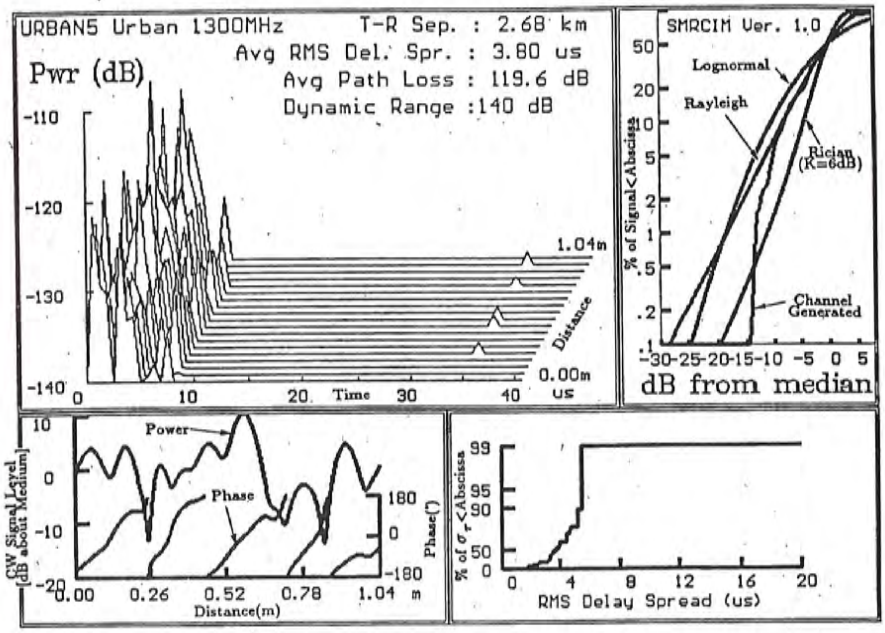

Figure 4.27
Urban wideband impulse responses simulated by SMRCIM at 1.3 GHz. Also shown are the distributions of the rms delay spread and the narrowband fading. T-R separation is 2.68 km. The rms delay spread is 3.8 μs. All multipath components and parameters are saved on disk. [From [Rap93a] © IEEE].

sion) to be used?

(c) What is the required IF passband bandwidth for this system? How is this much better than a direct pulse system with similar time resolution?

4.2 If a particular modulation provides suitable BER performance whenever $\sigma/T_s \leq 0.1$, determine the smallest symbol period T_s (and thus the greatest symbol rate) that may be sent through RF channels shown in Figure P4.2.

4.3 For the power delay profiles in Figure P4.2, estimate the 90% correlation and 50% correlation coherence bandwidths.

4.4 Approximately how large can the rms delay spread be in order for a binary modulated signal with a bit rate of 25 kbps to operate without an equalizer? What about an 8-PSK system with a bit rate of 75 kbps?

4.5 Given that the probability density function of a Rayleigh distributed envelope is given by $p(r) = \frac{r}{\sigma^2}\exp\left(\frac{-r^2}{2\sigma^2}\right)$, where σ^2 is the variance, show that the

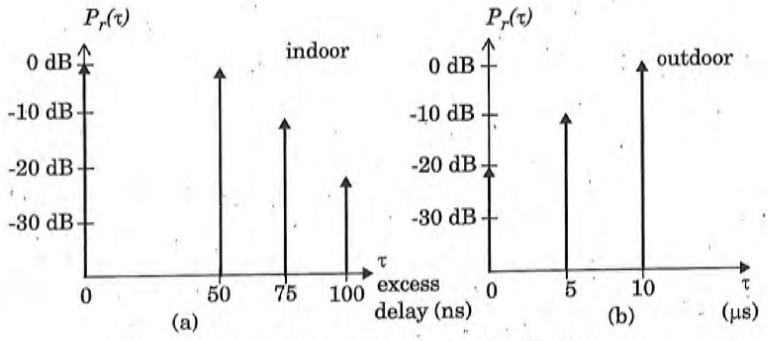

Figure P4.2: Two channel responses for Problem 4.2

cumulative distribution function is given as $p(r<R) = 1-\exp\left(\frac{-R^2}{2\sigma^2}\right)$. Find the percentage of time that a signal is 10 dB or more below the rms value for a Rayleigh fading signal.

4.6 The fading characteristics of a CW carrier in an urban area are to be measured. The following assumptions are made:
(1) The mobile receiver uses a simple vertical monopole
(2) Large-scale fading due to path loss is ignored.
(3) The mobile has no line-of-sight path to the base station.
(4) The pdf of the received signal follows a Rayleigh distribution.
(a) Derive the ratio of the desired signal level to the rms signal level that maximizes the level crossing rate. Express your answer in dB.
(b) Assuming the maximum velocity of the mobile is 50 km/hr, and the carrier frequency is 900 MHz, determine the maximum number of times the signal envelope will fade below the level found in (a) during a 1 minute test.
(c) How long, on average, will each fade in (b) last?

4.7 A vehicle receives a 900 MHz transmission while traveling at a constant velocity for 10 s. The average fade duration for a signal level 10 dB below the rms level is 1 ms. How far does the vehicle travel during the 10 s interval? How many fades does the signal undergo at the rms threshold level during a 10 s interval? Assume that the local mean remains constant during travel.

4.8 An automobile moves with velocity $v(t)$ shown in Figure P4.8. The received mobile signal experiences multipath Rayleigh fading on a 900 MHz CW carrier. What is the average crossing rate and fade duration over the 100 s interval? Assume $\rho = 0.1$ and ignore large-scale fading effects.

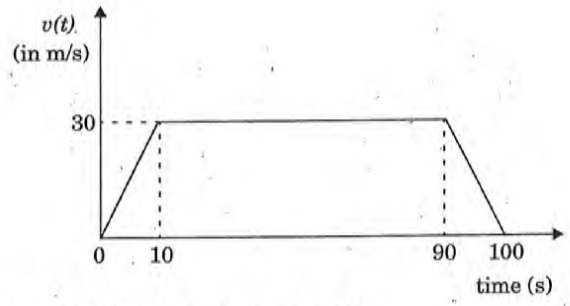

Figure P4.8 Graph of velocity of mobile.

4.9 For a mobile receiver operating at frequency of 860 MHz and moving at 100 km/hr.
(a) sketch the Doppler spectrum if a CW signal is transmitted and indicate the maximum and minium frequencies
(b) calculate the level crossing rate and average fade duration if $\rho = -20$ dB.

4.10 For the following digital wireless systems, estimate the maximum rms delay spread for which no equalizer is required at the receiver (neglect channel coding, antenna diversity, or use of extremely low power levels).

System	RF Data Rate	Modulation
USDC	48.6 kbps	π/4DQPSK
GSM	270.833 kbps	GMSK
DECT	1152 kbps	GMSK

4.11 Derive the RF Doppler spectrum for a 5/8λ vertical monopole receiving a CW signal using the models by Clarke and Gans. Plot the RF Doppler spectrum and the corresponding baseband spectrum out of an envelope detector. Assume isotropic scattering and unit average received power.

4.12 Show that the magnitude (envelope) of the sum of two independent identically distributed complex (quadrature) Gaussian sources is Rayleigh distributed. Assume that the Gaussian sources are zero mean and have unit variance.

4.13 Using the method described in Chapter 4, generate a time sequence of 8192 sample values of a Rayleigh fading signal for
(a) $f_d = 20$ Hz and (b) $f_d = 200$ Hz.

4.14 Generate 100 sample functions of fading data described in Problem 4.13, and compare the simulated and theoretical values of R_{RMS}, N_R, and $\bar{\tau}$ for $\rho = 1$, 0.1, and 0.01. Do your simulations agree with theory?

4.15 Recreate the plots of the CDFs shown in Figure 4.17, starting with the pdfs for Rayleigh, Ricean, and log-normal distributions.

4.16 Plot the probability density function and the CDF for a Ricean distribution having (a) $K = 10$ dB and (b) $K = 3$ dB. The abscissa of the CDF plot should be labeled in dB relative to the median signal level for both plots. Note that the median value for a Ricean distribution changes as K changes.

4.17 Based on your answer in Problem 4.16, if the median SNR is -70 dBm, what is the likelihood that a signal greater than -80 dBm will be received in a Ricean fading channel having (a) $K = 10$ dB, and (b) $K = 3$ dB?

4.18 A local spatial average of a power delay profile is shown in Figure P4.18.

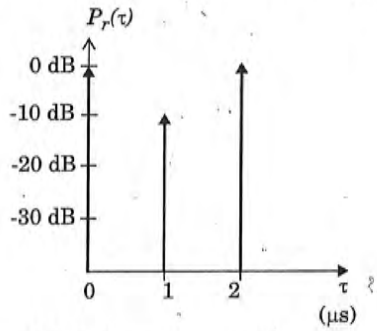

Figure P4.18. Power delay profile.

(a) Determine the rms delay spread and mean excess delay for the channel.
(b) Determine the maximum excess delay (20 dB).
(c) If the channel is to be used with a modulation that requires an equalizer whenever the symbol duration T is less than $10\sigma_\tau$, determine the maximum RF symbol rate that can be supported without requiring an equalizer.
(d) If a mobile traveling at 30 km/hr receives a signal through the channel, determine the time over which the channel appears stationary (or at least highly correlated).

4.19 A flat Rayleigh fading signal at 6 GHz is received by a mobile traveling at 80 km/hr.
(a) Determine the number of positive-going zero crossings about the rms value that occur over a 5 s interval.
(b) Determine the average duration of a fade below the rms level.
(c) Determine the average duration of a fade at a level of 20 dB below the rms value.

4.20 Using computer simulation, create a Rayleigh fading simulator that has 3 independent Rayleigh fading multipath components, each having variable multipath time delay and average power. Then convolve a random binary bit stream through your simulator and observe the time waveforms of the output stream. You may wish to use several samples for each bit (7 is a good number). Observe the effects of multipath spread as you vary the bit period and time delay of the channel.

4.21 Based on concepts taught in this chapter, propose methods that could be used by a base station to determine the vehicular speed of a mobile user. Such methods are useful for handoff algorithms.